AMINO ACIDS: BASOLATERAL EFFLUX AND EXTRACELLULAR HOMEOSTASIS CONTROL *IN VIVO*

Dissertation

zur

Erlangung der naturwissenschaftlichen Doktorwürde
(Dr. sc. nat.)

vorgelegt der

Mathematische-naturwissenschaftlichen Fakultät

der

Universität Zürich

von

Luca Carlo Olivio Mariotta

von

Muralto TI

Promotionskomitee

Prof. Dr. med. François Verrey
Prof. Dr. Hannelore Daniel
Prof. Dr. med. Gerd A. Kullak-Ublick

Zürich, 2012

To my growing family

Table of contents

1. Summary

In all living organisms, amino acids (AA) are essential building blocks, metabolites and signaling molecules. To reach their site of action AA need to pass through polar epithelial cells. Because AA cannot freely diffuse through the cell membrane, specific AA carriers ensure their transport across the apical and the basolateral membrane. Despite numerous flux studies and huge progress in the identification and characterization of these carrier proteins, AA transport across the basolateral membrane is not fully understood. The best characterized basolateral transporters in the small intestine and kidney proximal tubule are the obligatory exchanger (antiporter) Lat2-4F2hc (Slc7a8) and y^+Lat1-4F2hc (Slc7a7). Both require the presence of a "one-way transport" (uniporter) to achieve a net AA efflux. TAT1 (Slc16a10) and LAT4 (Slc43a2) fulfill this requirement with different substrate selectivities: TAT1 facilitates the diffusion of aromatic AA, whereas Lat4 transports branched chain AA, some aromatic AA, Met and Pro. The functional cooperation between TAT1 and Lat2-4F2hc has previously been shown using the *X. laevis* oocyte expression system (Ramadan, Camargo et al. 2007). An analogous functional cooperation was also shown for Lat4. Indeed, TAT1 shows the same localization as LAT2-4F2hc in epithelial cells and is further present in muscle sarcolemma and perivenous hepatocytes. The precise localization of Lat4 is still unknown and appears to overlap partially with that of TAT1.

The question addressed in this dissertation is: what is the function of TAT1 and Lat4 *in vivo*? Using global knock out mouse models we have examined the effect of the absence of the two uniporters on the AA homeostasis and epithelial transport.

By inducing specific aminoaciduria in TAT1 defective mice (*tat1*$^{-/-}$) under high protein diet, we could confirm the functional collaboration between TAT1 and LAT2-4F2hc *in vivo*. Furthermore, *tat1*$^{-/-}$ showed elevated aromatic AA in plasma, skeletal muscles and kidney, but not in liver. Thus, we could conclude that the absence of TAT1 prevents the maintenance of AA balance between plasma and liver and the consequent regulation of AA homeostasis. By means of everted gut sacs and microSPECT/CT imaging, we could show that the impairement of AA epithelial transport was caused by an intracellular accumulation of the AA substrates. The mild phenotype of *tat1*$^{-/-}$ strongly suggests a compensatory role by Lat4, which is also functionally redundant in the oocyte. In fact, Lat4 defective mice (*lat4*$^{-/-}$) prematurely died within the first five days of life. After birth, the normal size, skin color and behavior of *lat4*$^{-/-}$ pups excluded possible prenatal impairments. Normal suckling behavior further excluded possible severe neurological disability. The reduced growth recorded between 24 and 48 hours indicated a disorder in food intake or absorption. Further investigations should aim to decipher the cause of death.

In conclusion, this study analyzes the function of two basolateral uniporters for the first time *in vivo*. We show that the basolateral transport machinery is still functional in the absence of TAT1, whereas it appears to be more impaired in the absence of Lat4. Furthermore, we have shown a new important role of TAT1 in the regulation of the aromatic AA concentrations by the coupling of liver cells and blood plasma. Further research should aim to better characterize the *in vivo* interplay between AA transporters by the study of combinatorial knock out mice. Finally, the results of the different protein rich diets and their influence on the urinary pattern open new questions about the regulation of AA transporters *in vivo*.

2. Zusammenfassung

In allen Lebewesen sind Aminosäure (AS) essentielle Bausteine, Metaboliten und Signal-Moleküle. Um ihren Aktionsort zu erreichen, müssen sie die polaren Epithelzellen passieren. Weil AS nicht frei durch die Zellmembran diffundieren können, stellen AS-Transporter an apikalen und basolateralen Membranen den spezifischen Transport sicher. Trotz zahlreicher Transport-Studien und grosser Fortschritte in der Identifizierung und Charakterisierung der beteiligten Proteine, ist der Transport durch die basolaterale Membran nicht vollständig aufgeklärt. Die am besten charakterisierten basolateralen Transporter im Dünndarm und proximalen Nierentubulus sind die obligatorischen Austauscher (Antiporter) Lat2-4F2hc (Slc7a8) und y+Lat1-4F2hc (Slc7a7). Beide benötigen für ihre Funktion einen „Ein-Weg-Transporter“ (Uniporter), um einen Netto-Export der AS zu ermöglichen. TAT1 (Slc16a10) und Lat4 (Slc43a2) erfüllen diese Anforderung, aber mit unterschiedlichen Substraten. TAT1 transportiert aromatische AS und Lat4 die verzweigtkettigen AS, die aromatischen AS, Met und Pro. Im *X. laevis* Oocyten System wurde die Zusammenarbeit von TAT1 und Lat2-4F2hc funktionell gezeigt (Ramadan, Camargo et al. 2007). Lat4 konnte im Oocyten eine äquivalente Funktion zu der von TAT1 übernehmen. TAT1 teilt die Lokalisierung mit Lat2-4F2hc in Epithelzellen und ist ebenfalls in Muskel und Leber exprimiert. Die genaue Lokalisierung von Lat4 ist unbekannt. Die Expression der beiden Uniporter überlappt scheinbar nur teilweise.

Was ist die Funktion von TAT1 und Lat4 *in vivo*? Mittels globaler knock-out Maus-Modelle haben wir die Auswirkung deren Abwesenheit auf die AS-Homöostase und den Epithel-Transport untersucht.

Unter hoher Eiweiss-Ernährung bestätigte die Auslösung einer spezifischen Aminoazidurie in TAT1 knock-out Mäusen (*tat1*$^{-/-}$) die funktionale Zusammenarbeit zwischen TAT1 und Lat2-4F2hc *in vivo*. Weiter, zeigten *tat1*$^{-/-}$ Mäuse erhöhte aromatische AS im Plasma, Muskel und in den Nieren, im Gegensatz zur Leber. Somit, verhindert die Abwesenheit von TAT1 in Leberzellen den AS-Ausgleich mit dem Blut und nachfolgend die AS-Homöostase-Regulation. Mittels „Everted Gut Sac“ und „microSPECT“ Experimenten konnten wir zeigen, dass die Beeinträchtigung der epithelialen Funktionalität durch eine intrazelluläre Akkumulation der AS-Substrate verursacht wurde. Der milde Phänotyp deuted darauf hin, dass Lat4, der funktionell in Oocyte redundant ist, eine zentrale kompensatorische Rolle spielt. In der Tat sterben Lat4 Knock-out Mäuse (*lat4*$^{-/-}$) innerhalb der ersten fünf Lebenstage. Die Grösse, die Hautfarbe und das Verhalten der *lat4*$^{-/-}$ Tiere nach der Geburt liegen im normalen Bereich, welches pränatale Gründen ausschliesst. Neurologische Ursachen wurden wegen normalem Saugverhalten ausgeschlossen. Der reduzierte Wachstum zwischen 24 und 48 Stunden deutet auf eine Störung der Nahrungsaufnahme oder -absorption hin. Weitere Untersuchungen sollen die Todesursache entschlüsseln.

Im meiner Dissertation haben wir erstmals *in vivo* zwei bekannte basolaterale Uniporter analysiert. Die basolaterale AS Transportmachinerie ist in der Abwesenheit von TAT1 funktionsfähig, während sie ohne Lat4 scheinbar versagt. Ausserdem, haben wir eine wichtige neue Rolle von TAT1 in den Leberzellen für die Regulation der aromatischen AS-Konzentrationen gezeigt. Weitere Forschung soll darauf aufbauen, das *in vivo* Wechselspiel zwischen AS-Transportern mittels Doppel-Knock-out Mäusen weiter zu charakterisieren. Schließlich, haben die Resultate der verschiedenen eiweißreichen Diäten und deren Einfluss auf das Urin-Profil neue Fragen über die Regulierung von AS-Transportern *in vivo* eröffnet.

3. Introduction

3.1. Amino acids

3.1.1 Amino acids: structure and variety

Amino acids (AAs) are defined as organic substances which contain an amino group and an acidic carboxyl group (Wu 2009) (Fig. 1). AAs can join together with the help of the previously mentioned groups forming a peptide bond, and giving rise to a linear polymer of AAs, called polypeptide or protein (Fig. 2). Except for glycine, all AAs have both L- and D-isoforms due to their chirality with reference to glyceraldehydes, however only the L- isoforms are used for protein formation. Indeed, most of the D-AAs can be converted into L-AAs catalized by several oxydases and transaminases, which are species specific (Baker 2009; Fang, Luo et al. 2009). Variations in the AA side chain (Fig. 1, R-group) distinguish the AA among each other and confer different biochemical properties: nonpolar, polar uncharged, polar charged acidic and polar charged basic (Fig. 3). According to the chemical conformation of the side chain AAs can also be classified as aromatic AA, which are AAs with an aromatic ring and includes phenylalanine, tryptophan, tyrosine and histidine. Another group is the one of branched chain AA (BCAA), which includes leucine, isoleucine and valine. The side chain also confers its chemical property to the peptides or the part of the protein, which might consequently be more hydrophilic or hydrophobic, and the exact AA sequence is crucial for the proper formation of secondary and tertiary protein structures. Among more than 300 AA found in nature, only 20 serve as building blocks of proteins during mRNA translation (Wu 2009). In addition, four other AAs are found in mature proteins as consequence of posttranslational modifications: γ-carboxyglutamic acid, hydroxylysine, 4-hydroxyproline and 3-hydroxyproline (Galli 2007). Accordingly to the international IUPAC nomenclature AAs are classified with a trivial name (e.g. alanine), a symbol code (e.g. Ala or A) and systematic name (e.g. 2-Aminopropanoic acid) (Recommendations 1976). For convenience, in this work we refer to the 3-letter code or to the trivial name, always implying the L-isoform (Fig. 3).

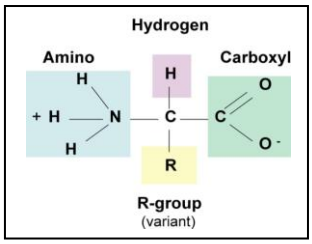

Fig. 1: Chemical structure of an amino acid. Amino acids (AAs) are organic molecules containing an amino and a carboxyl group. The variable side chain (R-group) confers the chemical properties and distinguish each AA.

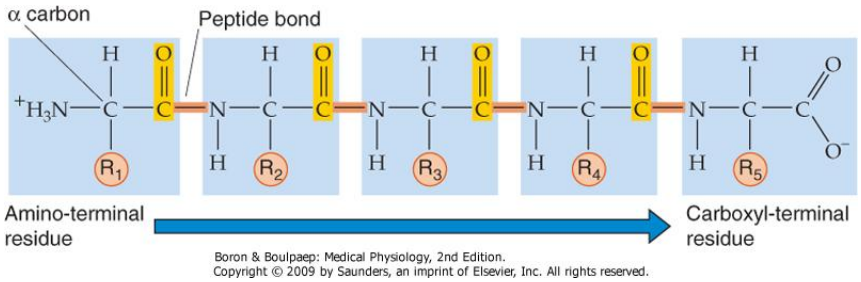

Fig. 2: L-AAs can be linked together to form peptides and proteins. Amino and carboxyl group of AA can be linked together via peptide bond. Side chains (R) confers specific chemical properties to the peptide. From (Boron and Boulpaep 2005).

Trivial name[a]	Symbol	One-letter symbol[b]	Systematic name[c]	Formula
Alanine	Ala	A	2-Aminopropanoic acid	$CH_3–CH(NH_2)–COOH$
Arginine	Arg	R	2-Amino-5-guanidinopentanoic acid	$H_2N–C(=NH)–NH–[CH_2]_3–CH(NH_2)–COOH$
Asparagine	Asn[d]	N[d]	2-Amino-3-carbamoylpropanoic acid	$H_2N–CO–CH_2–CH(NH_2)–COOH$
Aspartic acid	Asp[d]	D[d]	2-Aminobutanedioic acid	$HOOC–CH_2–CH(NH_2)–COOH$
Cysteine	Cys	C	2-Amino-3-mercaptopropanoic acid	$HS–CH_2–CH(NH_2)–COOH$
Glutamine	Gln[d]	Q[d]	2-Amino-4-carbamoylbutanoic acid	$H_2N–CO–[CH_2]_2–CH(NH_2)–COOH$
Glutamic acid	Glu[d]	E[d]	2-Aminopentanedioic acid	$HOOC–[CH_2]_2–CH(NH_2)–COOH$
Glycine	Gly	G	Aminoethanoic acid	$CH_2(NH_2)–COOH$
Histidine	His	H	2-Amino-3-(1*H*-imidazol-4-yl)propanoic acid	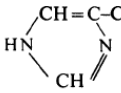
Isoleucine	Ile	I	2-Amino-3-methylpentanoic acid[e]	$C_2H_5–CH(CH_3)–CH(NH_2)–COOH$
Leucine	Leu	L	2-Amino-4-methylpentanoic acid	$(CH_3)_2CH–CH_2–CH(NH_2)–COOH$
Lysine	Lys	K	2,6-Diaminohexanoic acid	$H_2N–[CH_2]_4–CH(NH_2)–COOH$
Methionine	Met	M	2-Amino-4-(methylthio)butanoic acid	$CH_3–S–[CH_2]_2–CH(NH_2)–COOH$
Phenylalanine	Phe	F	2-Amino-3-phenylpropanoic acid	$C_6H_5–CH_2–CH(NH_2)–COOH$
Proline	Pro	P	Pyrrolidine-2-carboxylic acid	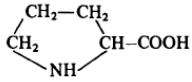
Serine	Ser	S	2-Amino-3-hydroxypropanoic acid	$HO–CH_2–CH(NH_2)–COOH$
Threonine	Thr	T	2-Amino-3-hydroxybutanoic acid[e]	$CH_3–CH(OH)–CH(NH_2)–COOH$
Tryptophan	Trp	W	2-Amino-3-(1*H*-indol-3-yl)propanoic acid	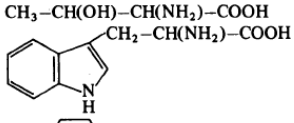
Tyrosine	Tyr	Y	2-Amino-3-(4-hydroxyphenyl)propanoic acid	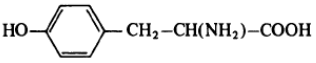
Valine	Val	V	2-Amino-3-methylbutanoic acid	$(CH_3)_2CH–CH(NH_2)–COOH$
Unspecified amino acid	Xaa	X		

Fig. 3: the 20 proteinogenic AA according to the IUPAC nomenclature. Taken from Nomenclature and Symbolism for Amino Acids and Peptides, (Recommendations 1976).

3.1.2 Amino acid functions and requirements

Amino acids are crucial elements for life with a plethora of functions. As already mentioned, AAs serve as proteins building blocks and are essential for the production of functional proteins (e.g. enzymes, regulatory proteins and signal peptides) and for structural proteins (e.g. collagen and proteins of the cytoskeleton). Furthermore, free AAs play an important role in cell metabolism, as metabolic intermediates, in inter-organ communication, neurotransmission, regulation of gene expression, hormonal synthesis, oxidative defense, immune defense and acid-base balance (Grillo and Colombatto 2007; Kim and Wu 2009; Wu 2009). Representing 40-45% of total body weight, the skeletal muscles are the major reservoir of AAs. In fact, the body of a 70 kg man contains approximately 12 kg of protein (17%) and 200 g of free AAs (0.3%) with a continuous exchange between both pools. The protein turnover was estimated to amount to approximately 300 g per day (Deutz, Wagenmakers et al. 1999). Since many free AAs are lost to energy conversion and urea, the daily requirement of dietary AAs amount to 70 g approximately (Deutz, Wagenmakers et al. 1999). Based on their specific requirement and on the ability (or not) to be sufficiently synthesized in the body, the 20 proteinogenic AAs were classified in essential (indispensible) and non-essential (dispensible) (Tab. 1). Furthermore AAs that can normally be synthesized by the organism, but need another AA as precursor, are classified as conditionally essential AAs. For example, Tyr can be synthesized in the liver and in the kidney by the enzyme phenylalanine hydroxylase (PAH), which however needs adequate amounts of starting substrate, Phe (Lichter-Konecki, Hipke et al. 1999). The classification might differ among species, due to different metabolism and food composition.

Essential AA	Non-Essential AA	Precursor
Histidine	Alanine	
Isoleucine	Arginine[g]	Glutamine/ate, Aspartate
Leucine	Asparagine	
Lysine	Aspartate	
Methionine	Cysteine[b,c,g]	Methionine, Serine
Phenylalanine	Glutamate	
Threonine	Glutamine[g]	Glutamate, Ammonia
Tryptophan	Glycine	
Valine	Proline[b,g]	Glutamate
	Serine	
	Tyrosine[c]	Phenylalanine

Tab. 1: Essential and Non-essential AA in mammals and their respective precursor. Conditional essential AA are labeled with letters accordingly whether they are required under growth[g], premature birth[b] or cirrhosis[c]. Modified from (Gropper 2005; Wu 2009).

3.1.3 Amino acid metabolism and nutrition

Besides proteins, a normal meal contains different components like sugars, fatty acids, vitamins, water and salts. Therefore it is fair to conclude that the body rarely faces a strict protein meal. Peters and Harper tested the effect of diets containing different levels of proteins and showed that several metabolic adaptations took place (Peters and Harper 1981; Peters and Harper 1985; Harper and Peters 1989). In plasma, BCAA (Val, Ile and Leu) directly correlated with the dietary load, whereas Ala and Gln were hallmarks for low protein diets, similarly to starvation status. Interestingly, aromatic AA remained stable. Therefore the majority of free AA in plasma are maintained within normal concentrations and their excess can result in severe adverse effects like reduced food intake, abnormal behavior, impaired growth and death (Boron and Boulpaep 2005). The plasma concentration of each AA is the result of its rate of appearance (Ra) and disappearance (Rd) from plasma (Cynober 2002). The Ra is influenced not only by the dietary intake but also by the protein turnover and AA catabolism in different organs. Similarly, the Rd is influenced by the anabolism with the abduction in different organs and by body losses. Both rates are AA specific, especially the Rd because of different AA fates. Furthermore, differences were found between gender, age and body mass (Cynober, Blonde et al. 1983; Caballero, Gleason et al. 1991; Cals, Bories et al. 1994; Klassen, Furst et al. 2001). Other studies, in which AAs were administered in presence or absence of glucose, showed an ambivalent effect on insulin, glucose and AA concentrations (Gannon, Nuttall et al. 2002; Gannon, Nuttall et al. 2002; Nuttall, Schweim et al. 2006; Kalogeropoulou, Lafave et al. 2008). Furthermore, it was shown that different protein loads and AA compositions of the diet affect the feeding behavior (Koehnle, Russell et al. 2003; Tome 2004; Langhans 2010). Thus, the correlation between dietary intake, metabolic status and AA plasma concentrations is extremely elaborate and appears to require complex network approaches to be understood (Bier 2003; Noguchi, Zhang et al. 2006; Shikata, Maki et al. 2007).

Considering the simple case of a strict protein meal, the food is first homogenized mechanically in the mouth and subsequently digested in the gastrointestinal tract. Peptide bonds are cleaved by different peptidases present first in the stomach (i.e. pepsin) and afterwards in the small intestine (i.e. trypsin, chymotrypsin, carboxypeptidase and aminopeptidase). Specialized cells called enterocytes (epithelial layer) absorb, besides other nutrients, the free AA and the di/tri-peptides. These cells might use part of the AAs as energy source for own requirements or deliver the rest to the extracellular fluid (Boron and Boulpaep 2005; Gropper 2005; Wu 2009). The AAs that enter the blood stream have an obligatory passage through the liver via the portal vein, where the glucogenic AAs are captured and converted into pyruvate for glycogen production (Fig. 4). The other AAs, that are still present in the circulation, are used for protein synthesis by other tissues, especially in muscles.

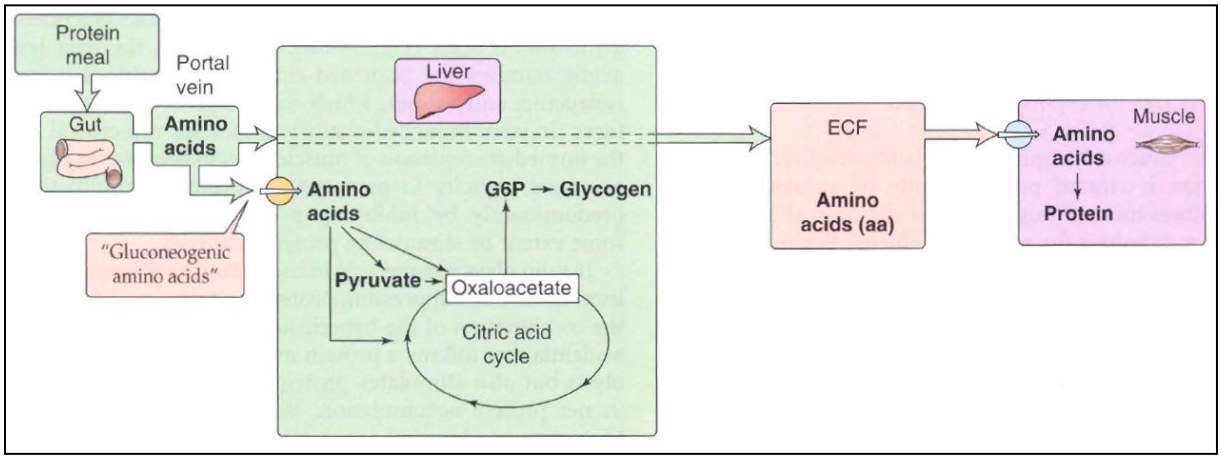

Fig. 4: Fate of AAs after a protein meal. From (Boron and Boulpaep 2005).

In contrast under starvation, the first priority is to maintain the glucose level constant for proper brain functionality, and only in a second instance to maintain protein reserves constant (Boron and Boulpaep 2005; Gropper 2005). Thus, after an overnight starvation, three major adaptations are taking place: the Cori cycle, the glucose-alanine cycle and the lipolysis (Fig. 5). In the Cori cycle, the liver converts the lactate, which has been energetically produced from anaerobic metabolism, into glucose and releases it into the plasma. In the glucose-alanine cycle, muscles and splanchnic tissues release newly synthesized alanine and glutamine produced as a consequence of protein degradation into the blood. Afterwards, the two AAs are taken up by the liver and used for gluconeogenesis. Both cycles are thus used for energy transfer. Finally, the insulin drop causes the release from fat stores of fatty acids and glycerol that are used by the liver to further generate energy. Prolonged starvation moderates the proteolysis in muscles and accelerates lipolysis.

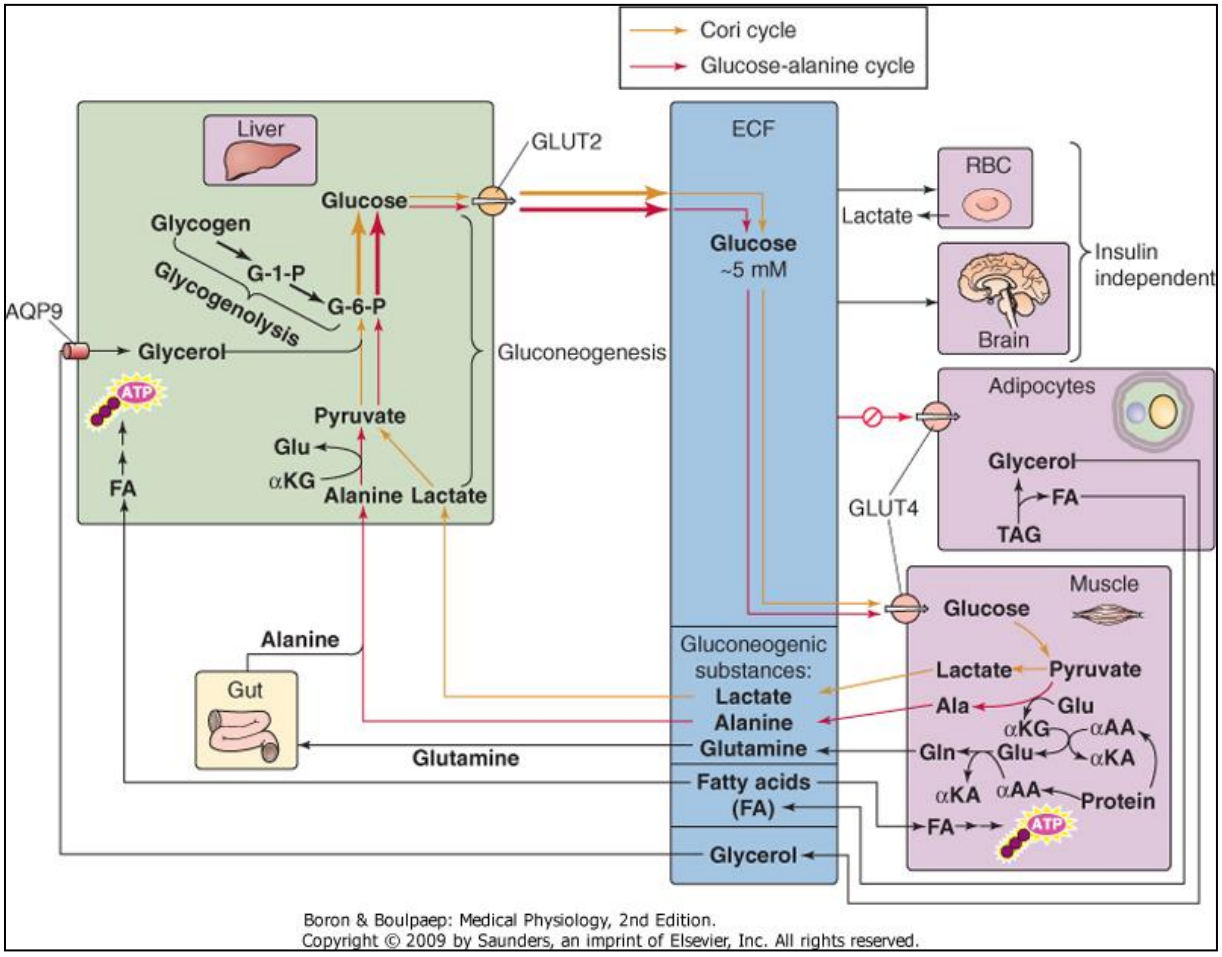

Fig. 5: Adaptation after an overnight fast: Cori cycle, glucose-alanine cycle and lipolysis. From (Boron and Boulpaep 2005).

3.1.4 The metabolism of aromatic amino acids in mammals

As discussed in section 3.1.1, the members of the aromatic AA group present an aromatic ring in their side chain and include phenylalanine, tryptophan, tyrosine and histidine. All of them can be considered as essential AA, since Tyr is dependent on Phe availability (Tab. 1). However, His differs from all other aromatic AA because its aromatic ring contains nitrogen (imidazole ring). This shows a pKa of approximately 6, thus gets protonated at pH lower than 6 where it has a positive charge (Fig. 3). As consequence of its peculiar chemical structure, His degradation differs from the other 3 aromatic AAs: it might be catabolized into Glu, it might be combined with β-Ala to generate carnosine or it might be decarboxylated to form histamine (Gropper 2005).

Of more interest are the other three aromatic AAs that display a benzyl ring (Phe, Tyr and Trp) and share a similar fate, being mostly degraded in the liver (Schimassek and Gerok 1965; Dietrich 1992; Brosnan 2003; Gropper 2005). Phe and Tyr are partially glucogenic and partially ketogenic, catabolized to acetoacetate. The first interconversion of Phe into Tyr is carried out by the enzyme phenylalanine hydroxylase (PAH), which was found in kidney and liver (Lichter-Konecki, Hipke et al. 1999). The catabolism of Tyr is not strictly liver specific but many obligatory reactions for its degradation occur primarily in the liver. Besides, other tissues use Tyr to produce different important compounds. In neurons and adrenal medulla, Tyr is the precursor of L-dopa and catecholamines (dopamine, noradrenaline and epinephrine), that shows a half-life of a few minutes when circulating into the blood. Furthermore, in melanocytes Tyr is transformed into melanin and in thyroid gland into thyroid hormones. Interestingly, the defect in Phe and Tyr metabolism (i.e. in the PAH enzyme) causes an autosomal genetic disorder named phenylketonuria, which results in a buildup of Phe and it derivates in the blood and causes neurologic disorders among others (Lichter-Konecki, Hipke et al. 1999; Thony 2010; Kostandyan, Britschgi et al. 2011). Concerning Trp, approximately 95% of its metabolism takes place in the liver, where it is transformed to pyruvate or acetyl CoA for energy production. Important by-products of Trp degradation are niacin (vitamin B_3) and NADP (Gropper 2005; Yao, Fang et al. 2011).

In addition Trp is used for the production of serotonin (5-HT), an important monoamine neurotransmitter (Lesch, Bengel et al. 1996), and melatonin, an hormone capable of influencing the daily cycle (Altun and Ugur-Altun 2007). Not surprising, an imbalance of Trp metabolism causes several disorders like α-ketoadipic aciduria (Przyrembel, Bachmann et al. 1975) and glutaric aciduria type I (Strauss, Puffenberger et al. 2003).

In conclusion, if not used for the synthesis of protein, the aromatic AA (Phe, Tyr and Trp) are mainly degraded in the liver, which thus act as a sink and regulates their plasma concentration. As evidence of this role during cirrhosis, liver failure or liver resection, the aromatic AA accumulate in plasma (Dejong, van de Poll et al. 2007). Besides this main fate, other tissues use little portions of those AAs to produce important signal molecules, among them catecholamines and monoamines. Their imbalance causes several disorders.

3.2. Amino acid transport

Dietary AAs must cross several barriers before reaching their final destination. First of all there is the intestine, where AAs are taken from the lumen and enter the blood stream. Furthermore, AAs in the blood stream might be filtered by the kidney, where they are reabsorbed. In both, intestine and kidney, specialized epithelia assure a proper trafficking. Finally, to reach the intracellular space of each cell, but also to pass through the epithelial cells, AAs need to cross the lipid bilayer of the cellular membrane, where they cannot freely diffuse and thus they need specialized proteins for their import and export. In the next subchapters these different aspects are more exhaustively explained, starting with the epithelial structure, continuing with the organization of gastrointestinal tract and kidney nephron, the membrane transport, the AA transporter proteins and finishing with particular families of AA transporters (i.e. *Slc16* and *Slc43*).

3.2.1 The epithelium

The epithelium is composed of a specialized sheet of cells that form a tight barrier between the internal and the external *milieux* such that the organism can regulate its internal fluid and separate it from the variable and potentially toxic external environment. In order to achieve this goal, the epithelium can actively import and expel substances, sometimes even against a steep gradient. To form a dynamic barrier, the epithelium presents two characteristic features: a tight connection between cells (tight junction) and a polarization of its cellular membrane, which is divided into an apical and a basolateral part (Fig. 6).

The tight junctions limit the free diffusion of solutes and fluids and define the boundary between the apical and the basolateral membrane. It is a complex structure of parallel strands of closely packed particles (Fig. 6). The degree of impermeability is roughly proportional to the number of these strands and small molecules that can pass through are termed to take a paracellular diffusion (i.e. between cells). The principal structural elements are a family of proteins called claudins. Interestingly, tight junctions display tissue specific degrees of permeability and thus partially modulate the transport of some solutes. For example, in the renal proximal tubule the tight junction is quite leaky whereas in the thick ascending limb it is impermeable to water.

The membranes separated by the tight junction present different proteins and lipid components on their surface that allow to enroll different functions. The apical membrane faces the lumen or extracorporeal world and generally presents typical infoldings also known as brush border, which amplifies the surface area in order to present more digestive enzymes and transport proteins. This is the case for intestinal cells, where the apical membrane forms microvilli and therefore increases the area by approximately 20 times. In contrast the basolateral membrane faces the inside of the body or the extracellular fluid compartment and is thus indirectly in contact with the blood. Other junctional complex types present in the lateral membrane interconnect the different cells and allow intercellular communication. The basolateral surface is also amplified by infoldings, however generally to a less extend than the apical one. Besides their morphological variance, the major difference relies in their protein composition, which also confers different biochemical properties. For example, in the intestine the apical membrane has to efficiently digest and import the different nutrients present in the lumen. In contrast, the basolateral membrane has to efficiently export the nutrients into the extracellular fluid and at the same time balance the import of other solutes that are necessary for cell survival and that are not present in the lumen. Importantly, in some tissues this process can work on the opposite way, like in the liver where toxic metabolites are sequestered from the blood and expelled into the bile. The proper trafficking and sorting of the different proteins in the appropriate membrane is thus crucial.

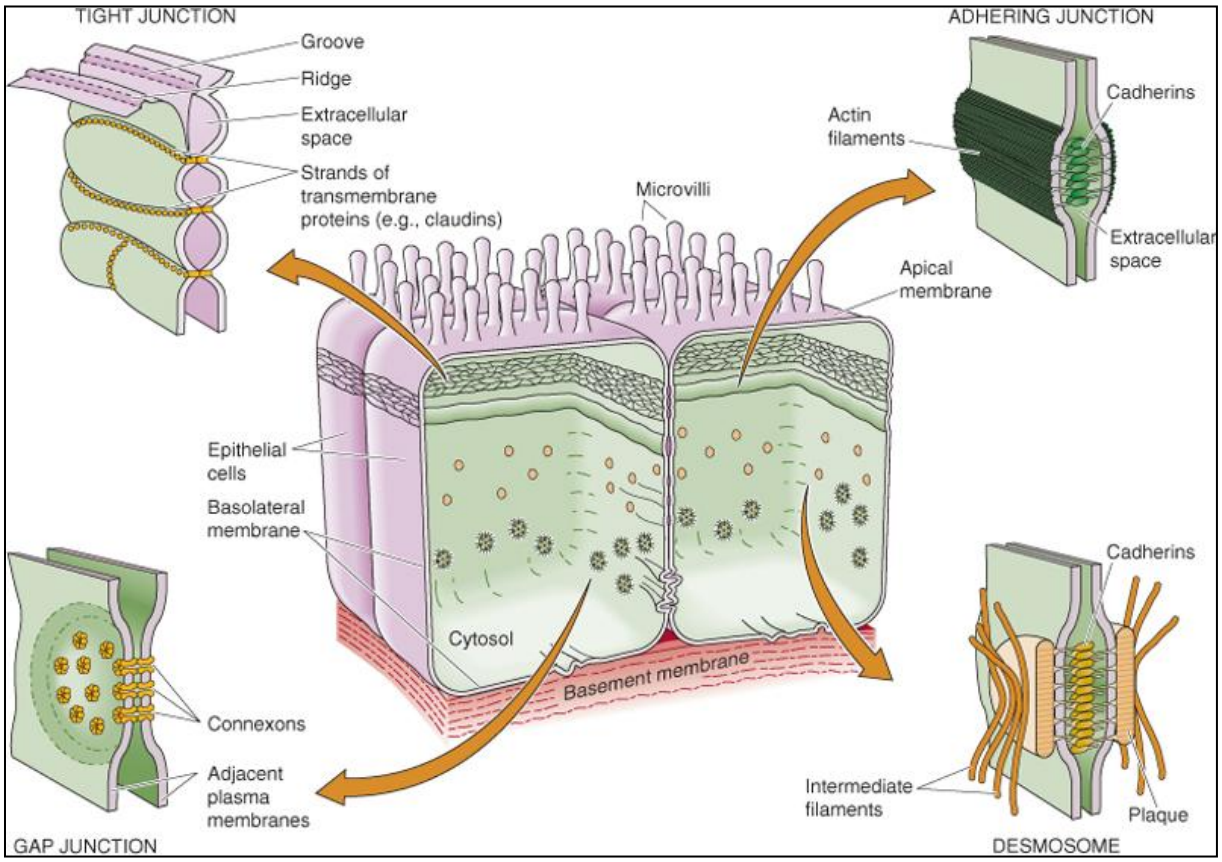

Fig. 6: Schema of an epithelium composed of polarized cells. The apical and the basolateral membrane are delimited by the tight junctions that connect the cells and limit the free diffusion of solutes and fluids. Other junction types are also illustrated. (Boron and Boulpaep 2005).

3.2.2 The gastrointestinal tract

The gastrointestinal tract consists of a series of hollow organs that stretch from the mouth to the anus (Fig. 7A). Each of those organs covers a specialized function and is divided by the presence of sphincters. The mouth is responsible for chewing, lubricating the food and initiating carbohydrate and fat digestion.

The stomach homogenate the food, secretes acids and initiates the protein digestion with the help of pepsins. The small intestine, which is divided into duodenum, jejunum and ileum, is the primary site for the absorption of nutrients. The large intestine reabsorbs fluid and electrolytes. Further accessory organs include the salivary glands, the pancreas and the liver. The liver is important for fat digestion, since it secretes the bile. In a second instance the liver also selectively removes from the circulation several freshly absorbed nutrients that obligatory pass through the portal vein. Thus, the liver plays also a key role in regulating plasma values of different components including the aromatic AA (see 3.1.4). The pancreas secretes several digestive enzymes and is important for the digestion of the protein and for the neutralization of gastric acids. The protein digestion is completed in the small intestine not only by the pancreatic enzymes but also by enzymes present in the brush border membrane.

Anatomically the gastrointestinal tract varies along its length, however several structures are common (Fig. 7B). The internal part facing the lumen is the mucosa, which consists of epithelial cells (see 3.2.1). Underneath there is the *lamina propria*, which contains capillaries, neurons and immune cells, and the *lamina muscularis mucosae*. Afterwards, the submucosa consists of loose connective tissue and larger blood vessels. Beneath, several layers of smooth muscles can be found (i.e. the *muscularis externa*) and enteric neurons. Finally, the serosa envelops the whole with connective tissues and squamous epithelial cells. A complex enteric nervous system controls the GI peristalsis via complete

reflex circuits. The small intestine presents a "villus – crypt" organization which enables to further increase the surface area (Fig. 8). Villi are finger-like projections of the mucosa and lamina propria where the epithelial cells are lined on. Together with the folds of Kercking and the microvilli, the villi enable to increase the surface area of approximately 600 folds compared to a simple cylinder. Thus, the total surface area of a human small intestine reaches approximately 200 m^2 (Boron and Boulpaep 2005). In contrast, the colon has more in crypts, thus its surface area is estimated in about 25 m^2.

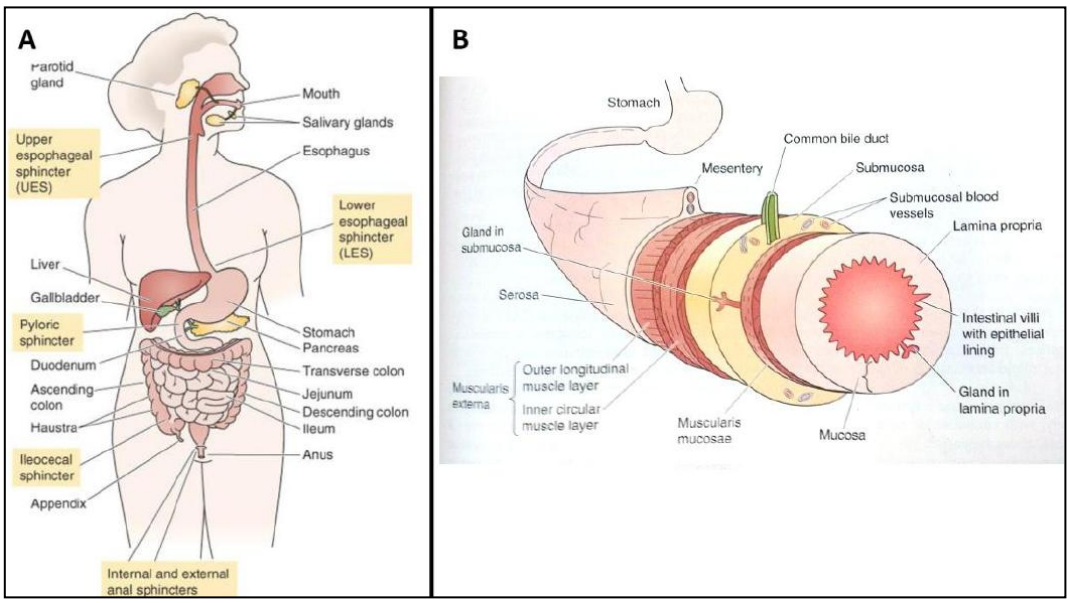

Fig. 7: Organization of the gastrointestinal tract. A. The GI tract is composed by several hollow organs, divided by sphincters, and other accessory glands and organs. B. The wall of a generic segment consists of different structures among which the epithelium in the inside (mucosa), different layers of muscles and the serosa on the outside. From (Boron and Boulpaep 2005).

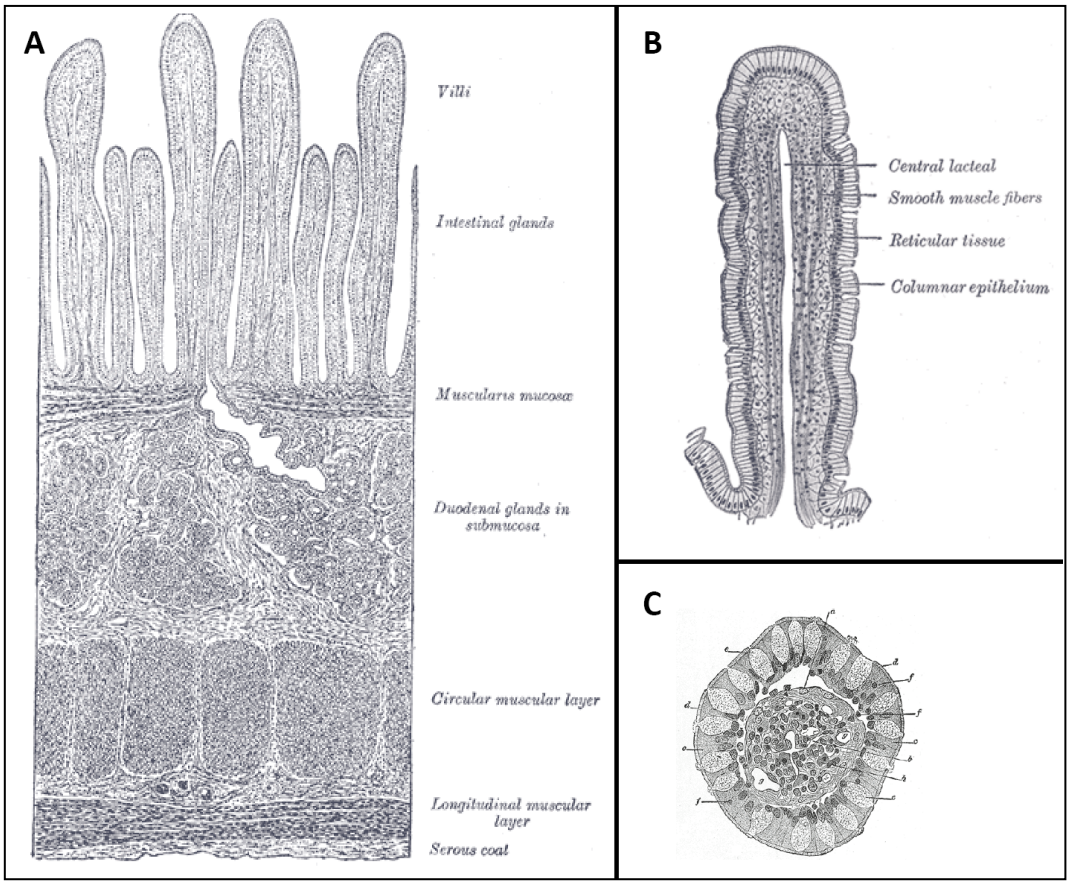

Fig. 8: The small intestine presents "villi – crypts" structures. A. Section of a duodenum with on top the villi (finger like-projections). B. Vertical section of a villus. C. Transverse section of a villus. From (Gray 1918).

3.2.3 The kidney

The kidneys are paired bean shaped structures that lie behind the peritoneum and are responsible for three different functions: (1) to filter and remove unwanted metabolic products and toxins, (2) to regulate the fluids, electrolyte and acid-base balance and (3) to produce and activate different hormones. Together they account for less than 0.5% of the total body mass, but they receive a considerable amount of blood (up to 20% of the cardiac output). Their functional unit is the nephron, which consists of a glomerulus and a tubule (Fig. 9). Each human adult kidney consists of about 1 milion of such nephrons (100'000 in mice). In the glomerulus, the afferent blood reaches a cluster of blood vessels where the plasma is filtrated and passes to the tubular system. The glomerular barrier consists of endothelial cells that forms fenestrated capillaries surrounded by the glomerular basement membrane and the podocytes. In a simplified view, 70 nm holes provide free passage of water and small solutes out of the vessels down in the tubule, whereas big particles like erythrocytes remains in the blood stream. The tubule is an epithelial structure with many subdivisions and different functions, as shown in Fig. 9. The first part, the proximal tubule, is further divided in two parts (proximal convoluted and proximal straight tubule). All parts present a brush border membrane and reabsorb the bulk of filtered fluid back in the circulation. Importantly, the proximal tubule is also the place where amino acids are reabsorbed, besides glucose, NaCl, $NaHCO_3$, divalent ions and water. After the proximal tubule, the Henle's loop, the thick ascending limb the distal tubule, the distal convoluted tubule, the connecting tubule and the final collecting duct are found. The tube of Henle concentrates or dilutes the ultrafiltrate, whereas the distal tubule and collecting duct system are responsible for the fine control of water and for the salt excretion.

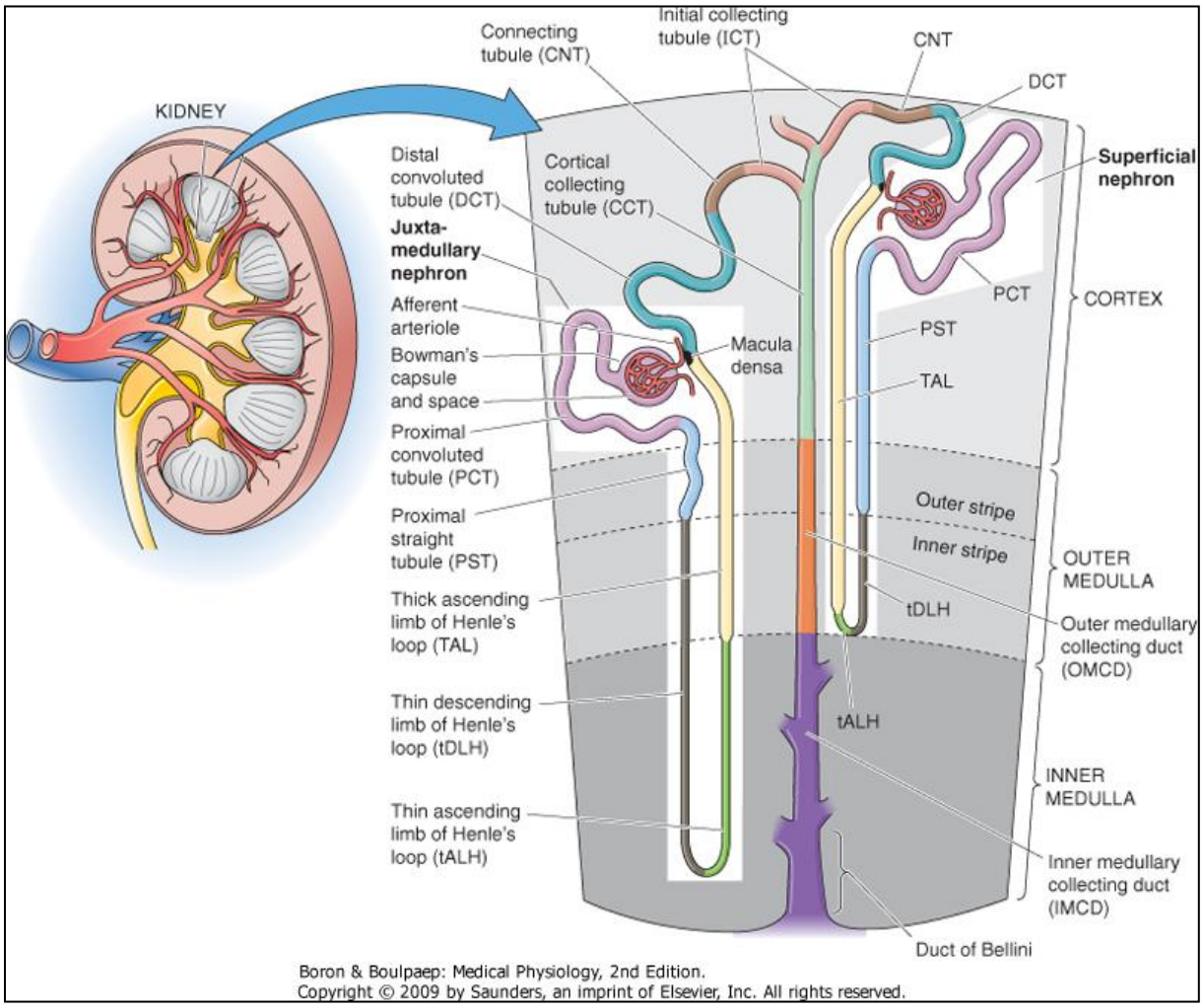

Fig. 9: The kidney and its functional unit, the nephron. The different tubular parts are listed. (Boron and Boulpaep 2005)

All solutes found in the urine come from the blood plasma perfused in the kidney. Thus, the rate at which the kidney excretes a solute equals the rate at which it disappears from the plasma, if the kidney does not produce or consume such a solute. Otherwise, the amount of solute excreted in the urine equals the sum of the amount filtered minus the amount reabsorbed and the amount secreted (Fig. 10). The clearance is plasma volume cleared of a substance in a given time (i.e. in ml / min), thus indicates the rate at which a substance is removed or cleared from the body by the action of kidneys and can be calculated with the formula $C_x = (U_x \times V) / P_x$ where C_x is the clearance, U_x the urinary concentration of the substance X, V the volume of urine formed in a given time and P_x the concentration of substance X in the plasma. The glomerular filtration rate (GFR) is the volume of fluid filtered in the

glomeruli per unit of time. The GFR can be extrapolated from the clearance of a known substance (e.g. inulin), provided that it is neither absorbed nor secreted. Knowing the GFR is important to extrapolate another useful parameter: the fractional excretion (FE). The FE is the ratio of the amount excreted in the urine to the amount of the filter load, or $FE_x = (U_x \times V) / (P_x \times GFR)$, which is also the clearance to GFR ratio. In other words, the FE gives an indication if a solutes has been reabsorbed (if <1) or secreted (>1). The FE does however not reveal whether both occurred, but only the sum of both.

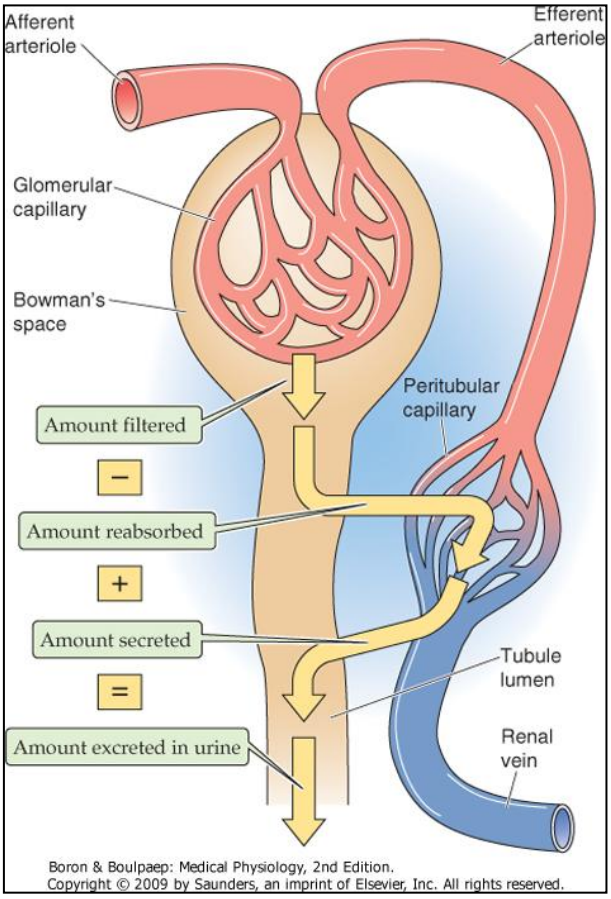

Fig. 10: Factors that contribute to the net urinary excretion of a substance. (Boron and Boulpaep 2005)

3.2.4 Membrane transport of small molecules

As already mentioned earlier, hydrophilic solutes can poorly diffuse into the lipid bilayer of the cellular membrane. Therefore, specialized pathways mediated by integral membrane proteins are required for their cellular import and export. Three types of such pathways are recognized: (1) the pore, which is always open, (2) the channel, which is alternatively open and closed (thus a gated pore) and (3) the carrier, which has two transmembrane gates that are never open at the same time and which presents a translocation cycle (Fig. 11). The pores allow the passive movement of solutes and enhance the membrane permeability, whereas the channel allows the movement down to an electrochemical gradient. The flow through channels is controlled by the open probability of the channel via gating mechanisms and the single channel conductance. In contrast, the carriers have a fixed stoichiometry of movement per translocation cycle and each carrier protein shows a specific affinity for binding one or more solutes. The simplest passive carrier-mediated transport is the facilitated diffusion (Fig. 11A). The facilitated diffusion differs from a simple diffusion by its transport rate which gets saturated above a certain concentration and which thus presents a maximum (Fig. 11B). Coupled transporters carry two or more solutes in the same direction (e.g. B^0AT1) and exchangers move them in opposite directions (e.g. Lat2-4F2hc) (Fig. 11A). All carriers that do not require ATP or coupled electron transport chain are members of the solute carrier (SLC) super-family. The SLCs are gatekeepers for all cells and organelles controlling the distribution of crucial compound such as sugars, nucleotides, ions, drugs and AAs. The Human Genome Organization (HUGO) provided a list of the SLC gene families, which were clustered upon their AA sequence homology (20-25% similitude among members) in 43 groups for a total of 298 genes in 2004 (Hediger, Romero et al. 2004) (Tab. 2). The members of the same family therefore do not necessarily show the same transport modalities. The genes were named using the root symbol SLC followed by the number of the family (i.e. SLC1 – SLC43), the letter A (as divider except for a few families) and finally the number of the individual gene, thus for example SLC16A10 (TAT1). Nevertheless, it became more evident that other membrane protein families were not yet classified because of their unknown function. A website with the latest updates has been created (http://www.bioparadigms.org/slc/menu.asp). At present, there are 51 families and 378 genes and among those 7 are families that account AA transporters (Tab. 2 and Tab. 3).

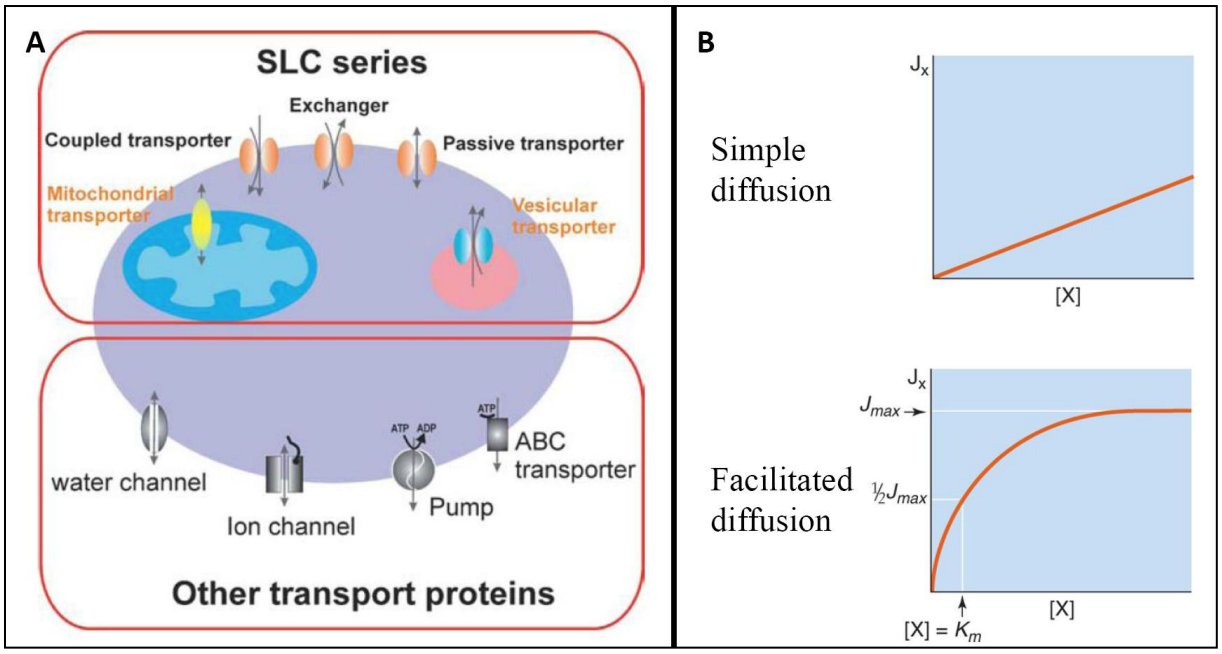

Fig. 11: the different membrane transport modalities. A. A cell with solute carriers (SLC) and non-SLC transporters expressed in its plasma membrane or in intracellular compartments. The different transport modalities of SLC members are also depicted (i.e. coupled transporter, exchanger and passive transporter). (Hediger, Romero et al. 2004). **B.** Transport rate upon solute concentration is different in a simple diffusion than in facilitated diffusion, where it is saturated and shows a half max flux. (Boron and Boulpaep 2005).

The HUGO Solute Carrier Family Series		Total
SLC1	The high-affinity glutamate and neutral amino acid transporter family	7
SLC2	The facilitative GLUT transporter family	14
SLC3	The heavy subunits of the heteromeric amino acid transporters	2
SLC4	The bicarbonate transporter family	10
SLC5	The sodium glucose cotransporter family	8
SLC6	The sodium- and chloride-dependent neurotransmitter transporter family	16
SLC7	The cationic amino acid transporter/glycoprotein-associated amino-acid transporter family	14
SLC8	The Na^+/Ca^{2+} exchanger family	3
SLC9	The Na^+/H^+ exchanger family	8
SLC10	The sodium bile salt cotransport family	6
SLC11	The proton coupled metal ion transporter family	2
SLC12	The electroneutral cation-Cl cotransporter family	9
SLC13	The human Na^+-sulfate/carboxylate cotransporter family	5
SLC14	The urea transporter family	2
SLC15	The proton oligopeptide cotransporter family	4
SLC16	The monocarboxylate transporter family	14
SLC17	The vesicular glutamate transporter family	8
SLC18	The vesicular amine transporter family	3
SLC19	The folate/thiamine transporter family	3
SLC20	The type-III Na^+-phosphate cotransporter family	2
SLC21/	The organic anion transporting family	11
SLC22	The organic cation/anion/zwitterion transporter family	18
SLC23	The Na^+-dependent ascorbic acid transporter family	4
SLC24	The $Na^+/(Ca^{2+}$-$K^+)$ exchanger family	5
SLC25	The mitochondrial carrier family	27
SLC26	The multifunctional anion exchanger family	10
SLC27	The fatty acid transport protein family	6
SLC28	The Na^+-coupled nucleoside transport family	3
SLC29	The facilitative nucleoside transporter family	4
SLC30	The zinc efflux family	9
SLC31	The copper transporter family	2
SLC32	The vesicular inhibitory amino acid transporter family	1
SLC33	The acetyl-CoA transporter family	1
SLC34	The type-II Na^+-phosphate cotransporter family	3
SLC35	The nucleoside-sugar transporter family	17
SLC36	The proton-coupled amino acid transporter family	4
SLC37	The sugar-phosphate/phosphate exchanger family	4
SLC38	The System A and N, sodium-coupled neutral amino acid transporter family	6
SLC39	The metal ion transporter family	14
SLC40	The basolateral iron transporter family	1
SLC41	The MgtE-like magnesium transporter family	3
SLC42	The Rh ammonium transporter family (pending)	3
SLC43	The Na^+-independent, system-L-like amino acid transporter family	2
Total		298

Tab. 2: list of solute carrier (SLC) families and number of their members in 2004, the updated list can be visualized at the link www.bioparadigms.org/slc/menu.asp (Hediger, Romero et al. 2004).

3.2.5 The SLC16 gene family

The SLC16 gene family accounts 14 members and is also known as the monocarboxylate cotransporter (MCT) family (Tab. 2). All family members are predicted to have 12 transmembrane domains, with intracellular N- and C-termini (Halestrap and Meredith 2004). The first four family members are known to transport important monocarboxylates such as lactate, pyruvate and ketone bodies. The other two characterized family members are MCT8 and MCT10, also known as XPCT and TAT1, respectively. MCT8 was shown to be a thyroid hormone transporter whereas TAT1 is the aromatic AA transporter (Friesema, Ganguly et al. 2003; Friesema, Jansen et al. 2005; Ramadan, Camargo et al. 2006). Interestingly MCT8 and MCT10 share 50% of homology in their sequence and are closely related to each other as opposed to other members (Fig. 12). Furthermore, they show a PEST sequence in their N-terminal (Fig. 13), which is thought to lead to rapid protein degradation (Rechsteiner and Rogers 1996). When tested, XPCT did however not mediate the transport of AA, whereas it is interesting to notice that both, TAT1 and XPCT, were able to mediate the transport of thyroid hormone triiodothyronine (T_3) (Verrey, Ristic et al. 2005).

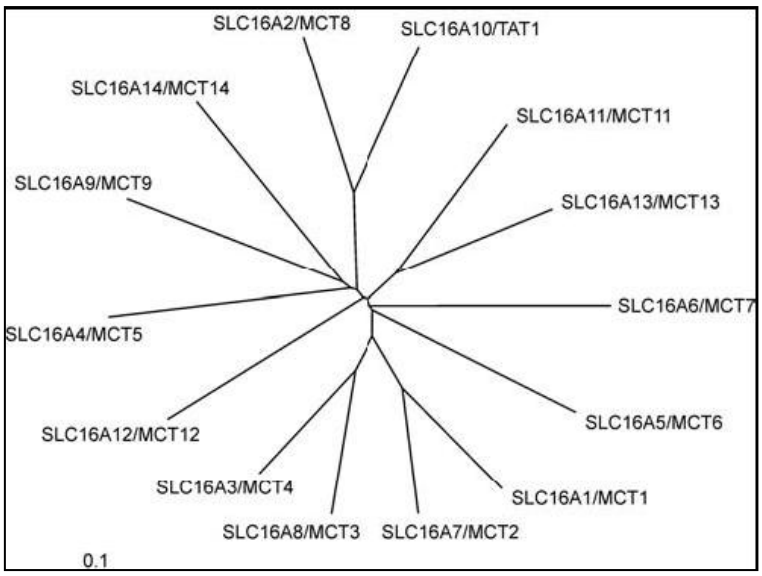

Fig. 12: Predicted phylogeny of SLC16 gene family. *tat1 (Slc16a10)* and *mct8 (Slc16a2)* share 50% of homology. (Halestrap and Meredith 2004).

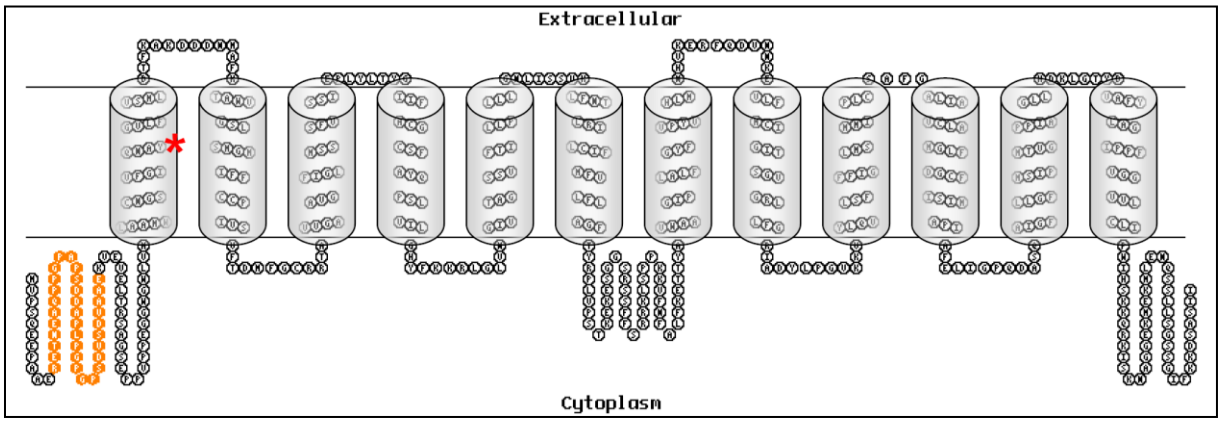

Fig. 13: Predicted topology of TAT1 with point mutation of *tat1*$^{-/-}$ in position 88 (asterisk). 12 transmembrane domains with intracellular N- and C- termini were predicted based on its AA sequence (Kim, Kanai et al. 2001) and on the predicted structure of MCT4 (Wilson, Meredith et al. 2005). The N-terminus presents a PEST sequence (orange).

3.2.6 The SLC43 gene family

The SLC43 gene family comprises 3 members: *lat3* (*Slc43a1*), *lat4 (Slc43a2)* and *eeg1* (*Slc43a3*) (Hediger, Romero et al. 2004; Broer 2008). When expressed in the oocyte heterologous system, *lat3* and *lat4* mediated the facilitated transport of several neutral AAs, being however structurally different from other L-system transporters (Stuart, Pavlova et al. 2001). *lat3* mRNA expression was confined to pancreas, skeletal muscles and liver (Babu, Kanai et al. 2003), whereas *lat4* seemed to be expressed in kidney nephron and small intestine (Bodoy, Martin et al. 2005). *eegl1* is an orphan transporter mostly expressed in fetus starting at embryonic day 7 but not during adulthood (Hediger, Romero et al. 2004). Furthermore *eegl1* has not show amino acid transport properties so far.

3.2.7 Amino acid transporters

The knowledge about the transport of AAs has evolved trough the past decades. Already at the beginning of 1900, Van Slyke and Meyer showed that AAs were absorbed from the blood to the tissues against a concentration gradient (Slyke and Meyer 1913). Afterwards, the pioneering work of Christensen in the early 1960 on tissue and cells, Heini Murer in the 1970 in membrane vesicles and Stevens in the 1980 allowed the classification of transport systems that were based on the physicochemical properties, stereospecificity, inhibition and selectivity (Christensen and Oxender 1960; Murer, Evers et al. 1976; Stevens, Ross et al. 1982; Christensen 1990). Thus 3 distinct systems were found: 1) system that prefer Leu and large hydrophobic neutral AA (system L), 2) system that prefer Ala and small and polar neutral AA (system A) and 3) system that prefer Ala, Ser and Cys (system ASC) (Broer 2008) (Tab. 3). An attempt to simplify the nomenclature was suggested in 1984, when the symbols y^+, x^- and ^{0} were proposed for basic, acidic and neutral transport systems and with additional letters indicating the substrate specificity. Sodium dependence was usually indicated by capital letter, although the previously characterized Na-independent system L was not modified (Broer 2008).

In the 1990s the molecular identification and the cellular expression of the transporter has been possible. Thus, a further step in the characterization of the transport systems has been made (Kanai and Hediger 1992; Palacin, Estevez et al. 1998; Hediger, Romero et al. 2004; Verrey, Singer et al. 2009). Usually, the system nomenclature was then followed by AT for AA transporter and a number for the different variants (e.g. Lat4; common names in Tab. 3). In particular, their function was studied in the heterologous *Xenopous laevis* expression system, by the injection of cRNA in the frog oocytes and by performing uptake and efflux studies with radiolabelled substrates. It has therefore also been possible to classify the AA transporters according to the SLC nomenclature (see 3.2.4, Tab. 3), which would be more preferable than the previous classification in systems that remained somehow inconsistent (Broer 2008). Furthermore, many AA transporters were localized by mean of specific antibodies. Lately, a few years ago, the function of AA transporters has been further analyzed by

the determination of the protein structures (Verrey, Singer et al. 2009). However, the knowledge about the AA transporter cooperation has been slowed down by several technical difficulties such as the overlapping selectivity, the lack of selective inhibitors, the transport nature of obligatory and symmetrical exchangers (Verrey, Ristic et al. 2005). Although AA transport takes place in all cells of the body, the most well characterized transport machinery is the one of the mammalian kidney and intestine. Therefore, the AA transporters were also divided accordingly to their contribution to the apical uptake, basolateral efflux, housekeeping function or presence in other tissues (Tab. 3).

Transport	SLC Name	Common Names	Luminal Substrates	Other Transported Species
Apical Uptake		**(System X_{AG})**		
(1)	SLC1A1	EAAT3 EAAC1	Anionic (or acidic) amino acids (Glu and Asp)	Cotransports 2 Na^+ and 1 H^+ inward, exchanges 1 K^+ outward (electrogenic uptake of net + charge)
(2)	Heterodimer: SLC7A9 SLC3A1	(System b^{0+}) $b^{0+}AT$ rBAT	Cationic (i.e., basic) amino acids (Lys^+ or Arg^+) or cystine (Cys-S-S-Cys)	Exchanges for neutral amino acid (electrogenic uptake of + charge when substrate is Lys^+ or Arg^+)
(3)	SLC6A18-20	(System B or B^0) B^0AT1	Neutral amino acids (not Pro), including aromatic amino acids (Phe, Trp, Tyr)	Cotransports with Na^+
(4)	SLC36A1	PAT1	Pro, Ala, Gly, and imino acids Cytoplasmic substrates	Cotransports with H^+ Other transported species
Basolateral Efflux				
(1)	Heterodimer: SLC7A7 SLC3A2	(System y^+L) y^+LAT1 4F2hc	Cationic (i.e., basic) amino acids (Arg^+, Lys^+, ornithine$^+$, His???)	Exchanges for extracellular neutral amino acid plus Na^+ (electrogenic uptake of + charge)
(2)	SLC16A10	TAT1	Aromatic amino acids (Phe, Trp, Tyr)	None (facilitated diffusion)
(3)	Heterodimer: SLC7A8 SLC3A2	(System L) LAT2 4F2hc	Neutral amino acids	Exchanges for neutral extracellular amino acid
(4)		(System ASC)	Ala, Ser, Cys, Thr	Exchanges for extracellular neutral amino acid plus Na^+ (electrogenic uptake of + charge)
(Apical in SI)	SLC1A4 SLC1A5	ASCT1 ASCT2	Basolateral substrates	Other transported species
Basolateral Uptake		(System N)		
(5)	SLC38A3	SNAT3	Gln, Asn, His	Cotransports Na^+ inward, exchanges H^+ outward
Amino Acid Transporters Present in Other Tissues				
	SLC1A2 SLC1A3 SLC1A6 SLC1A7	EAAT2, GLT-1 EAAT1, GLAST EAAT4 EAAT5	Anionic (or acidic) amino acids (Glu and Asp)	Cotransports 2 Na^+ and 1 H^+ inward, exchanges 1 K^+ outward (electrogenic uptake of net + charge)
	SLC6A1 SLC6A11 SLC6A12 SLC6A13	GAT1 GAT3 BGT1 GAT2	GABA (also betaine, β-alanine, taurine)	Cotransports Na^+ and Cl^-
		(System GLY)	Glycine (also *N*-methylglycine, i.e., sarcosine) Pro	Cotransports Na^+ and Cl^-
Basolateral membrane in small intestine	SLC6A9 SLC6A5 Pro	GLYT1 GLYT2 PROT (System A)		Cotransports Na^+ and Cl^-
Basolateral membrane in small intestine	SLC38A1,2,4 SLC38A3,5	SNAT1,2,4 (System N)	Gln, Ala, Asn, Cys, His, Ser Flu, His, Hln, Asn, Ser	Cotransports Na^+ Cotransports Na^+, exchanges H^+
Apical membrane in small intestine	SLC6A14	(System B^{0+}) ATB^{0+}	Neutral and cationic amino acids	Cotransports Na^+ and Cl^-

Tab. 3: Amino acid transporters. (Boron and Boulpaep 2005)

Several transport systems were identified through their involvement in the development of inherited disorders that displayed specific loss of AAs in the urine of patients (Verrey, Ristic et al. 2005; Broer 2008). Among those Hartnup disorder, Cystinuria, Lysinuric protein intolerance, Blue diaper syndrome and Glycinuria. The luminal transport of AA has been more extensively studied in the past. One of the key players is the broad neutral AA transporter B^0AT1 (SLC6A18), which transports the majority of free plasma AAs and whose defect causes the Hartnup disorder (Tab. 3 – 4, Fig. 14). Other known AA transporters are depicted in Fig. 14. The apical absorption of AA is driven by sodium or is proton mediated, thus it has been possible to measure their activity by electrophysiological approaches. Besides those luminal AA transporters, the di- and tri-peptide transporters, PEPT1 and PEPT2, exert a complementary role in the luminal AA uptake, in particular PEPT1, which is very important also in the intestine (Nassl, Rubio-Aliaga et al. 2011).

As illustrated in Tab. 4, the majority of the inherited disorders leading to aminoaciduria were attributed to a defective apical transport. Therefore, less is known about the contribution of the basolateral transporter. The difficulty to produce membrane vesicles for the functional studies and the electroneutral transport of the solutes further limits the investigation. In the past, many authors have simply referred to the exit from the epithelial cell as an unavoidable quick passage, which should not become the limiting step. However, compartmental analysis of the movement of Lys across the small intestine showed that the rate limiting step was the exit across the basolateral membrane (Cheeseman 1992). Furthermore, in order to preserve the cell, the basolateral membrane should not allow the total AA depletion but rather import nutrient from the blood in case of starvation. Thus, the basolateral membrane contains AA transporters important for the export but also housekeeping transporters that are found in other non-polarized cells (Fig. 14 and Tab. 3). It is well established that the two heterodimeric basolateral AA transporters, Lat2-4F2hc and y^+Lat1-4F2hc, cannot directly mediate the net efflux of AA from the basolateral membrane, because they are obligatory exchangers and thus require substrate for a 1:1 exchange (Fig. 14). It was postulated that one or more facilitated diffusion

pathway shall be present in the same membrane to allow the net efflux of at least some AAs that could then be exchanged for others (Verrey, Singer et al. 2009). It has also been shown with the *X. laevis* expression system that such a role can be mediated by *tat1* (*slc16a10*) and that indeed its co-expression allows the efflux of neutral AAs (Ramadan, Camargo et al. 2007). Furthermore, replacement of TAT1 by Lat4 and Lat2-4F2hc by Lat1-4F2hc, showed a similar functional cooperation. It became thus crucial to analyze the impact of the absence of those transporters *in vivo*, to better understand their functional cooperation.

	Kidney		Intestine			
Transporter	Apical	Basolateral	Apical	Basolateral	Disorder	cDNA
Neutral amino acids	+		+		Hartnup disorder	B^0AT1
Cationic amino acids, cystine	+		+		Cystinuria	rBAT/$b^{0,+}$AT
Cationic amino acids		+		+	Lysinuric protein intolerance	4F2 hc/y^+LAT1
Cationic amino acids	+		+		Hyperdibasic aminoaciduria	?
Tryptophan				+	Blue diaper syndrome	TAT1 (candidate)
Methionine, BCAA	+ (?)		+		Methionine malabsorption	?
Anionic amino acids	+		+		Dicarboxylic aminoaciduria	EAAT3 (candidate)
Glycine, proline, hydroxyproline	+		+		Iminoglycinuria	PAT1 (candidate) IMINO (candidate) PAT2 (candidate)
Glycine	+				Glycinuria	XT2 (candidate)
β-Amino acids	+				No transport defect reported	D-β-amino-isobutyrate:pyruvate aminotransferase

Tab. 4: Transport systems defined by inherited aminoacidurias. Most of the defects were attributed to the apical membrane transporters (Broer 2008).

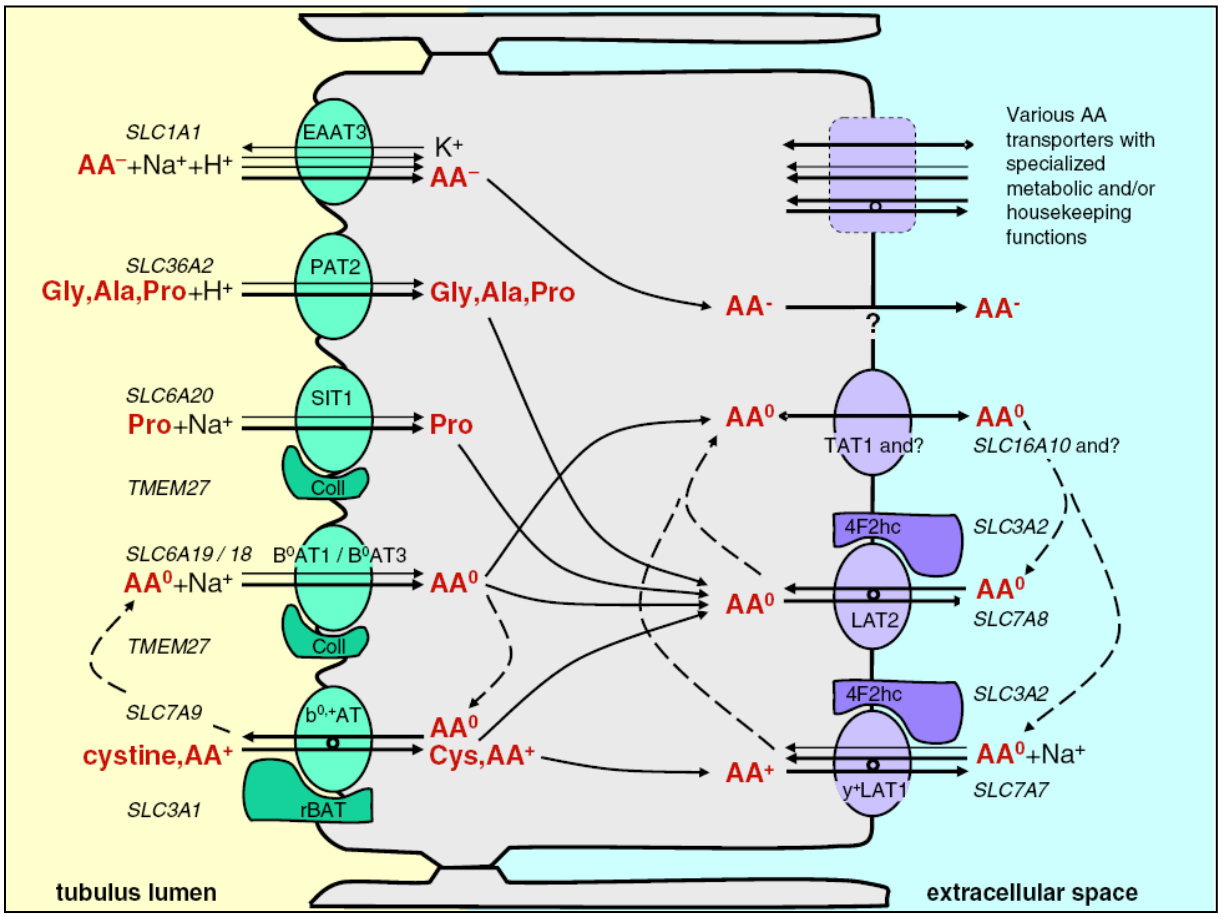

Fig. 14: Cellular model of a kidney proximal tubule cell with the different apical and basolateral AA transporters. SLC and common names are depicted. Transported AAs are labeled in red (AA^- means anionic AA, AA^0 neutral and AA^+ cationic). (Verrey, Singer et al. 2009).

4. Material and Methods

Luca Mariotta performed all the experiment described in this work, except for the microSPECT (4.1.7) that was done by Tony Lahoutte and Simone Camargo in the In vivo Cellular and Molecular Imaging Center Brussels. Furthermore *lat4*$^{-/-}$ characterization (6.2.2) was partially done by Dong Wang and protein analysis under protein diet study (5.3.1) was done by Marta Torrente. Several experiments were done by Luca Mariotta in collaboration with Dustin Singer Brigitte Herzog and Adriano Guetg.

4.1 Mice work

4.1.1 tat1$^{-/-}$ mouse

The *tat1* knock out mouse model was produced by Ingenium Pharmaceuticals AG (Germany) using the ENU (N-ethyl-N-nitrosurea) mutagenesis (Augustin, Sedlmeier et al. 2005; Keays, Clark et al. 2006). The nonsense mutation in the *tat1* gene leads to a premature stop at position 88 (Y88*). The mice were backcrossed 10 times in a C57Bl/6J inbred strain (Charles River, Germany), which was the background of the parental female, whereas the mutagenized sperm was C3HeBFeJ. Accordingly to the international ILAR News (1992) nomenclature the mice were named *B6;C3-(Slc16a10)mEug3(Y88*)Ingm.*

4.1.2 *lat4*$^{-/-}$ mouse

The *lat4* knockout mice (*lat4*$^{-/-}$) were generated at the Phenogenomic center of Toronto (http://www.phenogenomics.ca/). The mice were named accordingly to the ILAR identification *B6;129-(SLC43A2)Gt(IST13572E12)Tigm*. Cells of a repository clone (CMHD-GT_258C1) were identified to truncate *lat4* gene at the 6th intron with the insertion of a gene trap allele (UPA), as

described elsewhere (Shigeoka, Kawaichi et al. 2005). The ES cells were prepared for aggregation with diploid embryos to produce chimeric mice. R1 cells were in a 129 background, whereas germline testing was performed by crossing the chimera to CD-1 mice and assessing coat color. Subsequent breeding into C57BL/6 for the generation of F1 mixed animals.

4.1.3 Tracking newborn development

Breeding were set and male then separated 1 or 2 weeks after. Females were controlled daily until delivery. Afterwards, the litter was controlled twice a day. The compactness of the nest, the color of the skin of the pups and the milk spot were used as control parameters. Pups were labeled by daily coloring the extremities with a lab marker (Precision Dynamics Corporation, Secureline, USA). Weight of the pups was recorded daily. Between day 5 and day 9 of life, part of the 3rd phalanx was cut and used for preparing gDNA with Phire Animal Tissue Direct PCR kit (Finnzymes, Thermo Scientific, CH) by using it accordingly to the manufacturer instruction.

4.1.4 Genotyping

tat1 were genotyped by a modified tetra primer arms PCR protocol (Ye, Dhillon et al. 2001). For the PCR reaction the following cycling profiles for Taq polymerase were used: 95°C 5 min; (95°C 60 sec; 60.8°C 60 sec; 72°C 60 sec) x 35; 72°C 2 min; 10°C pause. The amplicons were detected on a 4% agarose gel where 3 bands were visible: 226, 195 and 87 basepairs. In the *wt* only the 226 and 195 should be found, whereas the 226 and 87 for the *tat1*$^{-/-}$. In the heterozygote all bands should be present. 4 primers were used for *tat1*:

A: 5’- GGG ACC CTC GGA TGT CTC -3’

C: 5’- GTC GGT GTT TGG CAT CCA GAA CGC CAA A -3’

D: 5’- GTG TCC AGC ATG GAC ACG AAG AGC ACC TGC -3’

E: 5’- GGC CAT GTT GTC ATC GTC CTT GGC CTT GA -3’

lat4 were genotyped by conventional PCR exploiting the following cycling profile for Taq polymerase: 95°C 5 min; (95°C 30 sec; 62°C 30 sec; 72°C 30 sec) x 35; 72°C 2 min; 10°C pause. Two amplicons should be detected in the heterozygote: 366 and 512 basepairs. The 366 bp band represent the *wt* allele and the 512 the *lat4* knock out allele. The following primers were used for *lat4*:

WTF1: 5'- CTT CAT GAA TGG GTG AAT CTG CTC T -3'

WTR1: 5'- TAC AAC TGC AGG GGA TTC TAG TCC A -3'

MUTR1: 5'- ACC TGA AAT GAC CCT GTG CCT TAT T -3'

4.1.5 Different protein diets and metabolic cages

10 week old *tat1*$^{-/-}$ and *wt* littermate mice were fed sequentially with a normal protein diet (20% casein rich) followed by 8 days of high protein diet (40% casein rich). The modified standard diet AIN93G (Reeves, Nielsen et al. 1993) was maintained isocaloric by adjusting the starch content (Kliba-Nafg, Switzerland). Chow was put as pellet directly in the normal cages or reduced to powder for the metabolic cage experiment. Mice were daily weighed and put into metabolic cages (Tecniplast, Buguggiate, Italy) every third day from 0830 to 1630 to adapt, and 24 hours (0830-0830) at the end of each diet period. At the end of the 24 hours, urine and feces were collected and food and water consumption recorded. Urinary pH was measured using a pH microelectrode (691 pH-meter, Metrohm). Urinary creatinine was measured by the Jaffe method (Seaton and Ali 1984). Urinary and plasma urea were measured using the diacetyl monoxime method (Wybenga, Di Giorgio et al. 1971). Urinary electrolytes (Na^+, K^+, Ca^{2+}, Mg^{2+}, Cl^-, $SO42^-$) were measured by ion chromatography (Metrohm ion chromatograph, Switzerland). Blood was collected through a single tail tip cut into Na-heparinized micro-haematocrit-tubes (Provet AG, Switzerland) and plasma collected after centrifugation at 6000 g at 4°C. After animal sacrifice, organs were harvested, frozen in liquid Nitrogen and stored at -80°C. For amino acid measurements, organs were lysed using MagNa Lyser

Green Beads (Roche, Switzerland) in PBS supplemented with 1ul/ml Protease Inhibitor Cocktail (Sigma, Switzerland), in a ratio of wet weight to PBS volume of 1:3. Supernatant was collected after two 15'000 g centrifugations for 15' at 4°C.

4.1.6 RotaRod Test

Mice were put on a rotating drum with an accelerating (day 1, 6 to 60 rpm) or fixed speed (day 2, average speed reached on day 1) (Sugiura, Kitagawa et al. 2005) (Ugo Basile, model 47600, Italy, courtesy of Dawid Wolfer lab). The time at which the animal drops off the drum was measured (maximal testing time: 300 s). Five trials were performed on each day. The average value of 4 different attempts was calculated.

4.1.7 Micro-SPECT

The analysis was performed in the In vivo Cellular and Molecular Imaging Center Brussels as before (Lahoutte, Caveliers et al. 2002; Lahoutte, Mertens et al. 2003; Lahoutte, Caveliers et al. 2004; Bauwens, Lahoutte et al. 2007; Vanhove, Defrise et al. 2011). Briefly, 30 minutes after i.v. injection of either 2-^{123}I-L-Phe or 2-^{125}I-L-Phe (courtesy of ICMIC, Brussel), animals were anesthetized and their blood and organs collected. The activity was counted with a gamma counter. Animals injected with 2-^{123}I-LPhe could be anesthetized and imaged with a micro-SPECT (e.cam 180, Siemens) and a micro-CT (Skyscan 1178, Skyscan, Belgium). Images were processed with the AMIDE 0.9.1 software (Loening and Gambhir 2003).

4.1.8 GFR measurement

Inulin clearance as measurement of the glomerular filtration rate (GFR) has been accordingly to Sällstrom and co-workers protocol (Sallstrom, Carlstrom et al. 2010). Briefly, animals were restrained and a 200 µL bolus injection of ^{3}H-methoxy-inulin (ART0278, American Radiolabeled Chemicals Inc., USA) performed in the tail vein. The ^{3}H-methoxy-inulin was priory divided into 5 µCi aliquots as decribed elsewhere (Shalmi, Lunau et al. 1991) in order to minimalise breakdown and consequent overestimations (Shalmi, Lunau et al. 1991). 5 µL tail vein blood was collected into heparinized

capillaries at different time points and plasma activity counted with scintillation counter. The clearance was calculated with the total AUC as described elsewhere (Qi, Whitt et al. 2004).

4.1.9 Kidney microdissection

All the procedures were performed by Dustin Singer as done before (Dustin Singer Diploma Thesis). Briefly, the mouse was anesthetized and ligations of abdominal aorta and vena cava twice posterior to kidney and once anterior to kidney prepared. After closure of the lowest ligation and after clamping of the abdominal aorta between kidney and ligation, a catheter was inserted in the aorta and legated. The clamp was opened, the renal artery cut and animals sequentially perfused with 8 ml DMEM/F12 and 8 ml DMEM/F12 supplemented with liberase (57.14 µl in 10 ml). Afterwards, kidneys were excised, cut and further incubated in the DMEM/F12 liberase solution for 40 min. After three times washing with ice cold DMEM/F12 supplemented with BSA (300µg/ml), the segments were microdissected under binocular in the same washing solution. The collected tubules were put into 300 µl RLT Buffer and snap frozen in liquid nitrogen. mRNA was then extracted with RNeasy-Micro Kit (Quiagen) with a final elution of 14 µl of water.

4.1.10 Everted gut sacs

Uptake on first 2/3 of proximal small intestine segments of radiolabeled L-Phe and D-mannitol was performed as described elsewhere (Nassl, Rubio-Aliaga et al. 2011)). Briefly, everted gut sacs were incubated for 10 minutes at 37°C in bubbling (Oxycarbon) Krebs-Tris buffer (pH 7.4) containing 100 µM L-Phe, 0.5 µCi ^{3}H-L-Phe/mL (Hartmann Analytic, Germany), 0.02 µCi ^{14}C-D-Mannitol/mL (ARC, USA). After brief washing, sacs were cut open and content activity counted. Sacs were further dried at 55°C O/N on cellulose (Sartorius AG, Germany) and weighed. The sacs were lysed in Solvable (Perkin Elmer, Switzerland) for 6 hours at 50°C, bleached with 200µl of 30% H_2O_2, and the radioactivity was determined by liquid scintillation in 15 ml of Ultima Gold (Perkin Elmer, Switzerland). Amino acid transport was expressed relative to the dry tissue weight.

4.2 Other Analysis

4.2.1 Amino acids measurement

Ice-cold methanol deproteinization of samples was performed as described elsewhere(Suresh Babu, Shareef et al. 2002). Deproteinized samples or mouse urine were then derivatized using AccQ Tag (Waters, Milford, USA) and analyzed on an Acquity UPLC (Waters) according to the manufacturer's instructions by the Functional Genomics Center Zurich (FGCZ) (Cohen and De Antonis 1994). Urinary creatinine was measured by the Jaffe method (Seaton and Ali 1984).

4.2.2 Immunofluorescence and Real-time Quantitative PCR

For *tat1* immunofluorescence, the polyclonal anti-mTAT1 antibody was used as previously described (Ramadan, Camargo et al. 2006). For *lat4*, a new polyclonal rabbit anti-mLat4 (Pineda, DE) was generated against the C-terminal of Lat4 protein (immunizing peptide sequence: NH2-CQLQQKREDSKLFL-CONH2) and affinity purified in SulfoLink column accordingly to the manufacturer instructions (Thermo Scientific, USA). B^0AT1 antybodies were described before (Romeo, Dave et al. 2006; Singer, Camargo et al. 2009). For immunofluorescence the tissues were processed as described elsewhere (Rossier, Meier et al. 1999). Briefly, tissues were 5-7 µm cut with a cryotome (Leica, DE) and post fixed in cold MeOH for 90 s. Antigen was retrieved with a microwave eating in 10mM Na-Citrate pH 6.0 at 98°C for 10 min. Primary antibody were diluted 1:600 or 1:1000 and incubated overnight at 4°C, whereas secondary 1:500 and incubated for 2 hours at RT.

The mRNA was extracted with RNeasy kit (Qiagen, USA) and quantified with TaqMan kit (Applied Biosystems, USA) as described before (Ramadan, Camargo et al. 2006). 1 ng of cDNA was loaded in each reaction, in a final volume of 20 µl.

4.2.3 Statistics

Statistical analysis was performed using GraphPad Prism 5.0 (GraphPad Software, USA) and R 2.14 (R Foundation of Statistical Computing). Unless mentioned otherwise, between-group comparisons were performed by Student's unpaired t-test or by repeated-measures one-way analysis of variance, followed by Bonferroni posttest. Statistical significance was accepted at $P < 0.05$ or as indicated. Data are presented as means ± SEM.

5. *tat1* Mouse Model

5.1 Introduction

As discussed in the general introduction of this work (see 3.2.7), since the two well-known basolateral AA transporters, Lat2-4F2hc and y^+Lat1-4F2hc, are obligatory exchangers they cannot directly contribute to the net basolateral efflux of AA in the epithelia. Thus, one or more facilitated diffusion pathway shall be present in the same membrane to allow the net efflux of at least one AA that could then be exchanged for others (Verrey, Singer et al. 2009). Previous work of Tamara Ramadan and co-workers clearly show that such a role can be mediated by the aromatic AA transporter TAT1 (Slc10a16): the co-expression of the facilitated diffusion pathway TAT1 and the exchanger Lat2-4F2hc in the *Xenopus* laevis oocyte allowed the net efflux of several neutral AAs (Ramadan, Camargo et al. 2007). It was also shown that the two transporters co-localize in the same basolateral membrane of kidney proximal tubule cells and small intestine enterocytes. Thus, to better understand the role of *tat1 in vivo* in the epithelial efflux of AAs and to quantify its contribution to the basolateral transport machinery, a *tat1* knock out mouse (*tat1*$^{-/-}$) has been generated. The mouse was produced by Ingenium Pharmaceuticals AG by random mutagenesis with the introduction of a premature stop codon (Y88*) as depicted in Fig. 13 in 3.2.5 and M&M 4.1.1 for details. Therefore, the first question was about the role of *tat1* in the epithelia in the context of the whole AA transport machinery. Furthermore, we investigated whether *tat1* does impact on the neurological function, since it transports important precursors of neurotransmitters. Last, we controlled whether *tat1* does impact on the systemic aromatic AA homeostasis.

The results concerning the work on *tat1*$^{-/-}$ are summarized in an original research article that is presented in the next section (5.2). Further data that were not shown in the manuscript are reported afterwards, in the addendum section (5.3).

5.2 Original research article: "T-type amino acid transporter TAT1 (Slc16a10) is essential for extracellular aromatic amino acid homeostasis control"

This manuscript summarizes the major finding about the characterization of the *tat1* knock out mouse. The first major discover is the role mediated by *tat1* in the flux of aromatic AA between plasma and liver, which in turn contributes to the control the aromatic AA homeostasis: when this is impaired the liver cannot anymore work as sink and thus aromatic AA accumulates in the blood. The second major issue is the role of *tat1* in the epithelia. When TAT1 is missing there is not a major loss of AAs, when a normal diet is provided. Under high protein diet a spillover of neutral AAs in the urine is found, suggesting for the functional cooperation of TAT1 and Lat2-4F2hc. In the small intestine the transport is less affected by the lack of *tat1*. The last founding is the experimental proofs for an intracellular accumulation of AAs after *tat1* depletion, which in turn blocks the apical import and results in AAs losses in the urine. The mild phenotype displayed by *tat1* knock out mice also revealed that there must be at least another transporter that compensates TAT1 absence.

The manuscript was submitted to the The Journal of Physiology on June 7th 2012.

T-type amino acid transporter TAT1 (Slc16a10) is essential for extracellular aromatic amino acid homeostasis control*

Luca Mariotta[1], Tamara Ramadan[1], Dustin Singer[1], Adriano Guetg[1], Brigitte Herzog[1], Claudia Stoeger[2], Manuel Palacín[3], Tony Lahoutte[4], Simone M.R Camargo[1] and François Verrey[1]

[1] Institute of Physiology and Zürich Center for Integrative Human Physiology (ZIHP), University of Zürich, Switzerland, [2] Ingenium Pharmaceuticals AG, Martinsried, Germany, [3] Institute for Research in Biomedicine (IRB Barcelona), Barcelona, Spain, [4] In Vivo Cellular and Molecular Imaging Laboratory, Vrije Universiteit Brussel, Brussels, Belgium

*Running title: Aromatic amino acid transport and homeostasis

To whom correspondence should be addressed: François Verrey, Institute of Physiology, University of Zurich, Winterthurerstrasse 190, CH-8057 Zurich, Switzerland, Tel.: +41 44 635 5044/46, Fax: +41 44 635 68 14, E-mail: verrey@access.uzh.ch

Keywords: liver; epithelial transport; basolateral membrane; lat4; microSPECT/CT

Background: The amino acid transporter TAT1 (Slc16A10) mediates facilitated diffusion of aromatic amino acids across membranes.
Results: TAT1 null mice lack liver control of aromatic amino acids and display altered epithelial amino acid transport.
Conclusion: TAT1 plays a central for the control body aromatic amino acid homeostasis.
Significance: Equilibrative essential amino acid membrane transport controls amino acid homeostasis

SUMMARY

The uniporter TAT1 (Slc16a10) mediates the facilitated diffusion of aromatic amino acids across basolateral membranes of kidney, small intestine and liver epithelial cells and across the plasma membrane of non-epithelial cells like skeletal myocytes. Its role for body amino acid homeostasis was now investigated using newly generated TAT1 (Slc16a10) defective mice (*tat1*$^{-/-}$). These mice grow and reproduce normally, show no gross phenotype and no obvious neurological defect. Histological analysis did not reveal abnormalities and there is no compensatory change in any tested amino acid transporter mRNA. TAT1 null mice display however increased plasma, muscle and kidney aromatic amino acid concentration under both normal and high protein diet, although this concentration remains normal in liver. A major aromatic aminoaciduria and a smaller urinary loss of all substrates additionally transported by L-type amino acid antiporter Lat2-4F2hc (Slc7a8) were revealed under high protein diet. This suggests an epithelial transport defect as also shown by the accumulation of intravenously injected ^{123}I-2-I-L-Phe in kidney and of ^{3}H-L-Phe in ex vivo everted gut sac enterocytes. Taken together, these data indicate that the uniporter TAT1 is required to equilibrate the concentration of aromatic amino acids across specific membranes. For instance, it enables hepatocytes to function as sink that controls the extracellular aromatic amino acid concentration. Additionally, it facilitates the release of aromatic amino acids across the basolateral membrane of small intestine and proximal kidney tubule epithelial cells, thereby driving the efflux of other neutral amino acids via the parallel system L antiporter Lat2-4F2hc into the extracellular space.

Dietary and endogenous proteins are hydrolyzed in the gastrointestinal lumen to tri-peptides, di-peptides and individual amino acids (AAs) that are taken up by small intestine enterocytes (Nassl, Rubio-Aliaga et al.). These cells hydrolyze the oligopeptides into single AAs and also further metabolize some of them. Finally, they release most AAs into the portal circulation, thereby strongly influencing the rate of AA appearance in plasma (Cynober 2002; Wu 2009). It is noteworthy that the amount of free AAs transported daily from the enterocytes into the circulation is much larger than the free AA pool of the plasma and extracellular space (~100 g per day versus less than 10 g), such that their uptake into tissues is crucial for maintaining extracellular AA homeostasis (Cynober 2002). In

the cells of different organs, AAs may then serve as building blocks for the synthesis of structural and functional proteins, may be used for cellular metabolism or function as signaling molecules (Verrey, Singer et al. 2009; Wu 2009). Therefore, AA transfer across plasma membranes via various cooperating AA transporters plays a crucial role for body AA homeostasis and the defect of transporters leads to several diseases (Verrey, Singer et al. 2009; Broer and Palacin).

The best characterized basolateral AA transporters of the small intestine and proximal kidney tubule (re)absorbing epithelia are the abundant Lat2-4F2hc (Slc7a8) and y^+Lat1-4F2hc (Slc7a7) that function as obligatory exchangers (antiporters). Thus, they do not mediate net AA transport, but are suggested to perform the directional transport of all their substrate AAs in exchange for AAs that can be recycled across the membrane by parallel transporters able to mediate a directional flux (Pfeiffer, Rossier et al. 1999; Rossier, Meier et al. 1999; Meier, Ristic et al. 2002; Fernandez, Torrents et al. 2003; Verrey 2003; Verrey, Singer et al. 2009). The role of Lat2-4F2hc has been recently investigated *in vivo* using a *lat2* defective mouse (Braun, Wirth et al.). Its phenotype was mild, presenting an increase in several small neutral AAs in serum and a corresponding minor aminoaciduria. Based on this published data we estimate that the observed small urinary AA loss of *lat2* null mice is not due to a decreased fractional excretion of AAs and therefore does surprisingly not point to a substantial epithelial AA transport defect (Braun, Wirth et al.). Interestingly, aromatic amino acids (AAAs) were not elevated in the serum of *lat2* null mice, suggesting that another AA transporter plays here a dominant role, possibly the T-type aromatic AA transporter TAT1 (Slc16a10) which was found slightly upregulated in the kidney of *lat2* null animals. This transporter was molecularly identified and first characterized in 2001 by Endou and coworkers (Kim, Kanai et al. 2001). In a later study, we have demonstrated using the *Xenopus laevis* oocyte expression system that TAT1 functions as a facilitated diffusion pathway which mediates the transport of AAAs L-Phe, L-Trp and L-Tyr with symmetric low apparent affinities, for instance with a $K_{0.5}$ of approximately 30 mM for L-Phe influx and efflux (Ramadan, Camargo et al. 2006). Interestingly, TAT1 protein was shown to co-localize in the kidney proximal tubule with the two exchangers mentioned above (Ramadan, Camargo et al. 2007) and also to localize to the basolateral membrane of small intestine enterocytes and the sinusoidal membrane of perivenous hepatocytes (Ramadan, Camargo et al. 2006). The analysis of *tat1* mRNA expression by real time PCR revealed its presence in the epithelial tissues mentioned above and also in muscles and brain (Ramadan, Camargo et al. 2006). Finally, it was demonstrated that AAAs effluxing via TAT1 can be recycled into the cell by the exchanger Lat2-4F2hc and thereby drive the efflux of other intracellular neutral AAs that are substrates of Lat2-4F2hc (Ramadan, Camargo et al. 2007). To investigate the role that TAT1 plays in whole body AA homeostasis maintenance and in epithelial AA transport, we generated a TAT1 knock out (*tat1*$^{-/-}$) mouse and present here its first characterization.

EXPERIMENTAL PROCEDURES

The *tat1* knock out mouse model was produced by Ingenium Pharmaceuticals AG (Germany) using ENU (N-ethyl-N-nitrosurea) mutagenesis (Augustin, Sedlmeier et al. 2005; Keays, Clark et al. 2007). The nonsense mutation in the *tat1* gene leads to a premature stop at position 88 (Y88*). The mice were backcrossed 10 times in a C57Bl/6J inbred strain (Charles River, Germany), which was the background of the parental female, whereas the mutagenized sperm was C3HeBFeJ. All animals were housed in standard conditions in normal light cycle and fed a standard diet prior to experiment. All procedures for mice handling were according to the Swiss Animal Welfare laws and approved by the Kantonales Veterinäramt Zürich.

Immunofluorescence and real-time PCR. The anti-mTAT1 antibody used has been previously characterized (Ramadan, Camargo et al. 2006) and tissues were processed as described elsewhere (Rossier, Meier et al. 1999). mRNA was extracted and quantified as described before (Ramadan, Camargo et al. 2006).

RotaRod Test. Mice were put on a rotating drum with an accelerating (day 1, 6 to 60 rpm) or fixed speed (day 2, average speed reached on day 1) (Ugo Basile, model 47600, Italy) (Sugiura, Kitagawa et al. 2005). The time at which the animal drops off the drum was measured (maximal testing time: 300 s). Five trials were performed on each day. The average value from 4 different experimental days was calculated.

Different protein diets and metabolic cages experiments. Ten week old *tat1*$^{-/-}$ and *wt* littermate mice were fed sequentially with a normal protein diet (20% casein) followed by 8

days of high protein diet (40% casein). The modified standard diet AIN93G was maintained isocaloric by adjusting the starch content (Kliba-Nafg, Switzerland). Chow was put as pellet directly in the normal cages or reduced to powder for the metabolic cage experiment. Mice were daily weighed and put every third day into metabolic cages (Tecniplast, Buguggiate, Italy) from 08:30 to 16:30 to adapt, and 24 hours (08:30-08:30) at the end of each diet period. At the end of the 24 hours, urine and feces were collected and food and water consumption recorded. Urinary pH was measured using a pH microelectrode (691 pH-meter, Metrohm). Urinary creatinine was measured by the Jaffe method (Seaton and Ali 1984). Urinary and plasma urea were measured using the diacetyl monoxime method (Wybenga, Di Giorgio et al. 1971). Urinary electrolytes (Na^+, K^+, Ca^{2+}, Mg^{2+}, Cl^-, SO_4^{2-}) were measured by ion chromatography (Metrohm ion chromatograph, Switzerland). Blood was collected through a single tail tip cut into Na^+-heparinized micro-haematocrit-tubes (Provet AG, Switzerland) and plasma collected after centrifugation at 6000 g at 4°C. After animal sacrifice, organs were harvested, frozen in liquid nitrogen and stored at -80°C. For AA measurements, organs were lysed using MagNa Lyser Green Beads (Roche, Switzerland) in PBS supplemented with 1 µl/ml Protease Inhibitor Cocktail (Sigma, Switzerland), in a ratio of wet weight to PBS volume of 1:3. Supernatant was collected after two 15'000 g centrifugations for 15 minutes at 4°C.

Amino acids measurement. Ice-cold methanol deproteinization of samples was performed as described elsewhere (Suresh Babu, Shareef et al. 2002). Deproteinized samples or mouse urine were then derivatized using AccQ Tag (Waters, Milford, USA) and analyzed on an Acquity UPLC (Waters) according to the manufacturer's instructions by the Functional Genomics Center Zurich (FGCZ) (Cohen and De Antonis 1994). The *tat1*$^{-/-}$ plasma AA ratios represented in Fig. 3B were normalized to the *wt* ones that were measured within the same diet and that are directly depicted in Fig. 3A. The same procedure was used to obtain the normalized urinary values depicted in Fig. 5B.

Micro-SPECT/CT imaging and biodistribution analysis. Imaging and biodistribution of the aromatic amino acid analog ^{123}I-2-I-L-Phe was performed in *wt* and *tat*$^{-/-}$ mice. ^{123}I-2-I-L-Phe was synthetized as decribed before (Bauwens, Lahoutte et al. 2007). Animals injected with ^{123}I-2-I-L-Phe were anesthetized and imaged 30 min after i.v. injection with a micro-SPECT (e.cam 180, Siemens) and a micro-CT (Skyscan 1178, Skyscan, Belgium) system as described before (Lahoutte, Caveliers et al. 2002; Lahoutte, Mertens et al. 2003; Lahoutte, Caveliers et al. 2004; Bauwens, Lahoutte et al. 2007; Vanhove, Defrise et al.). Images were visualized with the AMIDE 0.9.1 software, where MicroCT is represented in gray scale and MicroSPECT in NIH color scale (Loening and Gambhir 2003). After imaging, animals were sacrificed and dissected. All major organs and tissues were collected and counted in a gamma camera counter (Canberra, Belgium) and expressed as percentage of injected activity per gram of organ or tissue.

Everted gut sacs. Uptake on first 2/3 of proximal small intestine segments of radiolabeled L-Phe and D-Mannitol was performed as described elsewhere (Nassl, Rubio-Aliaga et al.). Briefly, everted gut sacs were incubated for 10 minutes at 37°C in bubbling (Oxycarbon) Krebs-Tris buffer (pH 7.4) containing 100 µM L-Phe, 0.5 µCi ^{3}H-L-Phe/mL (Hartmann Analytic, Germany), 0.02 µCi ^{14}C-D-Mannitol/mL (ARC, USA). After brief washing, sacs were cut open and content activity counted (serosa). Sacs were further dried at 55°C O/N on cellulose (Sartorius AG, Germany) and weighed. The sacs (tissue) were lysed in Solvable (Perkin Elmer, Switzerland) for 6 hours at 50°C, bleached with 200 µl of 30% H_2O_2, and the radioactivity was determined by liquid scintillation in 15 ml of Ultima Gold (Perkin Elmer, Switzerland). AA transport was expressed relative to the dry tissue weight.

Statistics. Statistical analysis was performed using GraphPad Prism 5.0 (GraphPad Software, USA) and R 2.14 (R Foundation of Statistical Computing). Unless mentioned otherwise, between-group comparisons were performed by Student's unpaired t-test or by repeated-measures one-way analysis of variance, followed by Bonferroni posttest. Statistical significance was accepted at $P<0.05$ or as indicated. Data are presented as means ± SEM.

RESULTS

A *tat1* knockout mouse (*tat1*$^{-/-}$) was produced by ENU mutagenesis (Ingenium Pharmaceuticals AG, Germany) in the context of the former European EUGINDAT project. The nonsense mutation (Y88*) was confirmed by DNA sequencing and the mice were backcrossed 10 times into C57Bl/6J background. Absense of *tat1* expression was confirmed using

immunofluorescence and mRNA analysis. The TAT1 protein was indeed not detected in any of the knock out samples tested (Fig. 1, B and D) and the *tat1* mRNA levels were decreased in all tested tissues, but in white adipose tissue (Suppl. Tab. 1a and b, *tat1*), presumably due to non-sense mediated decay (Maquat 1995).

Mild phenotype under normal conditions. *tat1*$^{-/-}$ pups grew normally and showed no visible phenotype when compared to their wild type (*wt*) littermates (Suppl. Fig. 1). Once adult, *tat1*$^{-/-}$ mice showed no body weight difference compared to *wt* (Tab. 1), they were fertile and gave birth to normal litters matching the expected mendelian distribution (data not shown). AAAs transported by TAT1 such as L-Trp and L-Tyr are known to be precursors of serotonine, catecholamines and thyroid hormone. Thus, the absence of TAT1 transporter could potentially impact on neurotransmitter and thyroid hormone availability and lead to neurological disorders. Although no gross behavioral change was observed, the motor activity and coordination skills of the mice were tested using a RotaRod test (Karl, Pabst et al. 2003), which however showed no difference between *tat1*$^{-/-}$ and *wt* littermates (Fig. 2). In an attempt to exacerbate a potential phenotype, the same experiment was carried out after subjecting the mice to a 7% casein diet for 5 days, without revealing any difference between the two groups (data not shown). In order to visualize a potential abnormal behavior, the animals were as well video recorded in their normal cage prior and after fasting (data not shown) and their feeding and drinking behavior recorded for 24 hours in metabolic cages (Tab. 1). Again, no difference was observed between *tat1*$^{-/-}$ mice and their *wt* littermates. A histological analysis of kidney, liver and intestinal segments on hematoxylin eosin stained sections did also not reveal any abnormality (Suppl. Fig. 2). A possible upregulation of other AA transporters was then investigated as compensatory mechanisms for TAT1 absence, but no significant change was noticed at the level of any tested AA transporter mRNA (Suppl. Tab. 1a and b). Also the carbohydrate metabolism did not appear to be perturbed, as indicated by a normal oral glucose tolerance test (Suppl. Fig. 3).

Altered homeostasis of aromatic amino acids. To assess the general impact of TAT1 absence on AA homeostasis, we measured the plasma concentration of proteinogenic AAs. Surprisingly, the AAA plasma concentration of *tat1*$^{-/-}$ mice was 2, 3 and 7.5 times higher than in wt for L-Phe, L-Trp and L-Tyr, respectively (Fig. 3B). In contrast, many other AAs were significantly diminished in *tat1*$^{-/-}$ plasma (i.e. Gly, L-Ala, L-Met, L-Ser, L-Thr, L-Asn, L-Gln, L-Lys and L-Arg). In view of the mild general phenotype observed under normal protein diet (20%), the animals were challenged for 8 days with a high protein diet (chow containing 40% of casein). This treatment did not significantly affect their body weight and, besides the expected high creatinine and urea excretion, only an increased fluid intake probably due to the texture of the chow was observed (Tab. 1 and Suppl. Tab. 2). *tat1*$^{-/-}$ mice displayed similar values as their *wt* littermates with a more pronounced effect on fluid intake. Upon switch to high protein diet, the plasma AAs remained stable in *wt* animals with the exception of the branched chain ones (BCAAs) that increased (Fig. 3A). In *tat1*$^{-/-}$ mice, the diet had a similar effect as in *wt* mice and maintained the peculiar pattern observed under normal diet: an elevated concentration of AAAs and a low concentration of all other AAs, except the BCAAs, which followed the dietary effect observed in the *wt* (Fig. 3B).

To further investigate the cause of the AA imbalance, free cytosolic AAs were measured in organs that represent the major reservoirs and metabolic sites: kidney, liver and skeletal muscles. The cellular concentrations of 5 representative AAs are depicted in Fig. 4. The AAAs L-Tyr and L-Trp displayed values strictly parallel to plasma in kidney and skeletal muscle. In contrast, in liver AAAs remained at the same lower concentration in *tat1*$^{-/-}$ as in *wt*. The organ concentrations of all non-aromatic AAs were similar in *tat1*$^{-/-}$ as in *wt* animals, as shown for L-Val and L-Leu (Fig. 4). One peculiarity is the high L-Phe values measured in kidney. This value might be related to the role of the kidney for the production of L-Tyr from L-Phe.

Altered epithelial amino acid transport. The analysis of 24 hours urine collected in metabolic cages showed that the dietary switch did not affect the AA excretion in *wt* animals (Fig. 5A). *tat1*$^{-/-}$ mice presented an aromatic aminoaciduria under normal protein diet that paralleled the high plasma values (Fig. 5B). However, under high protein diet, L-Tyr was found to be 64 times more abundant in *tat1*$^{-/-}$ than in *wt* urine and L-Trp and L-Phe, 95 and 9 times, respectively. Furthermore, many other neutral AAs were also present in higher amounts in *tat1*$^{-/-}$ urine (i.e. between 2 and 9 fold), including all other substrates of the Lat2-4F2hc broad selectivity

neutral AA exchanger. This indicates that under normal protein diet *tat1*$^{-/-}$ mice had an almost normal or only slightly increased fractional excretion of all AAs. In contrast, the high protein diet provoked in *tat1*$^{-/-}$ mice a high urinary excretion of AAs corresponding to a major increase of their fractional excretion. This decompensation of kidney AA reabsorption was selective, since all other measured urinary parameters did not display any significant difference between *tat1*$^{-/-}$ and *wt* control mice (Tab. 1).

Since TAT1 is expressed in the basolateral but not in the apical membrane of kidney proximal tubule, we hypothesize that the observed aminoaciduria might derive from an impaired basolateral export rather than from a defective apical import into epithelial cells. To verify this hypothesis, we used the isotopes ^{123}I-2-I-L-Phe and ^{125}I-2-I-L-Phe. These iodinated AAs are used as markers for oncologic imaging outside the brain, since their accumulation reflects the increased AA transport activity of cancer cells (Jager, Vaalburg et al. 2001; Lahoutte, Mertens et al. 2003). Their biodistribution has already been assessed and their validity demonstrated (Lahoutte, Caveliers et al. 2001; Lahoutte, Mertens et al. 2003; Lahoutte, Caveliers et al. 2004). When tested in the *Xenopus laevis* oocytes expression system, the compound (2-I-L-Phe) was shown to efficiently compete for L-Phe transport, whether mediated by TAT1, Lat4 (Slc43a2) or Lat2-4F2hc (Suppl. Fig. 4). Exploiting microSPECT/CT technique, the ^{123}I-2-I-L-Phe isotope was used for live imaging of its distribution 30 minutes after i.v. injection (Fig. 6). Indeed a higher accumulation of the compound was clearly detected in both kidneys of the *tat1*$^{-/-}$ mouse (Fig. 6B). This qualitative observation was verified by the quantification of the accumulated counts after sacrifice (n = 3; Fig. 6C).

Since as in kidney proximal tubule, TAT1 is also expressed in the basolateral membrane of epithelial cells along the small intestine (Ramadan, Camargo et al. 2006) (Suppl. Tab. 1), AA transport was measured in everted gut sacs. A significant accumulation of ^{3}H-L-Phe was observed in the enterocytes after 10 minute incubation at 37°C (Fig. 7). Also a tendency for decreased net transepithelial transport into the serosal compartment was observed. This data support the hypothesis that TAT1 absence reduces the transepithelial transport of AAAs by decreasing their basolateral efflux.

DISCUSSION

Although the lack of TAT1 does not prevent the normal development and fertility of mice, the study of the newly developed *tat1*$^{-/-}$ mouse revealed a number of important functions of this low affinity AAA uniporter that impact on body AA homeostasis. For instance, the disruption of TAT1 is shown to prevent the liver of playing its central role for the metabolism of AAAs. It is indeed well known that the accumulation of AAs as response to high protein diet is counteracted by an increase in liver AA catabolism (Moundras, Remesy et al. 1993). In particular, the liver is the major metabolic organ for the catabolism of AAAs (Schimassek and Gerok 1965; Brosnan 2003) and its failure causes an increase of AAAs in plasma (Fischer, Rosen et al. 1976; Brosnan 2003). This leads to a decrease of the BCAAs / AAAs ratio (Fischer ratio) and the consecutive increase of AAA uptake into the brain has been suggested to be a major cause of hepatic encephalopathy (James, Ziparo et al. 1979; Dejong, van de Poll et al. 2007). Here we show that plasma AAAs are stably elevated in *tat1*$^{-/-}$ mice regardless of the dietary load (Fig. 3). This increase is reflected in skeletal muscles, suggesting that TAT1 is not necessary for the AAA equilibration between plasma and this compartment (Fig. 4; Suppl. Tab. 1b). In contrast, in the liver of *tat1*$^{-/-}$ mice the intracellular AAA values are normal, indicating that the transport between the plasma that contains an elevated AAA concentration and this organ is uncoupled. The present data document that *tat1* mediates the equilibration of the extracellular AAA concentration with the hepatocytes and suggests that the liver functions as sink for the AAAs and thereby sets their concentration and controls their body homeostasis.

AAAs play important roles in the brain and both increased and decreased levels are thought to impair brain function, as mentioned above for the increase in AAAs due to liver failure that contributes to hepatic encephalopathy. An example in which a decreased level of AAAs leads to an alteration of brain functions is that of dietary L-Trp restriction that was shown in mice to result in altered emotional response to stress and increased locomotor activity (Uchida, Kitamoto et al. 2005). However, a more recent study did not find a correlation between L-Trp depletion, central serotonin reduction and affective behavioral changes (van Donkelaar, Blokland et al.). The lack of hepatic encephalopathy or behavioral disorders in *tat1*$^{-/-}$,

suggests that the AAA concentration within the brain is maintained by the intact blood brain barrier at a level that has no gross functional consequences. Because *tat1* is not expressed in mouse blood brain barrier, it is not likely that the protection of the brain of *tat1* null mice is due to the lack of *tat1* expression (Lyck, Ruderisch et al. 2009).

In the light of the mild phenotype and normal growth of *tat1*$^{-/-}$ mice, it appears that these mice maintain the capacity to absorb AAs from nutritional sources. This indicates that intestinal AA absorption and in particular the basolateral efflux of (aromatic) AAs from enterocytes is possible also in the absence of TAT1. Yet another cellular barrier that expresses TAT1 but in which this transporter appears to be dispensable in laboratory conditions is the placenta (Meredith and Christian 2008). Indeed, *tat*$^{-/-}$ fetus develop normally and *tat1*$^{-/-}$ female mice are normally fertile. We therefore tested whether some other transporters that could compensate for the lack of TAT1 would be induced. However, none of the other basolateral neutral AA transporters was found to be upregulated at the mRNA level in intestine and kidney, suggesting that the residual AAA transport capacity and potential paracellular transport can compensate for *tat1* absence under normal diet.

An important finding is the massive loss of AAAs and more discrete loss of all substrate AAs of the neutral exchanger Lat2-4F2hc in the urine of *tat1*$^{-/-}$ mice under high protein diet (Fig. 5). This aminoaciduria implies that the maximal transport capacity for these AAs was exceeded in kidney proximal tubule and reveals the role of TAT1 for epithelial amino acid transport. Furthermore, it is suggested that this (aromatic) AA loss explains the fact that the *tat*$^{-/-}$ mouse plasma AA concentration does not additionally change much under high protein diet. In our assay the urine was collected over 24 hours, whereas the blood was collected once (i.e. 3 hours after the switch to the inactive light phase). It is thus conceivable that under normal protein diet the AA transport rate is near the maximal transport capacity of the proximal tubule, already within the so-called splay, where some nephrons have not the capacity of reabsorbing all substrates. Since the plasma AA levels depend also on nutritional intake and are higher during the absorptive phase, under high protein diet a transient increase in blood AAs might cause the AA spillover. The urinary AA pattern (very high TAT1 substrates, increased Lat2-4F2hc substrates) is in line with the suggested functional cooperation of the uniporter TAT1 with the exchanger Lat2-4F2hc for the net efflux of neutral AAs, as previously shown in the *Xenopus laevis* expression system (Ramadan, Camargo et al. 2007). Interestingly, the loss of L-Phe in the urine was lower than that of L-Tyr and L-Trp. We hypothesize that this is due to the ability of another basolateral uniporter to transport L-Phe. Indeed, we have shown that Lat4 (Slc43a2) is also localized in the basolateral membrane of proximal kidney tubule cells and of small intestine enterocytes (Bodoy, Martin et al. 2005) (Mariotta, Guetg and Verrey unpublished data). This transporter was first described by Bodoy et al. in 2005 and shown to mediate the facilitated diffusion of BCAAs, L-Met and L-Phe and to a lesser extend L-Pro, L-Tyr and L-Trp. The presence of this other uniporter for essential amino acids and its selectivity might explain the differential urinary AAA pattern observed in *tat1*$^{-/-}$ mice (9-fold more L-Phe versus 64 and 95-fold more L-Tyr and L-Trp, respectively). Furthermore, Lat4 could to a large extent compensate for the absence of TAT1 in kidney and intestine and thus explain the mild phenotype of tat1$^{-/-}$ mice. The lack of Lat4 expression in the liver does on the other hand explain the fact that in the absence of *tat1* expression, the liver cannot function as sink for aromatic amino acids (Bodoy, Martin et al. 2005).

To verify that AAAs are efficiently imported luminally into transporting epithelial cells of *tat1*$^{-/-}$ mice, where they accumulate due to their inefficient basolateral export and consequently inhibit the apical transport, *in vivo* microSPECT/CT and *ex vivo* everted gut sac experiments were performed. The results confirmed the accumulation of tracers inside the epithelial cells (Fig. 6 and 7). However, the everted gut sacs experiments did not allow us to detect a significant difference in the net transcellular flux of L-Phe (Fig. 7: Serosa). This was due to a substantial residual permeability of the small intestine epithelium of tat1$^{-/-}$ mice for AAAs that might explain the normal growth of *tat1*$^{-/-}$ mice. This residual permeability is presumably due to a large extent to the contribution of the other uniporter Lat4, as mentioned above. We hypothesize however that a paracellular leak might also contribute to this permeability, as previously suggested for glucose and phosphate (Danisi and Murer; Pappenheimer 1993; Ballard, Hunter et al. 1995).

A defect in *tat1* has been predicted to be the cause of the blue diaper syndrome (Kim, Kanai et al. 2001; Broer 2008; Broer and Palacin). This syndrome was initially described by Drummond and co-workers in 1964 and appears to be caused by an excess of unabsorbed L-Trp in the intestinal tract (Drummond, Michael et al. 1964). We did not observe any symptom reminiscent of this syndrome in *tat1*$^{-/-}$ mice. Furthermore the amount of L-Trp found in the distal part of the small intestine was similar to *wt* (Suppl. Fig. 5) and much less than observed in Hartnup disorder (Singer and Verrey, unpublished results).

In summary, the analysis of *tat1*$^{-/-}$ mice confirmed that a complex machinery of AA transporters functionally cooperates for the absorption and distribution of dietary AAs. Our data further indicate that TAT1 exerts a major homeostatic function by equilibrating the concentration of AAAs between plasma and hepatocytes, where the AAAs are in turn catabolized. The functional impact of TAT1 absence becomes more evident under high protein diet, when the transport capacity of the kidney is exceeded such that a massive aromatic and also a neutral aminoaciduria appear that contributes in maintaining AA plasma homeostasis. We show that the aminoaciduria originates from an accumulation of AAs in the epithelial cells and we postulate that another basolateral uniporter, Lat4 (Slc43a2), compensates to a substantial extent for the lack of TAT1, in particular for driving the export function of the exchangers Lat2-4F2hc and y^+Lat1-4F2hc in small intestine and kidney proximal tubule.

Acknowledgments. The authors thank David Wolfer for his help in using the RotaRod and Hannelore Daniel for helpful discussions. This work was supported by the Swiss National Science Foundation grant 31-130471 to FV.

REFERENCES

1. Nassl, A. M., Rubio-Aliaga, I., Fenselau, H., Marth, M. K., Kottra, G., and Daniel, H. (2011) *Am J Physiol Gastrointest Liver Physiol* **301**, G128-137
2. Cynober, L. A. (2002) *Nutrition* **18**, 761-766
3. Wu, G. (2009) *Amino Acids* **37**, 1-17
4. Verrey, F., Singer, D., Ramadan, T., Vuille-dit-Bille, R. N., Mariotta, L., and Camargo, S. M. (2009) *Pflugers Arch* **458**, 53-60
5. Broer, S., and Palacin, M. (2011) *Biochem J* **436**, 193-211
6. Fernandez, E., Torrents, D., Chillaron, J., Martin Del Rio, R., Zorzano, A., and Palacin, M. (2003) *J Am Soc Nephrol* **14**, 837-847
7. Meier, C., Ristic, Z., Klauser, S., and Verrey, F. (2002) *Embo J* **21**, 580-589
8. Pfeiffer, R., Rossier, G., Spindler, B., Meier, C., Kuhn, L., and Verrey, F. (1999) *Embo J* **18**, 49-57
9. Rossier, G., Meier, C., Bauch, C., Summa, V., Sordat, B., Verrey, F., and Kuhn, L. C. (1999) *J Biol Chem* **274**, 34948-34954
10. Verrey, F. (2003) *Pflugers Arch* **445**, 529-533
11. Braun, D., Wirth, E. K., Wohlgemuth, F., Reix, N., Klein, M. O., Gruters, A., Kohrle, J., and Schweizer, U. (2011) *Biochem J* **439**, 249-255
12. Kim, D. K., Kanai, Y., Chairoungdua, A., Matsuo, H., Cha, S. H., and Endou, H. (2001) *J Biol Chem* **276**, 17221-17228
13. Ramadan, T., Camargo, S. M., Summa, V., Hunziker, P., Chesnov, S., Pos, K. M., and Verrey, F. (2006) *J Cell Physiol* **206**, 771-779
14. Ramadan, T., Camargo, S. M., Herzog, B., Bordin, M., Pos, K. M., and Verrey, F. (2007) *Pflugers Arch* **454**, 507-516
15. Keays, D. A., Clark, T. G., Campbell, T. G., Broxholme, J., and Valdar, W. (2007) *Mamm Genome* **18**, 123-124
16. Augustin, M., Sedlmeier, R., Peters, T., Huffstadt, U., Kochmann, E., Simon, D., Schoniger, M., Garke-Mayerthaler, S., Laufs, J., Mayhaus, M., Franke, S., Klose, M., Graupner, A., Kurzmann, M., Zinser, C., Wolf, A., Voelkel, M., Kellner, M., Kilian, M., Seelig, S., Koppius, A., Teubner, A., Korthaus, D., Nehls, M., and Wattler, S. (2005) *Mamm Genome* **16**, 405-413
17. Sugiura, S., Kitagawa, K., Tanaka, S., Todo, K., Omura-Matsuoka, E., Sasaki, T., Mabuchi, T., Matsushita, K., Yagita, Y., and Hori, M. (2005) *Stroke* **36**, 859-864
18. Seaton, B., and Ali, A. (1984) *Med Lab Sci* **41**, 327-336
19. Wybenga, D. R., Di Giorgio, J., and Pileggi, V. J. (1971) *Clin Chem* **17**, 891-895
20. Suresh Babu, S. V., Shareef, M. M., Pavan Kumar Shetty, A., and Taranath Shetty, K. (2002) *Indian Journal of Clinical Biochemistry* **17**, 7-26
21. Cohen, S. A., and De Antonis, K. M. (1994) *J Chromatogr A* **661**, 25-34
22. Bauwens, M., Lahoutte, T., Kersemans, K., Caveliers, V., Bossuyt, A., and Mertens, J. (2007) *Contrast Media Mol Imaging* **2**, 172-177
23. Lahoutte, T., Caveliers, V., Camargo, S. M., Franca, R., Ramadan, T., Veljkovic, E., Mertens, J., Bossuyt, A., and Verrey, F. (2004) *J Nucl Med* **45**, 1591-1596
24. Lahoutte, T., Caveliers, V., Franken, P. R., Bossuyt, A., Mertens, J., and Everaert, H. (2002) *J Nucl Med* **43**, 1201-1206
25. Lahoutte, T., Mertens, J., Caveliers, V., Franken, P. R., Everaert, H., and Bossuyt, A. (2003) *J Nucl Med* **44**, 1489-1494
26. Vanhove, C., Defrise, M., Bossuyt, A., and Lahoutte, T. (2011) *Eur J Nucl Med Mol Imaging* **38**, 153-165
27. Loening, A. M., and Gambhir, S. S. (2003) *Mol Imaging* **2**, 131-137
28. Maquat, L. E. (1995) *RNA* **1**, 453-465
29. Karl, T., Pabst, R., and von Horsten, S. (2003) *Exp Toxicol Pathol* **55**, 69-83
30. Jager, P. L., Vaalburg, W., Pruim, J., de Vries, E. G., Langen, K. J., and Piers, D. A. (2001) *J Nucl Med* **42**, 432-445
31. Lahoutte, T., Caveliers, V., Dierickx, L., Vekeman, M., Everaert, H., Mertens, J., and Bossuyt, A. (2001) *Nucl Med Biol* **28**, 129-134

32. Moundras, C., Remesy, C., and Demigne, C. (1993) *Am J Physiol* **264**, G1057-1065
33. Schimassek, H., and Gerok, W. (1965) *Biochem Z* **343**, 407-415
34. Brosnan, J. T. (2003) *J Nutr* **133**, 2068S-2072S
35. Fischer, J. E., Rosen, H. M., Ebeid, A. M., James, J. H., Keane, J. M., and Soeters, P. B. (1976) *Surgery* **80**, 77-91
36. James, J. H., Ziparo, V., Jeppsson, B., and Fischer, J. E. (1979) *Lancet* **2**, 772-775
37. Dejong, C. H., van de Poll, M. C., Soeters, P. B., Jalan, R., and Olde Damink, S. W. (2007) *J Nutr* **137**, 1579S-1585S; discussion 1597S-1598S
38. Uchida, S., Kitamoto, A., Umeeda, H., Nakagawa, N., Masushige, S., and Kida, S. (2005) *J Nutr Sci Vitaminol (Tokyo)* **51**, 175-181
39. van Donkelaar, E. L., Blokland, A., Lieben, C. K., Kenis, G., Ferrington, L., Kelly, P. A., Steinbusch, H. W., and Prickaerts, J. (2010) *Neurochem Int* **56**, 21-34
40. Lyck, R., Ruderisch, N., Moll, A. G., Steiner, O., Cohen, C. D., Engelhardt, B., Makrides, V., and Verrey, F. (2009) *J Cereb Blood Flow Metab* **29**, 1491-1502
41. Meredith, D., and Christian, H. C. (2008) *Xenobiotica* **38**, 1072-1106
42. Bodoy, S., Martin, L., Zorzano, A., Palacin, M., Estevez, R., and Bertran, J. (2005) *J Biol Chem* **280**, 12002-12011
43. Danisi, G., and Murer, H. (1991) *in Comprehensive Physiology, John Wiley & Sons, Inc.*
44. Pappenheimer, J. R. (1993) *Am J Physiol* **265**, G409-417
45. Ballard, S. T., Hunter, J. H., and Taylor, A. E. (1995) *Annu Rev Nutr* **15**, 35-55
46. Broer, S. (2008) *Physiology (Bethesda)* **23**, 95-103
47. Drummond, K. N., Michael, A. F., Ulstrom, R. A., and Good, R. A. (1964) *Am J Med* **37**, 928-948
48. Park, S. Y., Kim, J. K., Kim, I. J., Choi, B. K., Jung, K. Y., Lee, S., Park, K. J., Chairoungdua, A., Kanai, Y., Endou, H., and Kim, D. K. (2005) *Arch Pharm Res* **28**, 421-432

FIGURE LEGENDS

FIGURE 1. TAT1 detection by immunofluorescence microscopy in sections of liver (A and B) and kidney (C and D). TAT1 is localized to the perivenous hepatocytes (A) and kidney proximal tubule cells (B) of *wt* tissues, whereas it is not detected in *tat1*$^{-/-}$ tissues (B and D). V: central vein, G: glomerulus, S1: proximal convoluted tubule segment S1.

FIGURE 2. Locomotor and coordination capability of *tat1*$^{-/-}$ and *wt* littermates. Mice were tested with a RotaRod assay at accelerating and constant speed. Represented is the latency time before the first roll occurs (solid bars) and until first fall (open bars). Given are means ± SEM (n = 5).

FIGURE 3. Free circulating amino acids in plasma: effect of high protein diet in *wt* mice (A) and altered amino acid profile in *tat1*$^{-/-}$ (B). A: absolute concentrations of amino acids measured in plasma of wild type mice subjected to normal (20%) and high (40%) protein diet. * indicates $P<0.05$. B: plasma amino acid concentrations in *tat1* knock out mice are shown relative to the values measured for their wild type littermates under the same diet. The horizontal line (y = 1) corresponds to the *wt* values. Represented are means ± SEM (n = 12). Groups were compared by one-way ANOVA, followed by Bonferroni posttest on selected pairs of columns. Values with letters are statistically different ($P<0.05$): 'a' and 'b' indicates difference of *tat1*$^{-/-}$ versus *wt* under normal protein diet and high protein diet, respectively, 'c' indicates difference between normal protein and high protein diet in *tat1*$^{-/-}$ mice, ns all comparison are not significant.

FIGURE 4. Concentrations of free amino acids in plasma and in cytosol of different organs. PL: plasma, Liv: liver, Sk. m: skeletal muscles (i.e. *M. gastrocnemius*), Kid: kidney. Represented means ± SEM (n = 6). ** indicates $P<0.01$ and *** $P<0.001$ by unpaired Student t-test.

FIGURE 5. Urinary amino acid profiles: the high protein diet has no effect on *wt* mice (A) but enhances the aminoaciduria in *tat1*$^{-/-}$ (B). A: total amino acids excreted in 24 hours by wild type mice subjected to normal (20%) and high (40%) protein diet. B: amino acids excreted in *tat1* knock out mice are shown relative to the values measured for their wild type littermates under the same diet. The horizontal line (y = 1) corresponds to normalized *wt* values. The selectivity of known basolateral amino acid transporters measured in *Xenopus laevis* oocyte expression system is indicated below (References: [1] corresponds to (Ramadan, Camargo et al. 2007), [2] to (Meier, Ristic et al. 2002; Park, Kim et al. 2005) and [3] to (Bodoy, Martin et al. 2005)). +++ indicates high, ++ intermediate, + low and empty space no selectivity. Represented are means ± SEM (n = 12). Groups were compared by one-way ANOVA, followed by Bonferroni posttest on selected pairs of columns. Values with letters are statistically different ($P<0.05$): 'a' *tat1*$^{-/-}$ versus *wt* in NPD, 'b' *tat1*$^{-/-}$ versus *wt* in HPD, 'c' *tat1*$^{-/-}$ NPD versus HPD, 'd' *wt* NPD versus HPD, 'ns' all comparison are not significant.

FIGURE 6. ^{123}I-2-I-L-Phe accumulation in kidney after i.v. injection. Fused micro-SPECT/CT and micro-CT coronal scans of a *wt* (A) and a *tat1*$^{-/-}$ (B) mouse: the *tat1*$^{-/-}$ animal presented a clear accumulation of the compound in both kidneys, whereas kidney accumulation was low in *wt*. C: quantification of the biodistribution in different organs after dissection. Represented is the percentage of injected activity of ^{123}I-2-I-L-Phe in each tissue or organ per gram. Given are means ± SEM (n = 3). ** indicates $P<0.01$ by unpaired Student t-test.

FIGURE 7. Significant accumulation of L-Phe in intestinal everted gut sacs. Everted sacs of *tat1*$^{-/-}$ and *wt* mouse small intestine were incubated at 37°C for 10 minutes in Krebs buffer containing 100 µM L-Phe and ^{3}H-L-Phe tracer. Radioactivity was counted inside of the sacs (serosa) and in the tissue (epithelial cells). Transport rates were calculated and normalized to weight of tissue. Represented are means ± SEM ($n \geq 8$). * indicates $P<0.05$ by unpaired Student t-test.

TABLE 1: Urinary and physiological parameters of males measured in metabolic cages for 24 hours.

Males	Normal Protein Diet (20% Casein)		High Protein Diet (40% Casein)	
	wt	*tat1*$^{-/-}$	*wt*	*tat1*$^{-/-}$
Urinary parameters:				
pH	6.36[1] ± 0.03	6.46 ± 0.07	6.05 ± 0.06 c[2]	6.11 ± 0.02 d
Creatinine (mg/24 hours)	0.174 ± 0.036	0.510 ± 0.088	1.150 ± 0.299 c	1.898 ± 0.316 d
Creatinine (mg/dl)	40.2 ± 2.6	32.1 ± 2.9	22.8 ± 5.9 c	17.8 ± 0.9
Urea (mg/dl)/crea (mg/dl)	166.7 ± 53.4	133.9 ± 23.4	332.1 ± 32.9 c	277.6 ± 29.5 d
Na^+ (mM)/crea (mg/dl)	8.58 ± 0.57	7.90 ± 0.49	9.45 ± 1.22	7.18 ± 0.98
K^+ (mM)/crea (mg/dl)	7.27 ± 0.26	6.38 ± 0.34	6.88 ± 0.71	5.38 ± 0.62
Ca^{2+} (mM)/crea (mg/dl)	0.041 ± 0.001	0.048 ± 0.009	0.089 ± 0.008 c	0.078 ± 0.009
Mg^{2+} (mM)/crea (mg/dl)	0.52 ± 0.06	0.36 ± 0.05	0.70 ± 0.13	0.59 ± 0.10
Osmolality (mOsm/Kg H2O)	3148 ± 174	2260 ± 192	2660 ± 497	2072 ± 199
Urine volume (ml)/g BW	0.046 ± 0.005	0.086 ± 0.009	0.112 ± 0.019 c	0.164 ± 0.013 d
Water intake (ml)/g BW	0.131 ± 0.014	0.244 ± 0.028 a	0.272 ± 0.023 c	0.362 ± 0.021 d
Food intake (g)/g BW	0.142 ± 0.013	0.165 ± 0.010	0.144 ± 0.009	0.153 ± 0.009
Feces (g)/g BW	0.021 ± 0.002	0.023 ± 0.001	0.020 ± 0.002	0.019 ± 0.002
Body weight (g)	28.1 ± 1.0	25.7 ± 0.3	27.6 ± 0.8	26.2 ± 0.6
Body weight (% change)	1.00 ± 0.00	1.00 ± 0.00	0.99 ± 0.01	1.02 ± 0.02

[1]Given are means ± SEM. (n = 6). [2]Groups were compared by one-way ANOVA, followed by Bonferroni posttest on selected pairs of columns. Values with letters are statistically different ($P<0.05$): 'a' indicates that *tat1*$^{-/-}$ and *wt* are significantly different under normal protein diet, 'c' that *wt* under normal and high protein diet are different and 'd' that *tat1*$^{-/-}$ under normal versus high protein diet are different. No gender difference was observed. Female data can be found in supplementary Tab. 2.

Figure 1

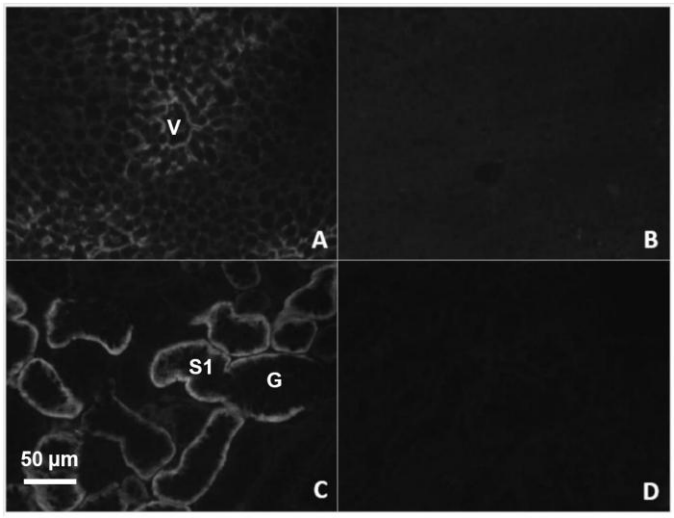

Figure 2

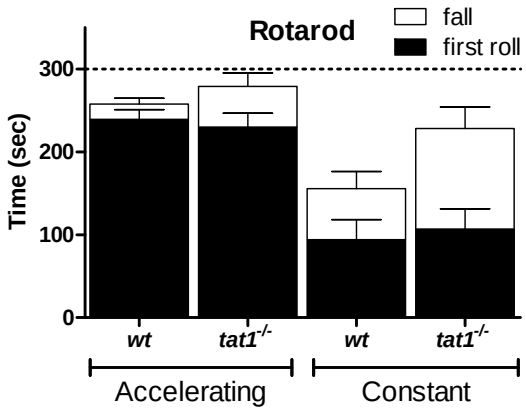

Figure 3

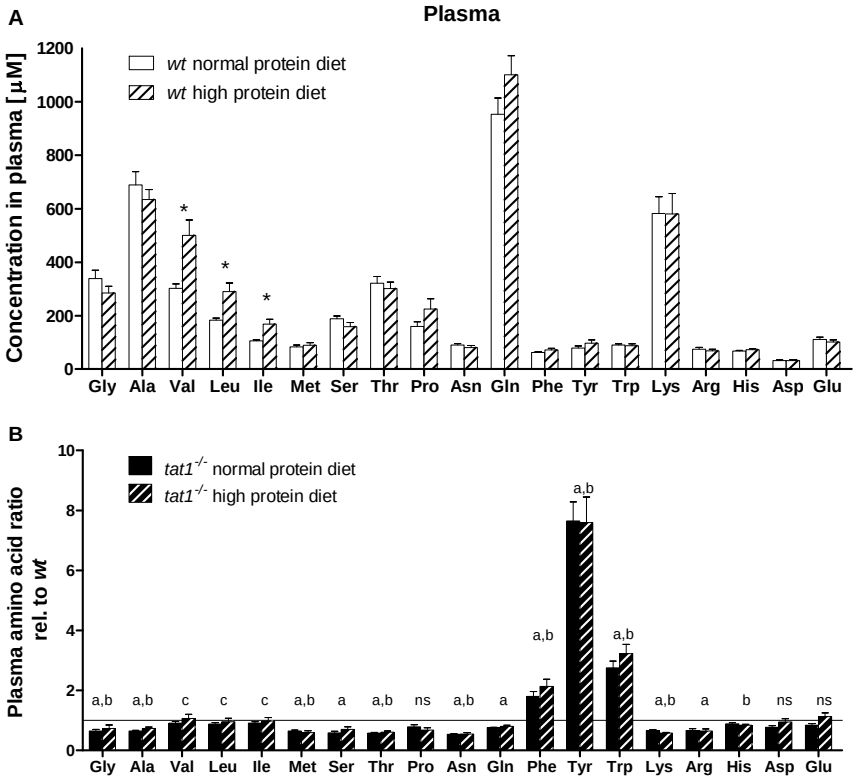

Figure 4

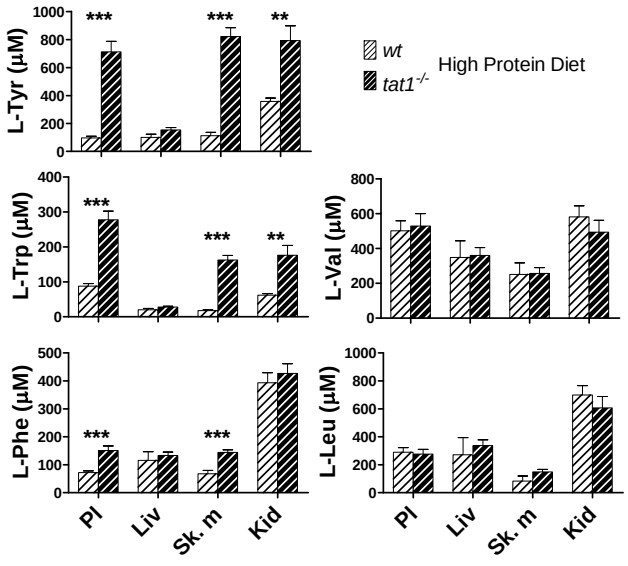

Figure 5

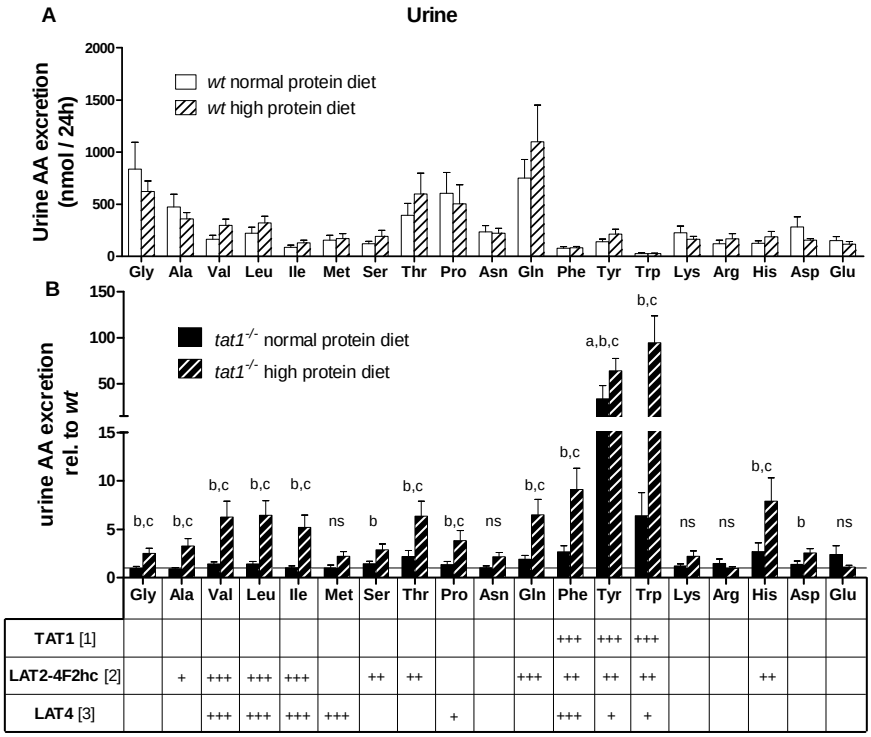

Figure 6

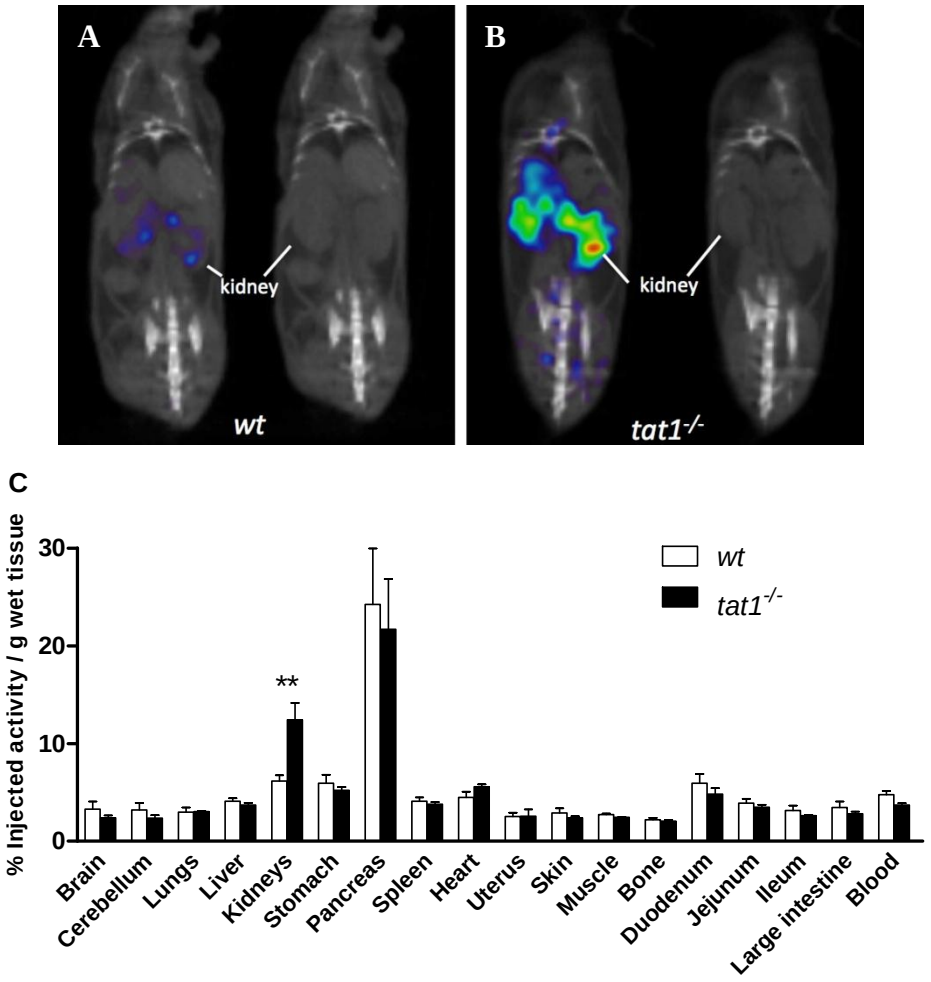

Figure 7

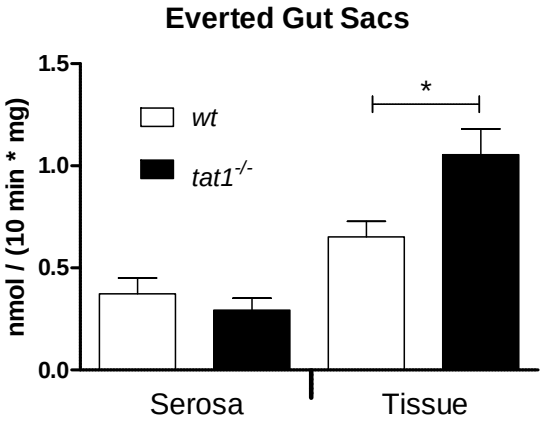

SUPPLEMENTARY MATERIAL

Material and methods

Growth Curve

Weights of pups from *tat1*$^{+/-}$ *inter se* breedings were recorded starting one day after birth. Animals were identified by marking the body with a Securiline alcohol-resistant lab marker (Precision Dynamics Corporation, USA). At day 6, fingers were clipped and animals genotyped by PCR.

Morphological analysis of organs

Tissues were harvested after heart perfusion with 50 ml 2.5% PFA in PBS, and 5 min incubation. After embedding in paraffin, organs were cut with a microtome (4 µm) and sections mounted and de-paraffinized. Classical staining was performed by incubating 2 min in Mayer’s Hematoxylin solution (Sigma-Aldrich, Switzerland) and 1 min in Eosin Y solution alcoholic (Sigma-Aldrich, Switzerland).

Oral glucose tolerance test

After O/N starvation, 0.25 mg / µl D-Sucrose solution was injected i.p. in a dose of 3 g / kg body weight. Blood was sampled from the tail vein and measured with Accu-Check Aviva (Roche, Switzerland) at different time points.

Oocytes uptakes

Injection and uptake in oocytes was performed as described previously (Meier, Ristic et al. 2002; Ramadan, Camargo et al. 2006). After injection of 10 ng of cRNA, oocytes were incubated for 18 hours (*lat2-4F2hc*) or 3 days (*tat1* and *lat4*) at 16°C in ND96 solution. Uptakes of 100 µM L-Phe were performed for 3 min. The 2-I-L-Phe used was kindly provided by the In vivo Cellular and Molecular Imaging Center Brussels. Depicted values were corrected by subtraction of the uptake of non-injected oocytes.

Content of distal small intestine

Experiment was performed as in Singer et al., (in revision). Animals were starved for 12 hours before the experiment to empty the intestine and reduce variation. A 10 ul / g bolus of PBS solution supplemented with amino acids (each AA was set at a final concentration that reflected 10x the plasma

values depicted in Fig. 3A) was given by oral gavage. Animals were kept in their own cages and sacrificed after 1h. The small intestine was carefully removed and the last 10 cm before the caecum cut at both ends. The content of this segment was collected by flushing with 1 ml of PBS and the amino acid concentration of this solution then measured by UPLC, as described before.

Suppl. Tab. 1a: mRNA abundance of several amino acid transporters in different tissue lysates relative to HPRT.

		Liver		Small intestine						Kidney	
				Duodenum		Jejunum		Ileum			
tat1	*wt*	3.3 ± 0.7[1]		10.5 ± 1.2		22.4 ± 2.9		10.3 ± 1.6		1.4 ± 0.2	
	tat1$^{-/-}$	0.4 ± 0.1	**[2]	1.4 ± 0.3	***	4.9 ± 0.7	***	2.3 ± 0.6	***	0.1 ± 0.01	***
lat2	*wt*	0.1 ± 0.02		7.7 ± 1.1		105.1 ± 21.5		17.5 ± 4.9		2.2 ± 0.5	
	tat1$^{-/-}$	0.1 ± 0.03		7.1 ± 1.1		72.4 ± 9.7		16.1 ± 3.2		2.0 ± 0.2	
lat4	*wt*	0.9 ± 0.2		33.2 ± 2.4		68.5 ± 10.6		44.9 ± 3.4		3.8 ± 0.2	
	tat1$^{-/-}$	0.3 ± 0.1	**	22.9 ± 2.8	*	61.0 ± 2.0		48.2 ± 7.5		4.2 ± 0.3	
4F2hc	*wt*	4.4 ± 0.7		49.2 ± 3.8		125.5 ± 17.3		48.7 ± 4.5		12.7 ± 2.1	
	tat1$^{-/-}$	4.1 ± 0.7		35.2 ± 4.4	*	136.3 ± 11.5		65.0 ± 17.5		11.9 ± 1.6	
B^{0}AT1	*wt*			21.8 ± 3.8		22.6 ± 3.7		35.5 ± 3.5		3.1 ± 0.5	
	tat1$^{-/-}$			17.4 ± 2.5		29.5 ± 4.3		31.4 ± 1.7		4.2 ± 0.4	

[1]means ± SEM. (n ≥ 10). [2] * indicates P<0.05, ** P<0.01 and *** P<0.001 by unpaired Student t-test.

Suppl. Tab. 1b: mRNA abundance of several amino acid transporters in muscles and fat relative to HPRT.

		Muscles			Fat
		Gastrocnemius	Soleus	Heart	
tat1	*wt*	3.41 ± 0.81[1]	1.00 ± 0.23	0.58 ± 0.25	0.31 ± 0.14
	tat1$^{-/-}$	0.76 ± 0.21 *[2]	0.55 ± 0.20	0.19 ± 0.10	0.70 ± 0.38
lat2	*wt*	0.18 ± 0.05	0.03 ± 0.01		
	tat1$^{-/-}$	0.30 ± 0.05	0.04 ± 0.02		
lat4	*wt*	0.30 ± 0.06	1.23 ± 0.43	0.27 ± 0.04	0.24 ± 0.02
	tat1$^{-/-}$	0.46 ± 0.08	1.03 ± 0.10	0.46 ± 0.25	0.24 ± 0.01
4F2hc	*wt*	1.73 ± 0.33	1.55 ± 0.68	2.84 ± 0.08	2.61 ± 1.40
	tat1$^{-/-}$	1.63 ± 0.27	1.79 ± 0.69	2.56 ± 0.22	6.78 ± 1.09

[1] means ± SEM. (n = 10-15). [2] means ± SEM. * indicates a P<0.05.

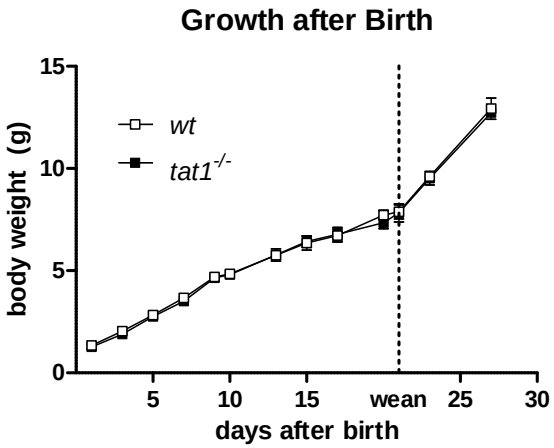

Suppl. Fig. 1: Growth after birth. Represented means ± SEM. (n = 4).

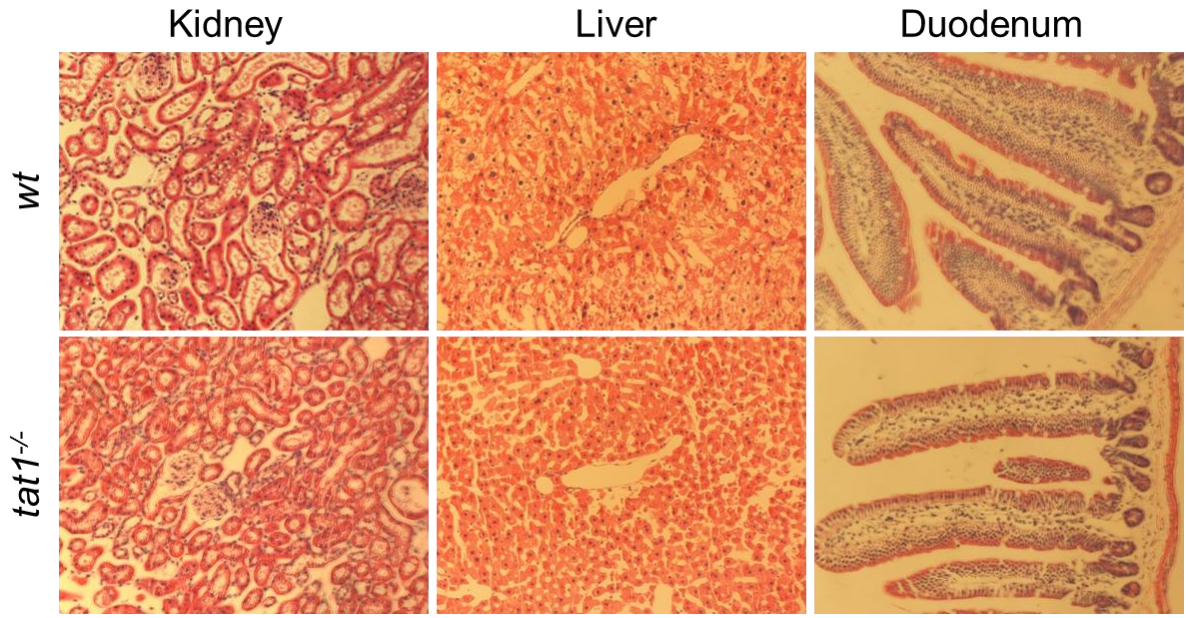

Suppl. Fig. 2: Organs have normal morphology: hematoxylin and eosin staining on 4 µm paraffin sections.

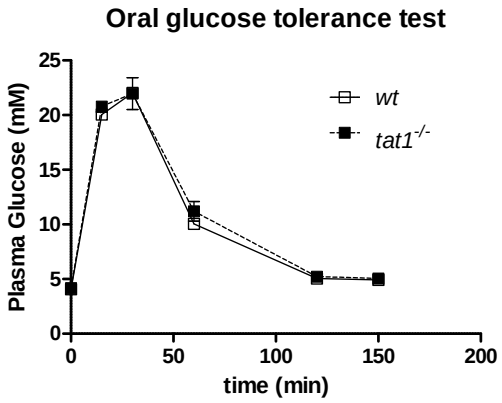

Suppl. Fig. 3: Oral glucose tolerance test. Represented means ± SEM. (n = 4).

Tab. 2: Urinary and physiological parameters of females measured in metabolic cages for 24 hours.

Females	**Normal Protein Diet (20% Casein)**		**High Protein Diet (40% Casein)**	
	wt	*tat1*$^{-/-}$	*wt*	*tat1*$^{-/-}$
Urinary parameters:				
pH	6.31[1] ± 0.06	6.36 ± 0.10	5.92 ± 0.07 c[2]	5.97 ± 0.04 d
Creatinine (mg/24 hours)	0.059 ± 0.047	0.199 ± 0.043	0.394 ± 0.116	1.045 ± 0.165 bd
Creatinine (mg/dl)	42.9 ± 10.6	23.1 ± 3.7	22.4 ± 3.2	18.1 ± 1.9
Urea (mg/dl)/crea (mg/dl)	247.0 ± 25.6	272.9 ± 22.2	561.1 ± 73.9 c	354.0 ± 69.1
Na^+ (mM)/crea (mg/dl)	12.39 ± 1.95	11.46 ± 0.99	11.02 ± 0.79	9.05 ± 0.66
K^+ (mM)/crea (mg/dl)	8.72 ± 1.14	9.15 ± 0.64	8.68 ± 0.57	6.60 ± 0.65
Ca^{2+} (mM)/crea (mg/dl)	0.089 ± 0.017	0.106 ± 0.019	0.184 ± 0.045	0.130 ± 0.016
Mg^{2+} (mM)/crea (mg/dl)	0.78 ± 0.18	0.76 ± 0.15	1.08 ± 0.24	0.98 ± 0.14
Osmolality (mOsm/Kg H2O)	4136 ± 990	2342 ± 348	3652 ± 589	2257 ± 204
Urine volume (ml)/g BW	0.023 ± 0.011	0.070 ± 0.008 a	0.086 ± 0.016 c	0.156 ± 0.013 bd
Water intake (ml)/g BW	0.277 ± 0.041	0.304 ± 0.022	0.353 ± 0.028	0.402 ± 0.020
Food intake (g)/g BW	0.185 ± 0.005	0.207 ± 0.010	0.186 ± 0.005	0.187 ± 0.008
Feces (g)/g BW	0.028 ± 0.005	0.029 ± 0.002	0.025 ± 0.002	0.026 ± 0.003
Body weight (g)	20.9 ± 0.6	19.7 ± 0.6	21.2 ± 0.5	20.5 ± 0.6
Body weight (% change)	1.00 ± 0.00	1.00 ± 0.00	1.02 ± 0.02	1.04 ± 0.01

[1]Given are means ± SEM. (n = 6). [2]Groups were compared by one-way ANOVA, followed by Bonferroni posttest on selected pairs of columns. Values with letters are statistically different (P<0.05): 'a' indicates that *tat1*$^{-/-}$ versus *wt* are statistically different under normal protein diet, 'b' that *tat1*$^{-/-}$ versus *wt* are different under high protein diet, 'c' and 'd' that there is a significant difference between normal and high protein diet in *wt and tat1*$^{-/-}$, respectively.

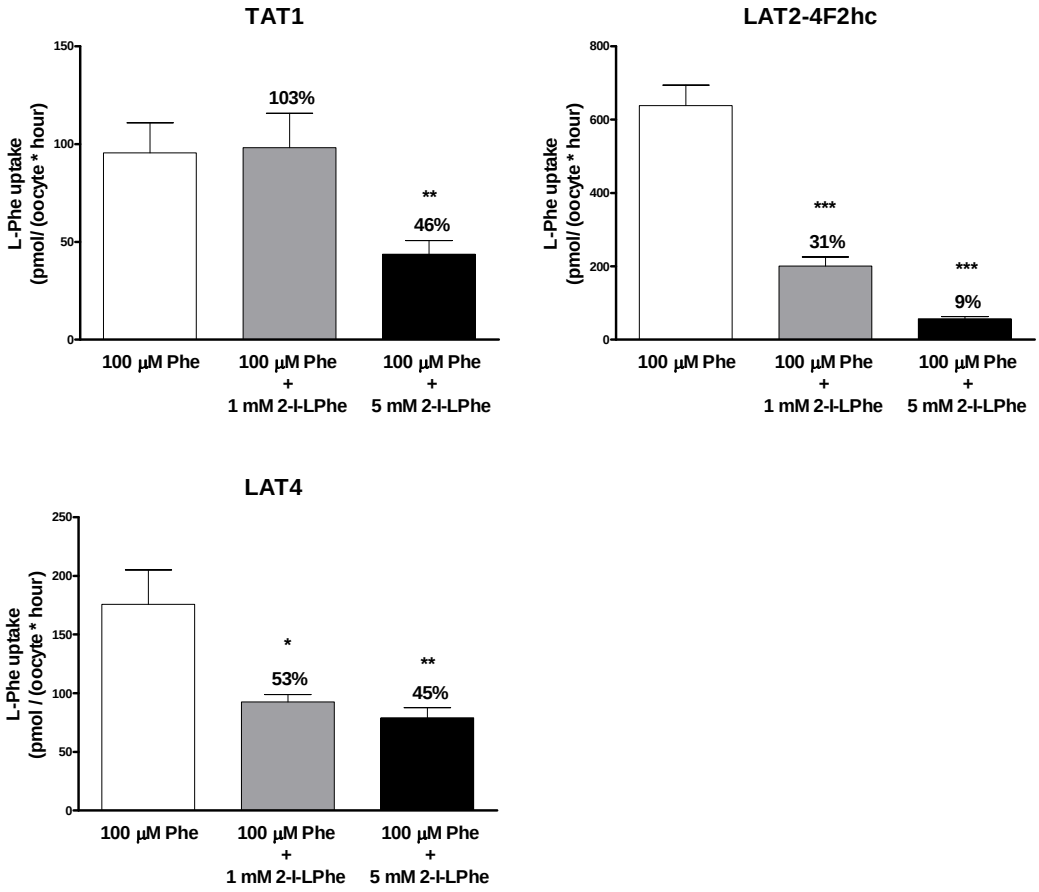

Suppl. Fig. 4: L-Phe uptake is competed by 2-I-L-Phe. Oocytes were injected either with *tat1*, *lat2-4F2hc* or *lat4* cRNAs and uptakes of 100 µM L-Phe were performed without competition (control, white bars), or in the presence of 1 mM 2-I-L-Phe (grey bars) and 5 mM 2-I-L-Phe (black bars). The residual uptake fractions are indicated above the bars as percent of control. The bars represent means ± SEM. (n = 8-10). * indicates a $P<0.05$, ** a $P<0.01$ and *** a $P<0.001$ by unpaired Student t-test.

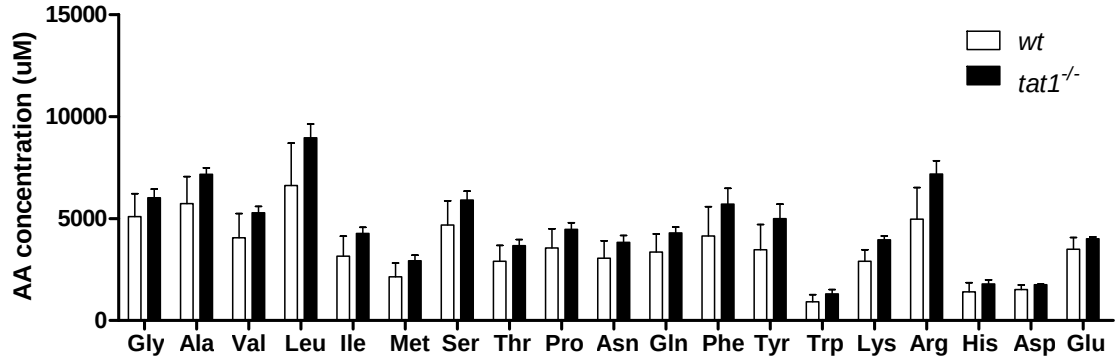

Suppl. Fig. 5: Amino acids reaching the distal part of the small intestine. 1 hour after an oral load of amino acids the animals were sacrificed and the content of the last 10 cm of small intestine (ileum) collected. The quantification did not reveal a statistical difference between *tat1*$^{-/-}$ and *wt* mice. Represented are means ± SEM (n = 4).

Supplementary References

1. Meier, C., Ristic, Z., Klauser, S., and Verrey, F. (2002) *EMBO J* **21**, 580-589
2. Ramadan, T., Camargo, S. M., Summa, V., Hunziker, P., Chesnov, S., Pos, K. M., and Verrey, F. (2006) *J Cell Physiol* **206**, 771-779
3. Singer D, Camargo SMR., Ramadan T, Schäfer M, Mariotta L, Herzog B, Huggel K, Wolfer D, Werner S, Penninger J, Verrey F (2012), in revision

5.3. Addendum

5.3.1 Low protein diet study

In concomitance with the high protein diet (PD) treatment, whose results are presented in the previous section, a low protein challenge was similarly performed. For this, an isocaloric casein free diet was provided for 8 consecutive days to the mice either at the end or at the beginning of the challenge. Under this condition the mice immediately displayed a considerable loss of body weight, which progressively continued (Fig. 15). Nevertheless, the animals presented a normal behavior as judged by the absence of signs of apathy, pain, weakness and diarrhea. Furthermore, the animals were able to regain the majority of their weight in the 48 hours consecutive to the normal PD switch, however without being able to fully recover (Fig.15B). The body weight progression along the whole dietary challenge was identical in *wt* and *tat1*$^{-/-}$.

The amino acid analysis in plasma of animals treated with the casein free diet revealed higher concentrations of Ala and Gln, which were shown to be hallmarks for low protein diet as a consequence of elevated muscle protein catabolism (Peters and Harper 1985; Moundras, Remesy et al. 1993) (Fig. 16A). Free plasma Arg was also slightly increased, probably as a consequence of diminished urea cycle. Indeed, when the urinary urea was measured with the diacetyl monoxyme method (Wybenga, Di Giorgio et al. 1971), all samples lied below the detection limit of the assay, which indicates an extremely low abundance (not shown). Many other essential amino acids were less concentrated, among those also the aromatic and the branched chain ones, as a consequence of the abolished dietary intake. In the urine after low PD, if compared to normal PD, a drastic decrease in all amino acid concentration was observed (Fig. 16B). The plasma of *tat1*$^{-/-}$ presented the same relative trend displayed under normal PD, although in a reduced smaller extend due to the dietary amino acid

deprivation: elevated aromatic amino acid in the circulation. Under low PD no difference between *wt* and *tat1*$^{-/-}$ was observed in the urinary content, not surprisingly in the light of the general extremely low values recorded. In conclusion, the steep decrease in body weight and the major differences observed in urinary amino acids indicates that the protein free diet is a too harsh intervention and that a 5-7% casein diet would be more adequate. Nevertheless, *tat1*$^{-/-}$ mice reacted to the treatment in a similar way as *wt* and seemed therefore not to be disadvantaged by their mutation.

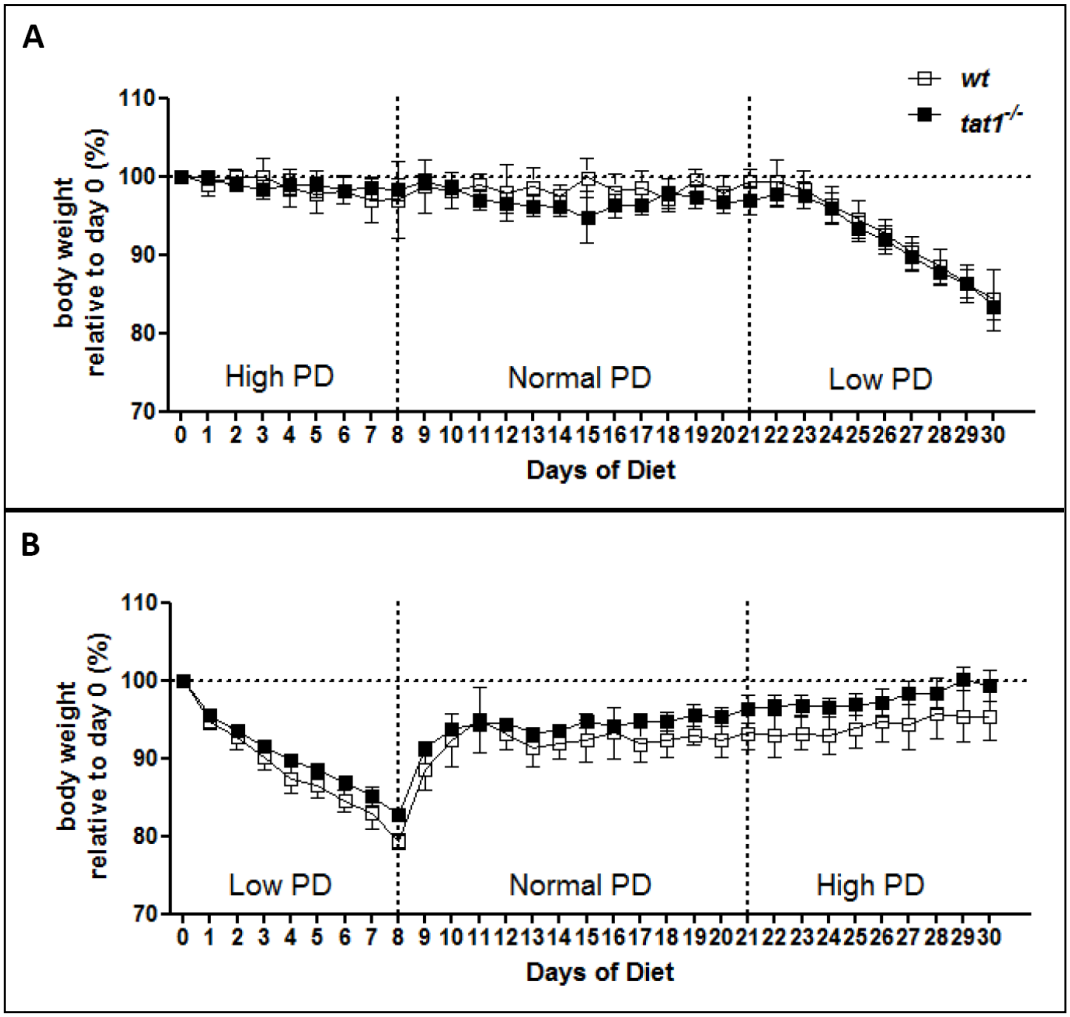

Fig. 15: Progression of body weight during the dietary challenge. Mice were divided into two groups: A. the first received sequentially the high (40% casein), normal (20%) and low (0%) protein diet (PD) and B. the second group received the diets in the opposite order. Represented means ± SEM (n = 6).

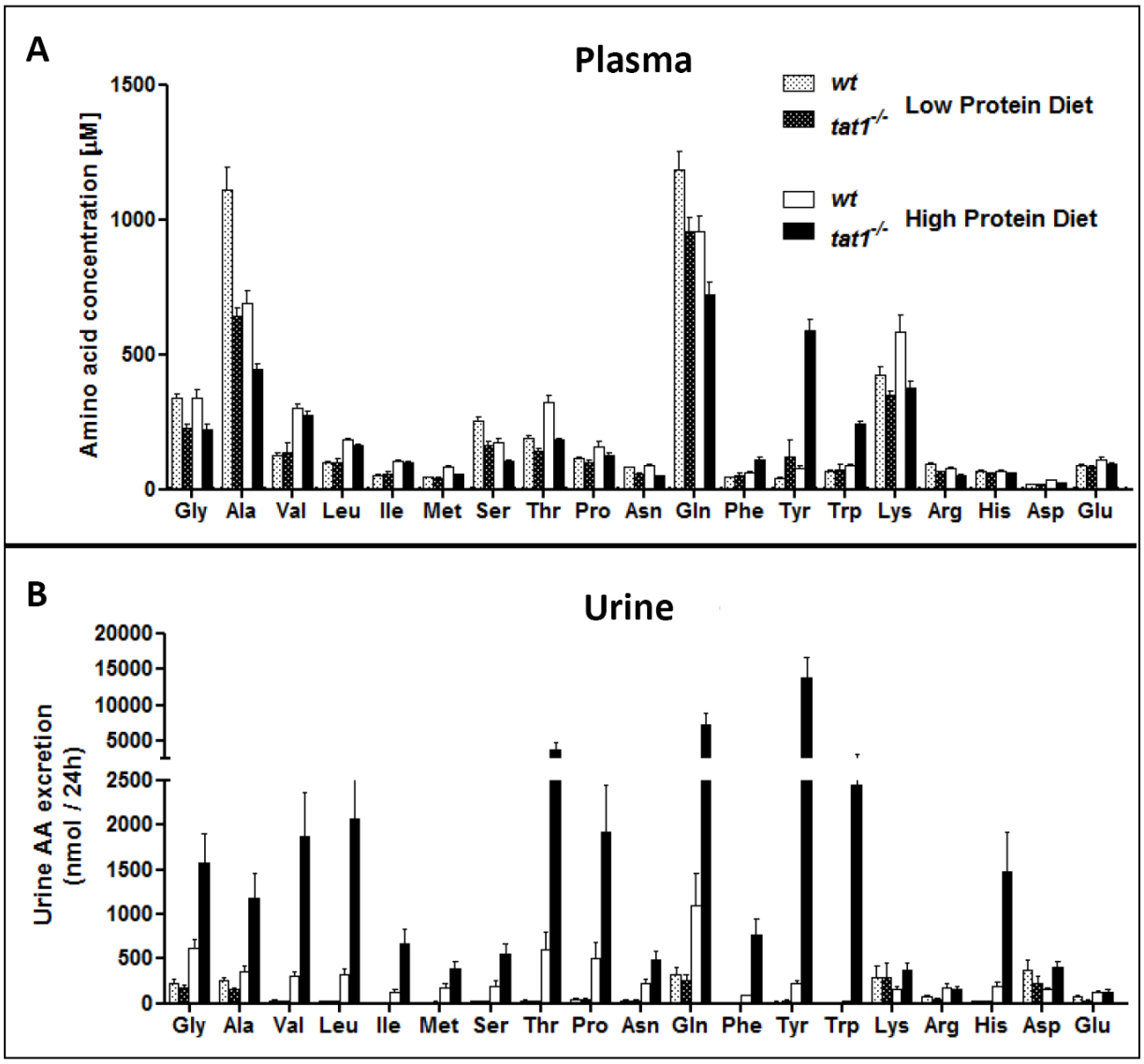

Fig. 16: Amino acid profiles showed hallmarks of low PD in plasma and a much less presence in the urine. A. plasma amino acid profiles showed increased Ala and Glu and decreased BCAA similar to other studies (Peters and Harper 1985; Moundras, Remesy et al. 1993). Although in a lesser extent, *tat1*$^{-/-}$ displayed the same relative trend observed under normal PD. **B.** Urinary amino acid excreted in 24 hours showed a drastic decrease under low PD in both, *wt* and *tat1*$^{-/-}$.

5.3.2 Validation of the everted gut sac technique

An improved system of the everted gut sac technique for rats has been reviewed in 1998 (Lloyd and Whelan 1969; Barthe, Woodley et al. 1998). With the mediation of Moritz Jüttner (University Hospital Zürich), the protocol used here has been further optimized for the application in mice, based on the experience of the Daniel's lab (Technische Universität München) (Stein, Daniel et al. 1994; Nassl, Rubio-Aliaga et al. 2011). The description of the procedure can be found in the material and methods section (4.1.10) and in the *tat1* manuscript (5.2). Briefly, 1.5 cm long pieces of small intestine (duodenum and jejunum) were everted so that the mucosa, which normally faces the lumen, was turned inside out (Fig. 17A). Thus, the inside of the newly formed sac reflected the extracellular space in the body and has been named serosa, referring to the last anatomical structure that can be found (see 3.2.2). The bags were ligated at both ends and a KREBS buffer was introduced in the inside with a syringe at one end. The exact volume introduced was calculated from the weight difference of the syringe. The bag was incubated in a 37°C pre-warmed oxygenated KREBS buffer supplemented with the tested substrates and their tracers (Fig. 17B). At the end of the incubation, the sacs were washed with 30 ml ice cold sodium deprived KREBS buffer, cut open and the sac contents were collected. The tissues were dried at 55° C over night, weighted and consecutively lysed with a dedicated kit (Solvable, Perkin Elmer). Since the intestine has been everted and since the substrates for uptake has been added at the mucosal part (Fig. 17A and B), the concentration inside of the bag indicates the sum of transepithelial (active) and paracellular (passive) transports. Therefore, in order to discriminate between both components, a co-incubation with ^{14}C-mannitol, which only diffuses paracellularly, was performed. The exclusion criterion for sacs presenting a serosal mannitol content higher than 5% of the total has been applied. Similarly, a threshold of 1% has been applied for the tissues.

Before performing the experiment presented in the *tat1* manuscript (see 5.2), several trial aiming at controlling the consistency of the new system were performed. First, the transport rate at 4°C was significantly diminished (Fig. 17C), which agrees to thermodynamic laws and to experiments in *X. laevis* heterologous expression system. Therefore, the majority of the measured transport was active and not paracellular. Second, compared to *wt* the transport rates of Leu were significantly decreased in *ace2*$^{-/y}$ (Fig. 17D), which is in agreement with the data published by Camargo, Singer and co-workers obtained with the intestinal ring technique where the same differences were observed (7 nmol/mg in *wt*; 2 nmol/mg in *ace2*$^{-/y}$) (Camargo, Singer et al. 2009). Last, time course plots showed a progressive increase in the transport rates and an accumulation of Phe in the serosa, which however stopped around 100 µM (Fig. 18).

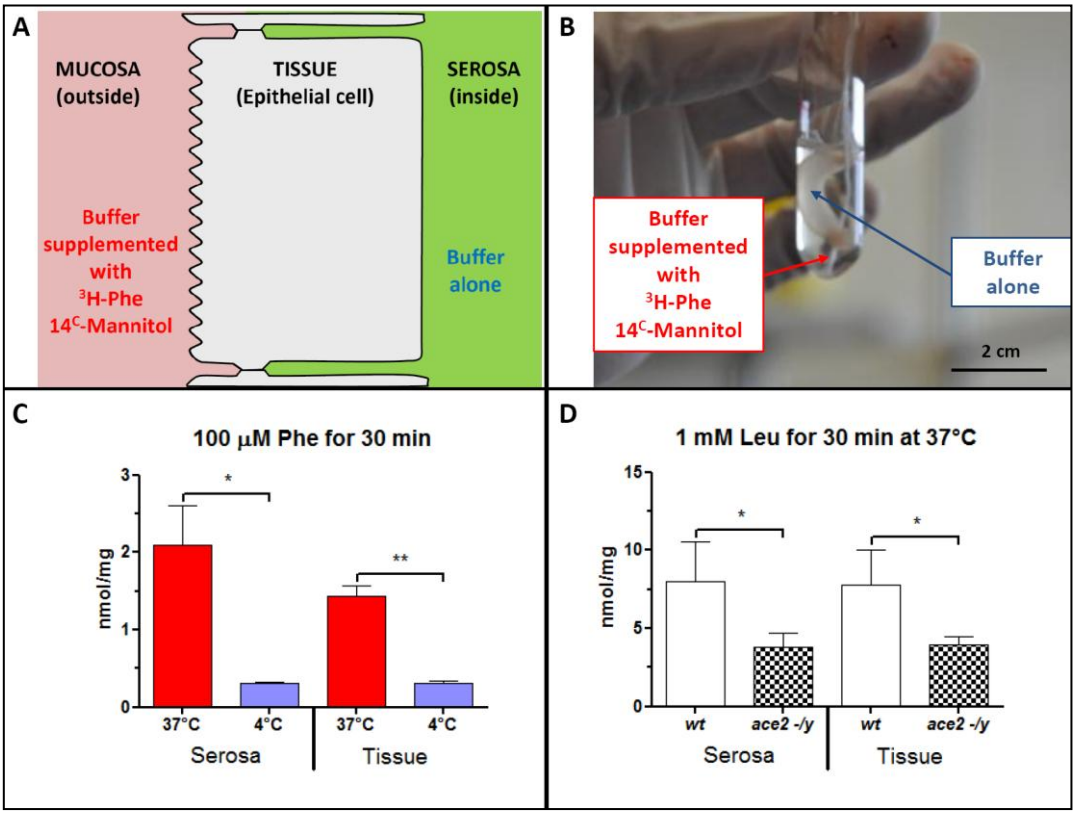

Fig. 17: the everted gut sacs technique and controls. A: schematic view of the epithelium in the everted gut sac assay. The substrates are applied form the outside of the bag, which after evertion corresponds to the mucosa. The buffer alone is applied in the serosa side (inside of the sac). Serosa and tissue radioactivity was measured with scintillation reaction. B: a representative picture of the experiment. Arrows indicate where the different buffers were applied. C: the transport was almost stopped when sacs were incubated in ice cold buffer. Thus, the majority of the transport measured at 37°C is active (transepithelial). D: *ace2*$^{-/y}$ tissues showed a reduced transport of Leu. This result is comparable to the one obtained with the intestinal ring technique (Camargo, Singer et al. 2009). Represented means ± SEM (n = 3 - 5). * indicates P<0.05 and ** P<0.01 by unpaired Student t-test.

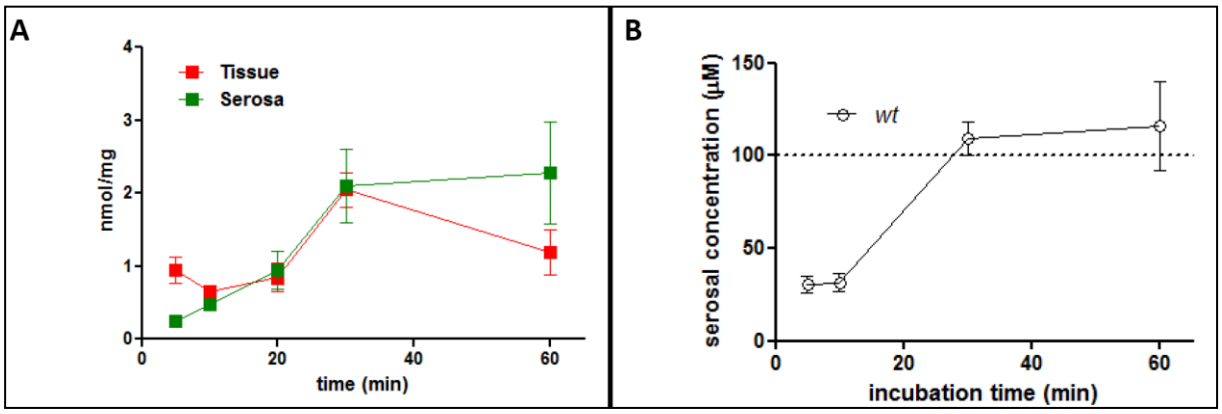

Fig. 18: Time course of transport rates and concentrations measured with everted gut sacs. A: time course in *wt* from mucosa to tissue (red) and mucosa to serosa (green). B: Absolute concentrations measured within the serosa at different time points. Represented means ± SEM (n = 5 - 10).

5.3.3 Everted gut sacs experiments with *tat1*$^{-/-}$

tat1$^{-/-}$ gut functionality was tested with the everted gut sacs technique to assess amino acids transport rates. The results for Phe are reported in the manuscript (see 5.2). The measured significant accumulation in the *tat1*$^{-/-}$ tissues parallels the 2-I-L-Phe accumulation in kidney epithelial cells observed with the microSPECT technique. However, due to the high variance, which is probably secondary to the heterogeneous expression of the transporters along the small intestine, and due to an effective small difference in transport, the transepithelial transport was not different (serosa). In the kidney this rate is likely to be impaired, as suggested by the aminoaciduria. Tyr has also been tested, since in contrast to Phe, Tyr is not well transported by *lat4* (Bodoy, Martin et al. 2005). Surprisingly, incubations of 10 and 60 min did not display a difference between *wt* and *tat1*$^{-/-}$ (Fig. 19). The measured rates were similar to the ones of Phe, with the exception of the 60 min serosa, which tended to reach much higher concentrations. More time points and probably higher concentrations should be considered in further analysis.

Using the *X. laevis* expression system, it was shown that Gln is released from oocytes expressing both *tat1* and *lat2*, but not from those expressing *lat2* solely (Ramadan, Camargo et al. 2007). To mimic that effect, Gln transport in *wt* and *tat1*$^{-/-}$ sacs was studied in presence and absence of Phe in mucosa or serosa (Fig. 20A). The concentrations were chosen in order to exceed the transport affinities (Meier, Ristic et al. 2002) in order to obtain an efficient apical transport and to saturate *lat2-4F2hc* exchanger. Indeed when a high concentration of Phe was applied in the serosa, a minor increase in Gln transport was observed in the *wt*. In contrast, the application of 100 µM Phe in mucosa did not reveal any trend of higher transport. In the same situation however, a significantly higher amount of Gln was transported in *tat1*$^{-/-}$. This unexpected trend was not reproduced by the transport of Ser in the presence of Phe (Fig. 20B) but only when Phe was substituted with Tyr (Fig. 20C). Currently there is no explanation for the unexpectedly high transport in the *tat1*$^{-/-}$. Nevertheless, since the measurement relies solely on the detection of the tritium in the solutions, the metabolism in the enteric cells must be taken into account. Indeed several non-essential amino acids, including Gln, have been shown to be extensively oxidized by the epithelial cells of the small intestine (Stoll, Henry et al. 1998; Wu 1998; Wu 2009). In contrast, Tyr should not be metabolized, as shown from first pass intestinal studies (Stoll, Henry et al. 1998; Wu 1998), whereas Phe is catabolized in a lesser extended (Biolo, Tessari et al. 1992; Hoerr, Matthews et al. 1993). In our assay the tracers could therefore have been degraded and the tritium transferred to water, which could consequently leave the cell and diffuse paracellularly. A validation of the transstimulation assay should therefore be achieved by measuring the effective concentration of the substrate by HPLC or by using 2-I-L-Phe, which would not be further metabolized. Furthermore, the turnover of the epithelial proteins should be investigated, to rule out the possibility of a different metabolism in *tat1*$^{-/-}$, which would cause the misinterpretations.

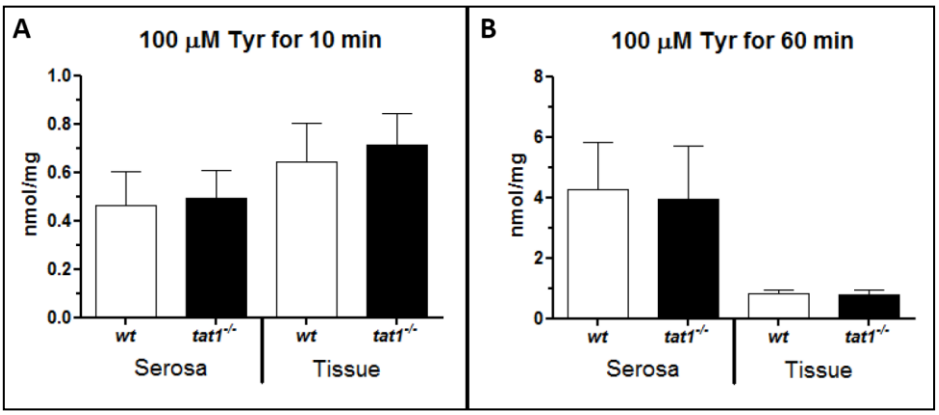

Fig. 19: *wt* and *tat1*$^{-/-}$ showed no difference in Tyr transport. Tyr transport displays similar rates than Phe upon 10 min incubation (A) and higher serosa accumulation after 60 min (B). *wt* and *tat1*$^{-/-}$ displayed the same rates overall. Represented means ± SEM (n = 5 – 6).

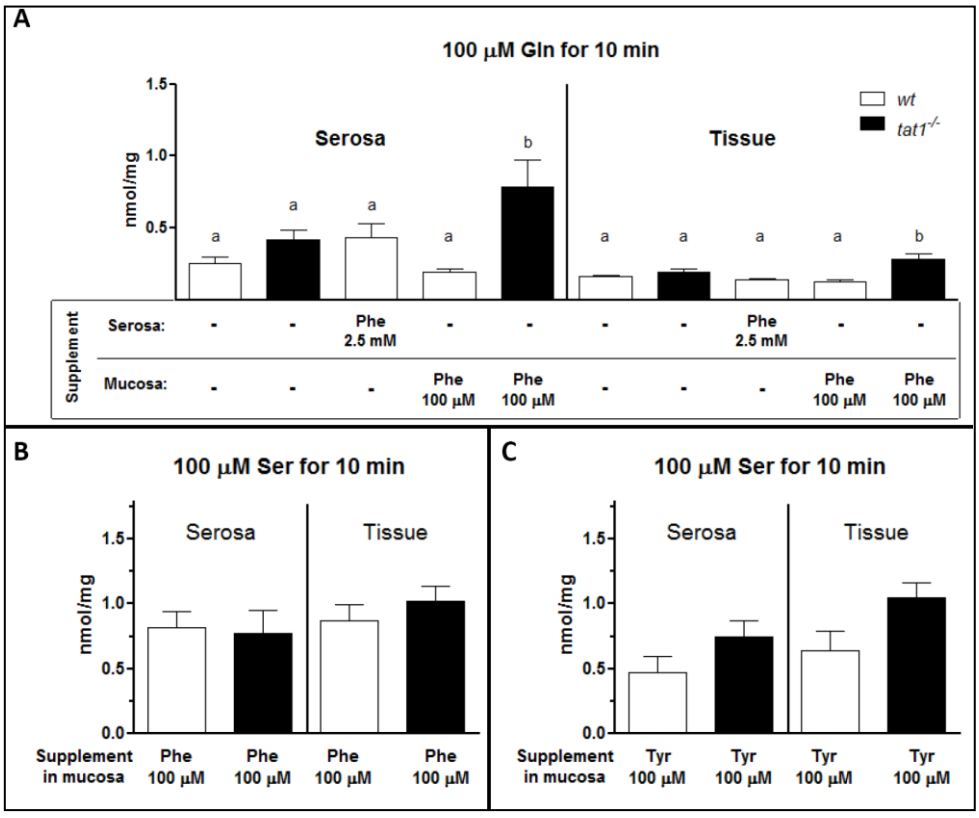

Fig. 20: Transstimulation of Gln and Ser transport by application of Phe and Tyr in mucosa or serosa. A: a small increase in serosal Gln transport was observed after application of Phe in serosa, but not in mucosa. *tat1*$^{-/-}$ tissues presented an unexpectedly high transport rate. B: no effect has been observed in the transport of Ser. C: after substitution of Phe with Tyr an effect in Ser transport was observed similarly to Gln. Groups were compared by one-way ANOVA, followed by Bonferroni post-test on selected pairs of columns. Values with letters are statistically different ($P<0.05$). Represented means ± SEM (n = 4 – 12).

5.3.4 Measurement of the glomerular filtration rate

It is well established that high plasma amino acids and postprandial state alters renal hemodynamics and lead to hyperfiltration (Castellino, Coda et al. 1986; Premen 1988; Castellino, Levin et al. 1990). It has been further demonstrated that different protein contents in the diet exert a similar effect (Sallstrom, Carlstrom et al. 2010). Since *tat1*$^{-/-}$ displayed high circulating aromatic amino acids (see manuscripts in 5.2 section), it is well conceivable that *tat1*$^{-/-}$ presents a higher gromerular filtration rate (GFR). In the assessment of the theoretical fractional excretion of amino acids in *tat1*$^{-/-}$, an invariable GFR was used as reference (Qi, Whitt et al. 2004). The data presented in the manuscript were derived by calculating the total amino acids excreted in 24 hours by knowing the total urinary volume. A common praxis in humans is to normalize the measured amino acid concentrations to the urinary creatinine. Although this is a well established procedure, the accuracy of such method in mice has been recently discussed: creatinine has been shown to be secreted along the nephron and therefore causes an overestimation of the real GFR; furthermore creatinine is proportional to the muscle mass and thus not homogeneous (Breyer and Qi 2010; Eisner, Faulhaber-Walter et al. 2010). Therefore an attempt to measure the real GFR by mean of inulin clearance has been made following a recently published protocol ((Sallstrom, Carlstrom et al. 2010) and material and methods section 4.1.8). The measurement were performed in 8 animals kept under normal protein diet (NPD, 20% casein) for baseline and under high (HPD, 40% casein) or low (LPD, 0% casein) protein diet for 8 days. The results indicated a clear decrease in the GFR in mice kept under the LPD, regardless of their genotype (Fig. 21A). In contrast under HPD there was an increase in GFR for the *wt*, but not for the *tat1*$^{-/-}$. This last observation contrasts with the initial hypothesis that in *tat1*$^{-/-}$ higher plasma amino acids would higher the GFR, however the high variability of the measured points suggest for caution in the interpretation. In fact, unsuccessful i.v. injections leaded to the exclusion of several animals (e.g. representative in Fig.21B and C): the wrong compartmental distribution of the bolus in the extracellular fluid caused an initial increase instead of a steep decrease in plasma activity. Furthermore the restrain of the animal caused variable stress, which in turn caused further difference in hemodynamics.

In conclusion, the use of the 24 hour volume to calculate the AA excreted amount appeared to be a more adequate system. However, if the unexpectedly low GFR observed in *tat1*$^{-/-}$ under HPD would be taken in account, it would not weaken the results but rather increase the magnitude of the presented phenotype in the manuscript (see 5.2).

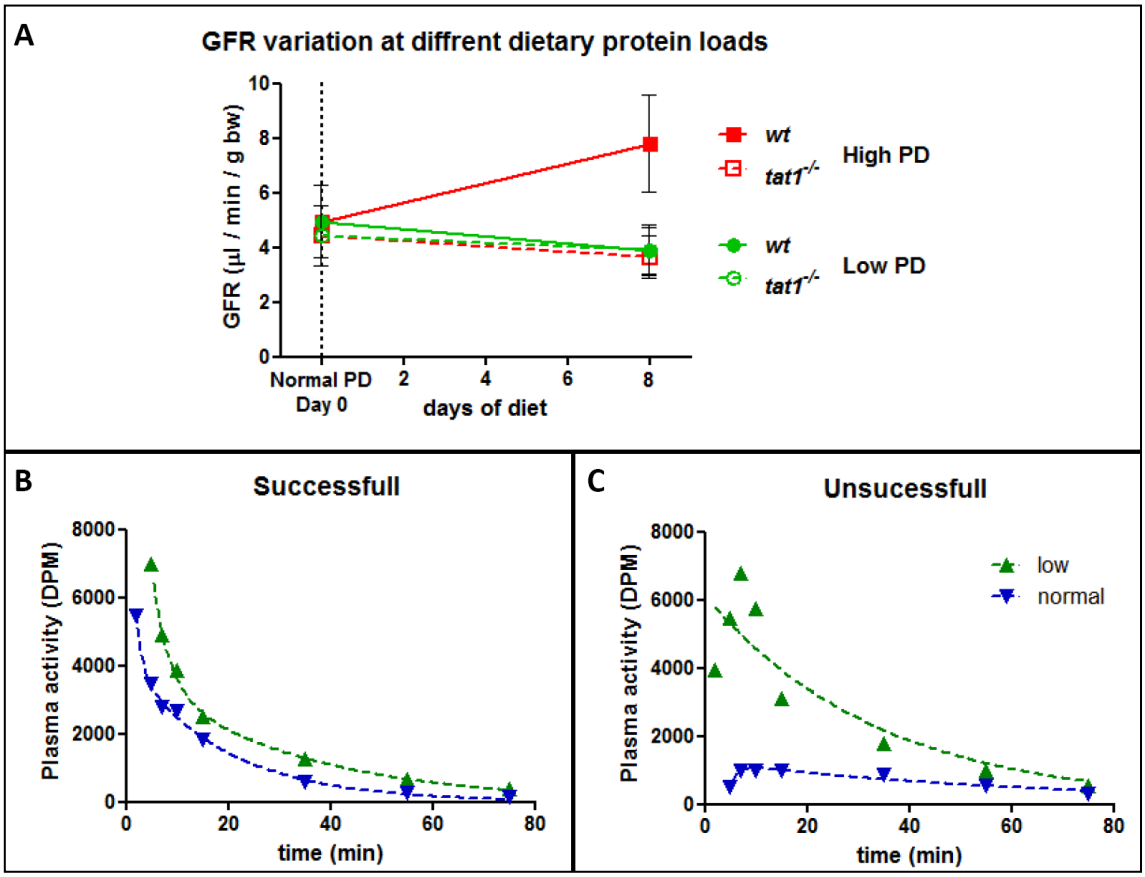

Fig. 21: Glomerular filtration rates (GFR) varies upon different protein loads in the diet. A: variation in the GFR measured after 8 days of low PD (0% casein) or high PD (40% casein). Represented means ± SEM (n = 6 – 8). **B**: example of a successful measurement in an animal, where a 2 exponential fit was possible. **C**: example of a bad quality measurement, discarded by the exclusion criteria: although fitting of the low PD data (green triangles) could be improved by the exclusion of the first 2 time points, the normal PD data (blue triangles) were abnormally low, probably due to a wrong i.v. injection.

6. *lat4* Mouse Model

6.1 Introduction

Immediately after the first *inter se* cross of *tat1*$^{+/-}$ animals, it appeared that the impact of *tat1* absence was not causing lethality. Furthermore, the analysis of *tat1*$^{-/-}$ urine showed an almost normal fractional reabsorption of all amino acids (Verrey, Singer et al. 2009). Thus, taken together all the results of the *tat1*$^{-/-}$ characterization discussed in the first part of this work (see section 5), suggest that one or more compensating mechanisms must take place to rescue the *tat1*$^{-/-}$ mice. As explained more extensively in the discussion of the manuscript (see 5.2), no upregulation of known amino acid transporters has been found in *tat1*$^{-/-}$. Therefore, one or more transporters normally present in the basolateral membrane should cover the compensatory role. We proposed that *lat4* (SLC43A2) could be involved in this action for several reasons. Firstly, Lat4 functions as facilitated diffusion transport for essential amino acids in a Na^+ independent manner (Bodoy, Martin et al. 2005), which exactly reflects the properties of *tat1*. Secondly, *lat4* present a narrow selectivity for BCAA, L-Met and L-Phe, thus sharing at least one substrate with *tat1*. Furthermore, *X. laevis* oocytes expressing *lat4* also showed minor transport of L-Trp and L-Tyr in both, uptake and competition assays (Bodoy, Martin et al. 2005). Third, *lat4* mRNA has been shown to be expressed in mouse small intestine and in kidney, but not in the liver (Bodoy, Martin et al. 2005). A last argument was provided by the substitution assay performed in the *X. laevis* oocytes expression system, where *lat4* could functionally cooperate with *lat2-4F2hc* in a way similar to *tat1* (Ramadan, Camargo et al. 2007).

As already discussed in the introductory part of this work, *lat4* belongs to the *slc43* gene family, which comprises 2 other members: *lat3* (SLC43A1) and *eeg1* (SLC43A3) (http://www.bioparadigms.org/slc, (Hediger, Romero et al. 2004; Broer 2008)). *eegl1* is an orphan transporter mostly expressed in fetus starting at embryonic day 7 but not during adulthood. Furthermore, *eegl1* did not show so far amino acid transport properties in the oocyte expression system (Stuart, Pavlova et al. 2001), in contrast to *lat3*, which transported several neutral amino acids. Nevertheless, *lat3* mRNA expression was confined to pancreas, skeletal muscles and liver (Babu, Kanai et al. 2003), and thus excluding its involvement in intestine and kidney. So far, the only other known amino acid uniporters are *CATs* (SLC7 family) (Verrey, Closs et al. 2004; Broer 2008; Verrey, Singer et al. 2009), that belong to the y^+ system because they transport cationic amino acids and that would thus not provide any neutral substrates to *lat2-4F2*.

In the light of all this evidences, we ordered a *lat4* knock out mouse (*lat4*$^{-/-}$) from the Phenogenomic center of Toronto (http://www.phenogenomics.ca/). ES cell line used to generate the knock out contained a gene trap allele with UPA gene trap vector (Shigeoka, Kawaichi et al. 2005) inserted in the 6th intron of *lat4* gene. This resulted in the truncation of the Lat4 protein. For more details, please consult the material and methods section (4.1.2).

6.2 Results

6.2.1 First crossings of *lat4* animals

The first crossings of animals from Toronto delivered in a mixed B6/ICR/129 background generated 89 pups, among which the majority of *lat4*$^{-/-}$ died prematurely. In fact, only one female survived and reached adulthood. The detailed list is reported in the following table:

Breeding pair Mother	Father		Number of pups at Birth	at weaning	Died	day of death
first round of crossing 01.2010						
lat4$^{+/-}$	***lat4***$^{+/-}$	A	8 (1k.o.)	7	1	8d
		B	14	12	2	5d/5d
		C	10	8	2	8d/8d
		D	no pups			
		E	8	5	3	8d/8d/8d
		F	6	5	1	8d
		G	8	5	3	8d/8d/8d
		H	9	9		
		I	no pups			
		K	5	3	2	8d/8d
		TOT:	68	54	14	
second round of crossing 07.2010						
lat4$^{+/-}$	***lat4***$^{+/-}$	A	6	5	1	8d (k.o.)
		B	10	7	3	6d/12d/12d
		C	3	3	0	
		D	9	8	1	9d (k.o.)
		E	6	4	2	3d/3d
		F	7	7	0	
		G	7	7	0	
		H	9	0	9	2d all
		I	3	2	1	4d
		K	6	6	0	
		L	8	8	0	
		M	8 (1k.o.)	8 (1k.o.)	0	
		N	7	6	1	4d
		TOT:	89	71	18	
first roud of crossing 01.2011						
lat4$^{-/-}$	***lat4***$^{+/-}$	A	11 (3k.o.)	10 (2k.o.)	1	4d (k.o.)
		B	0	0	0	
		TOT:	11	10	1	

6.2.2 Preliminary analysis of a survival family

As visible in table shown in section 6.2.1, the first generation of mice with mixed B6/ICR/129 background gave birth to one viable *lat4*$^{-/-}$ female (breeding pair M). The female presented no obvious phenotype and generated additional 3 *lat4*$^{-/-}$, among which 2 reached adulthood. Similar to their mother, the two survivors showed no obvious phenotype and, when paired with *lat4*$^{+/-}$ partners in the attempt to further generate knock outs, they both repeatedly failed. In particular, the offspring male failed to fecundate the respective *lat4*$^{+/-}$ partners, which did not show signs of pregnancy. The female never got pregnant either.

One *lat4*$^{-/-}$ animal was put into metabolic cage together with other *lat4*$^{+/-}$ and *wt*. The animals were sacrificed and organs prepared for histological and morphological analysis. The 7 month old *lat4*$^{-/-}$ male was slightly underweight (22.7 g) compared to the mean weight of its littermates (33.5 g). The *lat4*$^{-/-}$ presented a left renal hypertrophy (enlarged kidney) and a right renal atrophy (small kidney). The histological analysis of both kidneys on hematoxylin eosin stained sections showed a higher number of fibroblasts and mononuclear cells in the mesenchyme of the left kidney. Extensive fibrosis (collagenous fiber-like staining) and morphological similarities with a polycystic kidney were also observed. The right kidney showed less cell presence in the mesenchyme but higher level of fibrosis (Fig. 22). The other *lat4*$^{-/-}$ male showed less fibroblasts or mononuclear cells and no signs of kidney hypertrophy or atrophy.

In the overall, the kidney of *lat4*$^{+/-}$ showed no macroscopical difference. However, their section showed all over particular signs of local degeneration of the tubuli (e.g. arrows Fig. 23). Interestingly, this kind of microcyst formations were also reported in another haploinsufficient mouse, *pdk1*$^{+/-}$, which has been shown to be involved in the autosomal dominant polycystic kidney disease (ADPKD) (Bastos, Piontek et al. 2009). Nevertheless this observation must be confirmed by more detailed electron microscope images and a larger number of animals should be examined.

The testis the *lat4*$^{-/-}$ male showed less layers of spermatogenic epithelium in seminiferous tubule and fewer spermatogonium, primary and secondary spermatocytes have been found (Fig. 24). The spermatoid found in seminiferous tubule were also less numerous in *lat4*$^{-/-}$. Both, *lat4*$^{-/-}$ and *lat4*$^{+/-}$ presented no difference in liver, muscle, lung or heart if compared to *wt*. Similarly, there was no obvious bone marrow functional difference between groups, as judged by the ratio of cells with nucleus and those without nucleus in giemsa stained smeared slides.

At the age of 7 month, before sacrifice and organ collection, the *lat4*$^{-/-}$ male was housed in metabolic cages for urine collection. The total blood was also collected and the plasma analyzed for its amino acid content. The analysis of plasma showed minor differences in amino acid values between *lat4*$^{-/-}$ and *wt*: Pro and Asp were 30% less concentrated in the *lat4*$^{-/-}$ (Fig. 25A), whereas all other amino acids were only slightly less concentrated, with the exception of Trp, which was 20% more concentrated. The 24 hours urine analysis showed a peculiar pattern of amino acid loss: Ala, Val and Asp were more than 5 fold concentrated; Gly, Leu, Thr, Pro, Asn, Gln, Arg, His and Glu ranged between 2 and 5 fold more (Fig. 25B). Interestingly Ile and Met, two good substrates of *lat4*, were not significantly different. Surprisingly, the more prominent effect observed was the one of Asp, which is not a substrate of Lat4 (Bodoy, Martin et al. 2005). Phe was not detected in the urine of *lat4*$^{-/-}$. These data must be taken with caution, because the absence of further *lat4*$^{-/-}$ experimental mice limited the number to one single case. The comparison between *lat4*$^{+/-}$ and *wt* did not reveal differences (Fig. 25).

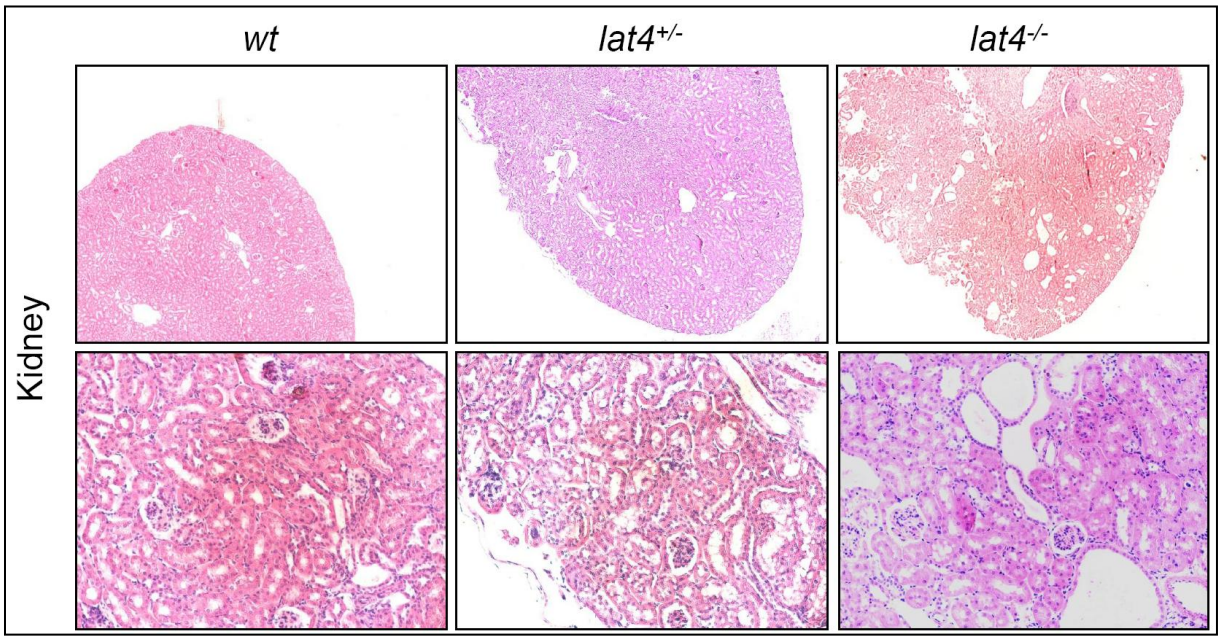

Fig. 22: Kidney sections stained with hematoxylin and eosin presented signs of fibroblast and mononuclear cells infiltration in the *lat4*$^{-/-}$ mesenchyma. Upper raw 4x magnification, below 20x.

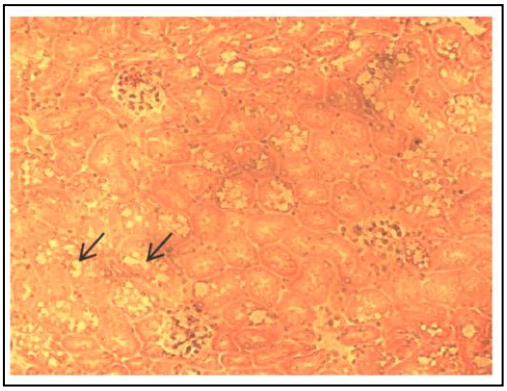

Fig. 23: Kidney section of *lat4*$^{+/-}$ showed microcyst formations, similarly to *pdk1*$^{+/-}$ phenotype (Bastos, Piontek et al. 2009). Hematoxylin and eosin kidney sections were overexposed. Microcysts were found all over the specimen. Arrows indicates two examples of microcysts. 20x magnification.

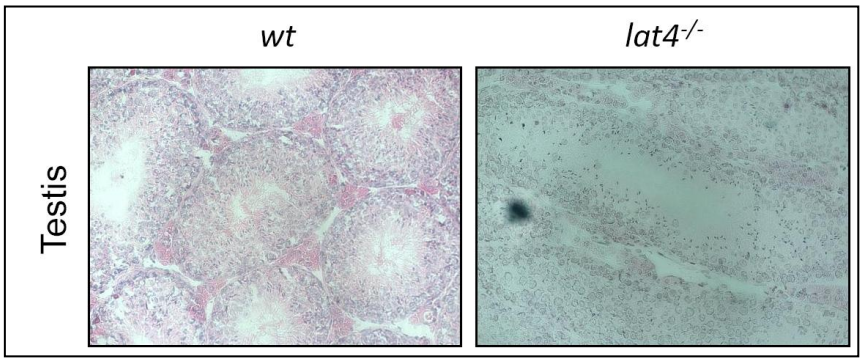

Fig. 24: sections of testis stained with hematoxylin and eosin presented less spermatocytes in the *lat4*$^{-/-}$. 20x magnification.

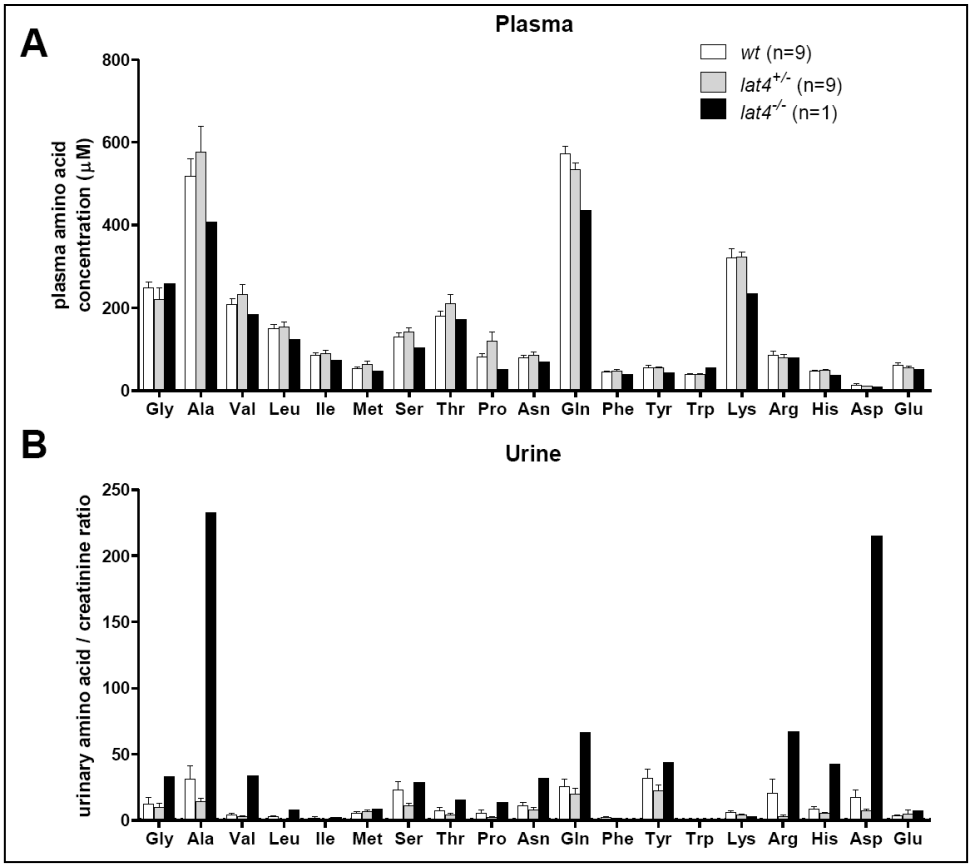

Fig. 25: The *lat4*$^{-/-}$ showed normal plasma values but higher urinary amino acids. A: plasma amino acid concentrations did not reveal significant differences between groups. Interestingly, Pro and Asp are less present in the knock out. B: many urinary amino acids normalized to the creatinine content showed much higher levels in the *lat4*$^{-/-}$. Represented mean ± SEM.

6.2.3 Preliminary analysis of animals backcrossed in C57BL/6 background

In parallel to the analysis of the B6/ICR/129 mixed *lat4*$^{-/-}$ mice, a backcross into the conventional C57BL/6 strain was set up. Once the 3rd backcross generation was reached, *lat4*$^{+/-}$ *inter se* crossings were set to further generate experimental animals. In the light of the small number of *lat4*$^{-/-}$ found in the first litters, an even more careful monitoring of the litter size and pup weight was performed. At birth, the nest presented a normal size (average of 8 animals per litter). Despite differences in each litter, the total number of animals per genotype was not significantly different than the ones obtained with a mendelian's distribution. The litters were distributed as follows:

Breeding pair			Number of pups			
Mother	Father		at Birth	***lat4***$^{-/-}$	***wt***	***lat4***$^{+/-}$
lat4$^{+/-}$	***lat4***$^{+/-}$	A	5	1	0	4
		A	9	1	7	1
		A	8	2	0	6
		B	7	2	4	1
		B	7	2	2	3
		B	8	2	0	6
		B	10	3	3	4
		TOT:	54	13	16	25
		Percentage:	100%	24%	30%	46%
		Expected:	100%	25%	25%	50%

At birth, all pups presented a normal color of the skin and the *lat4*$^{-/-}$ mice were undistinguishable from their littermates: the *lat4*$^{-/-}$ differed less than 15% in body size (average thorax length of 2.1 for *lat4*$^{-/-}$ versus 2.4 of *lat4*$^{+/-}$; Fig. 26). The milk spot, a white area in correspondence of the stomach caused by the presence of milk, was well visible 24 hours after birth and remained within the next days in all pups, suggesting that the suckling behavior was normal and all animals had normal access to food. 24 hours after birth the animals started to differ in their body weight and continued to have a smaller net weight gain in the following 24 hours (Fig. 27). Despite the fact that the percentage weight gain was only of 10% for the *lat4*$^{-/-}$ in contrast to the 25% of *wt* and *lat*$^{+/-}$, it stayed positive indicating that the mice did not lose weight. 48 hours after birth, the animals were sacrificed and their plasma and organs collected.

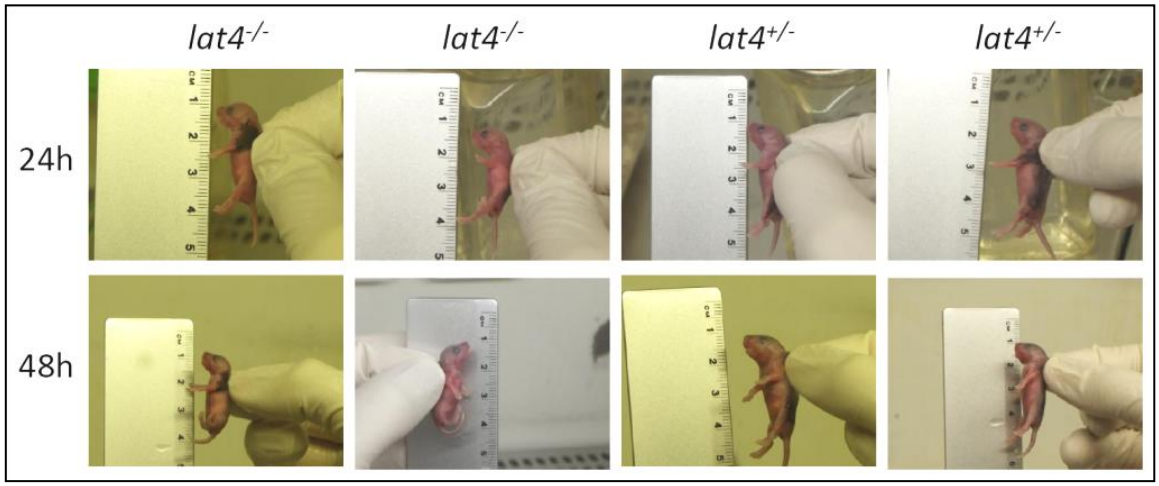

Fig. 26: the size of *lat4*$^{-/-}$ pups was less than 15% smaller than *lat4*$^{+/-}$ littermates and showed no other distinguishable marks. Pictures of littermates were taken 24 and 48 hours after birth. The thorax length was calculated as the measure between the basis of the neck and the basis of the tail: *lat4*$^{-/-}$ measured on average 2.1 cm whereas *lat4*$^{+/-}$ 2.4 cm.

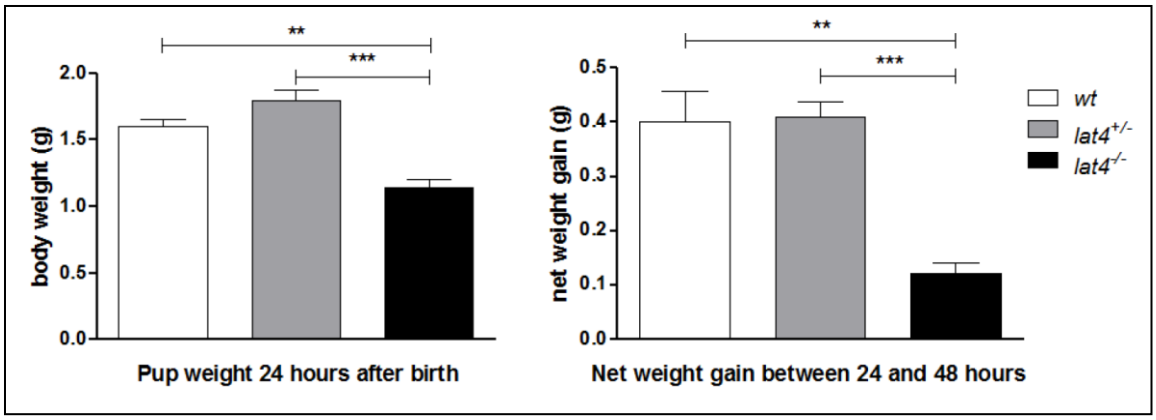

Fig. 27: 24 hours after birth, *lat4*$^{-/-}$ weighted less and continued to grow less within the following 24 hours. Left: average body weight measured 24 hours after birth in the same litter. Right: average net weight gain of the same animals between 24 to 48 hours after birth. Represented means ± SEM (n = 3 to 6). ** indicates P<0.01, *** P<0.001 and by unpaired Student t-test.

6.2.4 Lat4 localization

Bodoy and co-workers concluded based on "in situ hybridization" that *lat4* mRNA is presumably expressed in the epithelial cells of the distal tubule and the collecting duct of the kidney as well as in the intestine, being mainly present in the cells of the crypts (Bodoy, Martin et al. 2005). The inspection of the proposed images showed indeed strong signals in distal tubular segments and a fainter staining in proximal tubule cells. With regard to the intestine, a strong signal was present in the crypts and a faint signal was also visible in the enterocytes of the villi. The first approach was to micro-dissect the kidney into its different component (See introduction 3.2.3), extract mRNA from proximal convoluted (PCT) and proximal straight tubule (PST) and perform quantitative PCR analysis of different transporters. The results showed that *lat4* was expressed in both segments, with a higher expression in the PST, where *tat1*, *lat2* and *4F2hc* were no longer expressed (Fig. 28). Here *XT2* and B^0AT1 were used as markers for the proper selection of the segments: *XT2*, which was recently renamed B^0AT3, is expressed in the late proximal straight tubule (PST); B^0AT1 localizes to the early proximal convoluted tubule (PCT) (Romeo, Dave et al. 2006; Singer, Camargo et al. 2009).

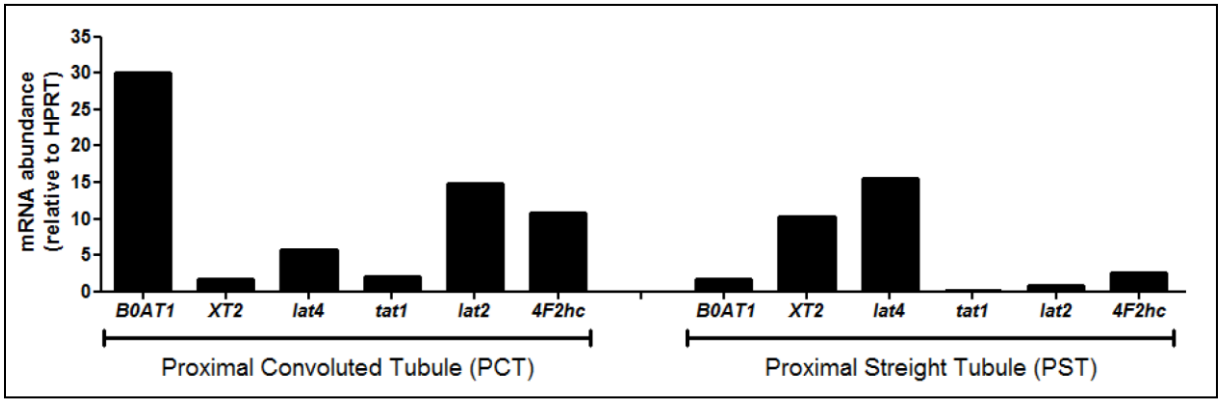

Fig. 28: microdissection of kidney revealed that *lat4* is expressed in PCT and PST, whereas *tat1*, *lat2* and *4F2hc* only in the PCT. B^0AT1 and *XT2* are controls for PCT and PST respectively. (n = 1).

7. Discussion and Outlook

7.1 Discussion

7.1.1 Advances in the characterization of the AA transporters

In the past decades, very large progress in the characterization of AA transporters has been made. For more details see the introductory part (3.2). Briefly, the first discoveries allowed the classification of transport systems based on their physicochemical, stereospecific, inhibitors and selectivity properties (Stevens, Ross et al. 1982; Verrey, Singer et al. 2009). A second big progress in the characterization of AA transporters was done with the molecular identification, DNA cloning and cellular expression that allowed the biochemical and more precise functional characterization of several AA transporter proteins (Verrey, Singer et al. 2009). In particular, the transport properties were studied with the expression of cloned transporters in *Xenopus laevis* oocytes and with the analysis of uptake and efflux rates of radiolabeled substrates. In parallel to the characterization of exogenously expressed AA transporters, the localization of several of these proteins in different tissues and at subcellular level has been established. Thereby the idea of complex transporter machineries that involves several membrane proteins and that work together took place. In this respect, the selective co-expression of selected transporters in the heterologous system allowed the identification of functional cooperations, like the one proposed for TAT1 and Lat2-4F2hc (Ramadan, Camargo et al. 2007). Finally, much progress in the identification of transport proteins has been made by the analysis of the etiology of inherited disorders that display specific losses of AAs in the urine (Verrey, Ristic et al. 2005; Broer 2008). Among those Hartnup disorder, Cystinuria, Lysinuric protein intolerance and Glycinuria. Many of these disorders were attributed to compromised apical transport (Tab. 4), contributing to the fact that the basolateral membrane transport remained less characterized.

A recent investigation tool is the analysis of specific knock out animal models. Similarly to the study of the inherited disorders, the knock out mouse models allow to study the impact of the absence of one transporter protein on the whole body. Several animal models of apical transporters have indeed been reported: B^0AT1, B^0AT3, Tmem27, Ace2, Pept1 and Pept2 (Bohmer, Broer et al. 2005; Daniel, Spanier et al. 2006; Danilczyk, Sarao et al. 2006; Camargo, Singer et al. 2009; Singer, Camargo et al. 2009; Broer, Juelich et al. 2011; Nassl, Rubio-Aliaga et al. 2011). Overall, these animals could at least partially compensate for the absence of the transporter and showed in general a mild phenotype similar to what we reported for *tat1*$^{-/-}$: minor reduction in body weight and mild aminoaciduria. This agrees with a certain degree of functional overlap, which is probably due to their essential role.

Only one knock out mouse of the basolateral AA transport machinery has been reported so far: *lat2*$^{-/-}$ (*slc7a8*) (Braun, Wirth et al. 2011). The knock out was generated by the insertion into the second *lat2* exon of a cassette, which causes a premature truncation of the protein. Similarly to apical knock outs, this *lat2*$^{-/-}$ mouse showed a mild phenotype: the mice were undistinguishable in body size and weight, but showed several small neutral AAs elevated in serum and lost in urine (Braun, Wirth et al. 2011). The parallelism between both suggested for an unchanged fractional excretion. Only a subset of Lat2-4F2hc substrates was affected and the aromatic AAs were normal. Based on this observation and on a slight, non significant, increase in *tat1* mRNA level, the authors proposed a compensatory involvement of TAT1. The impairment in the AA homeostasis was not further analyzed, since the authors aimed at investigating the involvement of *Lat2* in thyroid hormone homeostasis.

In this work we analyzed the impact of the absence of two uniporters, TAT1 and Lat4, using the respective knock out mouse models. The results presented in chapters 5 and 6 are discussed in the next paragraphs (7.1.2 and 7.1.3).

7.1.2 *tat1* mouse model

The main results on *tat1*$^{-/-}$ are discussed in the manuscript in section 5.2. An extended summary: is Described in this section:

1. We could show that elevated aromatic AAs in the circulation are caused by the lack of TAT1 function, which prevents their equilibration between plasma and liver cells. In the *wt*, the hepatocytes work as sink for aromatic AAs and therefore regulate the plasma concentration by clearing the aromatic AAs and further metabolizing them (Schimassek and Gerok 1965; Moundras, Remesy et al. 1993; Brosnan 2003; Gropper 2005). The absence of *tat1* prevented this action; therefore, the aromatic AAs were accumulated in the plasma. Indeed the cytosolic AA concentration in the hepatocytes was normal, whereas in the other major AA pool (i.e. the skeletal muscles) they paralleled the plasma (Fig. 29A). A similar investigation could potentially reveal the cause of the elevated AAs in the *lat2*$^{-/-}$ (see 7.1.2). Uptakes with primary derived hepatocytes of *wt* and *tat1*$^{-/-}$ could potentially allow a more detailed study of the fluxes between plasma and liver. Interestingly in the past, studies have similarly been conducted and transport system identified (e.g. (Fafournoux, Remesy et al. 1983), although without being done in specific knock out context. The liver homeostatic function has also been discussed in the context of hepatic encephalopathy, where a rise in the so-called Fisher ratio (AAA / BCAA) has been reported (James, Ziparo et al. 1979; Dejong, van de Poll et al. 2007). In this work we showed that TAT1 is involved in this homeostatic process and that interestingly an alteration in the Fisher ratio in our mouse model seems not to lead to the neurological disease, in contrast to what has been previously hypothesized (Fischer, Rosen et al. 1976; Dejong, van de Poll et al. 2007). Furthermore, we showed that the brain function in *tat1*$^{-/-}$ mice seems not to be affected. This is not completely surprising since *tat1* was not shown to be expressed in the blood brain barrier, which would prevent an accumulation of TAT1 substrates (Lyck, Ruderisch et al. 2009; Abbott, Patabendige et al. 2010). However a complete behavioral screen (e.g. open field, elevated T-maze, hanging resistance, etc.) in the search of signs of anxiety and fear has not been perform to definitively rule out such phenotype. Furthermore, a quantification of serotonin and catecholamine levels in the brain could also be performed.

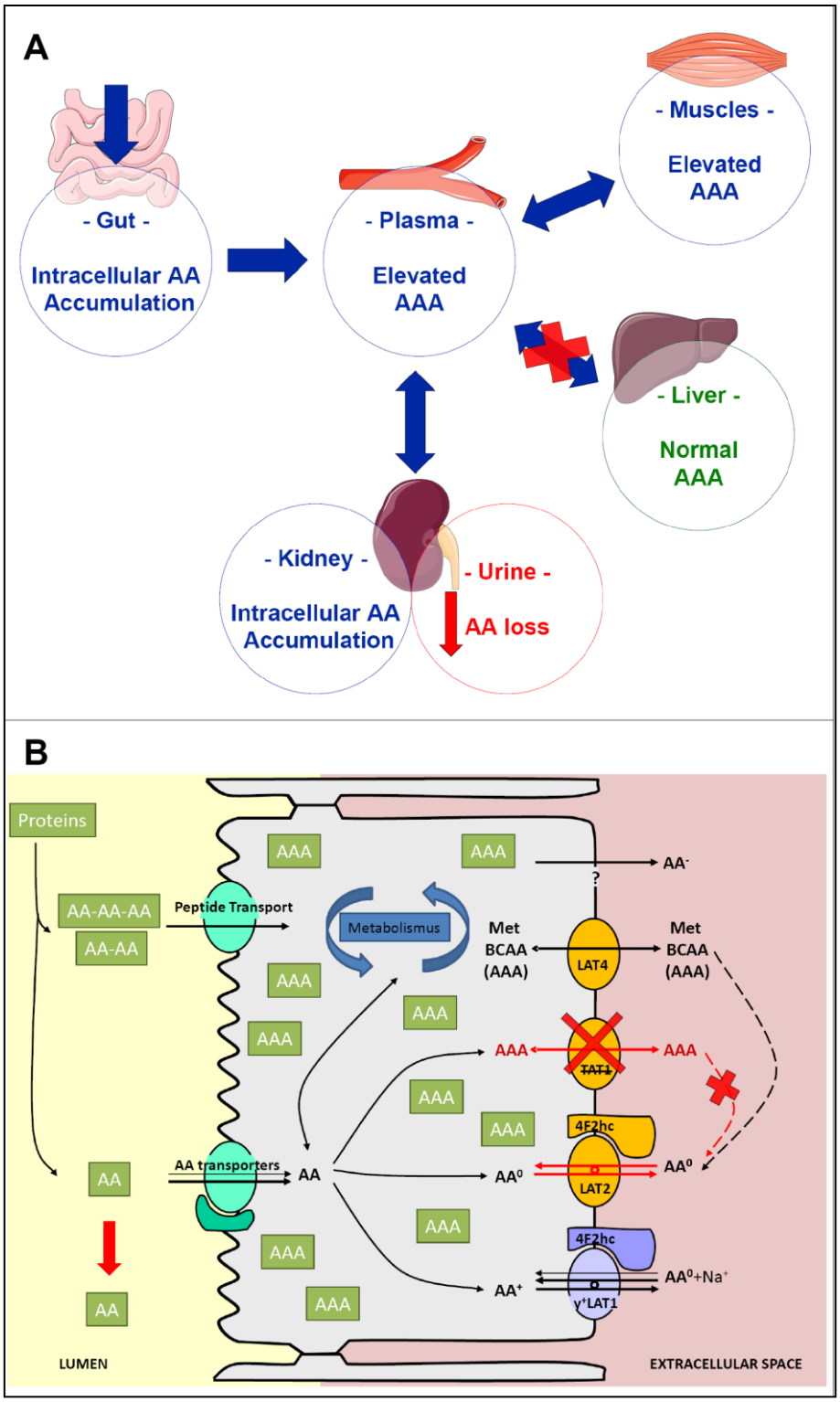

Fig. 29: schematic representation of the impairments observed in *tat1*$^{-/-}$ mice. A. The absence of TAT1 caused the uncoupling of liver and plasma aromatic AAs. As a result, *tat1*$^{-/-}$ show elevated aromatic AAs in plasma and skeletal muscle, whereas the liver metabolism regulates its own concentration. One or more compensatory transporter(s) with similar properties as TAT1 probably covers TAT1 function in muscles and epithelial cells of small intestine and kidney. We propose that this is done to a large extent by Lat4. An intracellular accumulation of AA due to defective basolateral export was observed in epithelia. Major losses of AAs were found in the urine of *tat1*$^{-/-}$ under high protein diet. B. Schematic representation of an epithelial cell, with intracellular accumulation of AAA due to impaired export caused by TAT1 absence and unpaired Lat2-4F2hc substrate recycle (red crosses). The accumulation leads to a consequent block of apical import and thus to AA losses (red arrow).

2. We could show that under normal diet conditions the basolateral transport machinery in kidney proximal tubule and small intestine epithelia is not severely impaired by the absence of TAT1. No compensatory increase of other AA transporters (mRNAs) was found suggesting that the residual aromatic AA transport capacity and the paracellular pathway could compensate TAT1 deficit. Under a dietary high protein load a massive presence of aromatic AAs and, in lesser extent, of Lat2-4F2hc substrates was found in *tat1*$^{-/-}$ urine suggesting that the maximal transport rate was exceeded in the kidney proximal tubule. We propose that under normal protein diet the concentration is already within the so-called splay, where some nephrons have not anymore the capacity of reabsorbing all substrates. Under high protein diet the transient absorptive increase of plasma AAs results in their spillover. To test this hypothesis the collection of the urine and the plasma could be divided into absorptive and postabsorptive phases. This would however require a difficult entrainment of the animals or an efficient monitoring. The urinary pattern further suggests the involvement of Lat4, which is also a facilitated diffusion pathway, because it transports more efficiently Phe than Tyr and Trp. The involvement of a paracellular component as compensatory mechanism remains controversial, especially in the intestine. Recently, the absence of the AA transporter B^0AT1 was reported to potentially influence the paracellular permeability, as indirectly studied by the decrease in thight junction proteins, Occludin and Claudin-2 (Broer, Juelich et al. 2011). Our data suggest that this pathway might be more pronounced in the small intestine, where the net transport measured with everted gut sacs did not show a significant difference between *wt* and *tat1*$^{-/-}$. However, the mannitol, which was especially used to control the paracellular permeability and leakiness, did never parallel the steep accumulation of the tested AAs (see 5.3.2 and 5.3.3). Furthermore, a difference between *tat1*$^{-/-}$ and *wt* in mannitol transport has not been observed. The Phe inside of the sac did never exceed the concentration in the outside, which suggest for a certain equilibration process in the sac. An enteric perfusion and portal vein sampling could be applied to further investigate the gastrointestinal functionality of *tat1*$^{-/-}$.

3. We showed with the microSPECT and everted gut sac techniques that the decreased epithelial transport may be caused by an intracellular AA accumulation, which leads to a subsequent decrease of apical transport (Fig. 29B). The impairment of TAT1 did not only affect the aromatic AA reabsorption but also the one of other neutral AAs transported by the exchanger Lat2-4F2hc, as indicated by the urinary pattern under high protein diet (see 5.2). In TAT1 absence thus it is most likely that the exchanger did not anymore have recycling substrate needed for its proper function. Therefore, these data agree with a functional cooperation between TAT1 and Lat2-4F2hc proposed by Ramadan et al. (Ramadan, Camargo et al. 2007). In the small intestine a significant accumulation of Phe has been observed in the *tat1*$^{-/-}$ tissue with the everted gut sac assay despite a high variability, which might reflect the heterogeneous expression of the transporters along the intestinal tract. MicroSPECT assay showed a clear accumulation of 2-I-L-Phe in both kidneys 30 minutes after i.v. injection (see 5.2). This tracer was shown previously in *X. laevis* oocytes expressing TAT1, Lat4 and Lat2-4F2hcto be transported as Phe. To test a potential change in liver accumulation of Phe an oral bolus administration of tritiated Phe was performed. This did not reveal a difference in liver accumulation between *tat1*$^{-/-}$ and *wt* (data not shown). We hypothesize that the enteric and hepatic metabolism degraded the traced AA and prevented a differential accumulation in the liver despite the absence of TAT1.

4. A defect in *tat1* has been predicted to be the cause of the blue diaper syndrome (Kim et al., 2001; Broer, 2008; Broer and Palacin 2011). This syndrome was initially described by Drummond and co-workers in 1964 and appears to be extremely rare since only 3 cases have been reported (Drummond et al., 2964; Chen et al., 1991; Hoffman, Zschocke and Nyhan). Since an excess of Trp was found in stool of the patients, it was proposed that the intestinal bacteria convert the Trp into indoles, which are in turn metabolized by the liver into indican and subsequently released into urine or feces. Upon oxydation excreted indicans become indigo, causing a peculiar bluish color of the diaper (Broer et al., 2008). Despite a different bacterial flora, which would not allow to ultimately exclude an involvement of *tat1* by the absence of bluish pigments in feces or urine in *tat1*$^{-/-}$, *tat1*$^{-/-}$ data suggest that this is more

unlikely to be. First of all, in contrast to what *tat1*$^{-/-}$ showed, the children suffered from low circulating Trp and did not present specific urinary losses (Drummond et al., 1964). Furthermore, an analysis of AA luminal content in the distal part of the small intestine did not reveal significant differences in Trp amounts between *tat1*$^{-/-}$ and *wt* littermates (See 5.2), which indicates that the defect on *tat1* is not sufficient to cause such a dramatic accumulation of Trp. It is possible that the etiology of the disease is polygenic involving *tat1* and other(s) AA transporters, as reflected in the low incidence of the disease.

5. When subjected to a low protein diet for 8 days both, *tat1*$^{-/-}$ and *wt*, showed a drastic decrease of urinary AAs (Fig. 16B in paragraph 5.3.1). This phenomenon is thus probably not related with the genotype but it opens new perspectives: how is this mechanism happening and why? It is conceivable that the kidney proximal tubule reacts upon starvation in order to protect the organism against deleterious AA losses. Since the AAs in plasma were maintained within normal levels, it could be that the kidney produces more transporter protein in order to reabsorb a larger fraction of AAs.

7.1.3 *lat4* mouse model

In light of the results about *tat1*$^{-/-}$ phenotype, a *lat4*$^{-/-}$ has been generated with the aim to identify a potential compensatory role. The results reported in chapter 6.2.2 about the mixed background *lat4*$^{-/-}$ survivor family should be taken with caution because the genotype was confirmed by repeated PCRs but not yet at protein level. Furthermore, the analysis was limited to very few animals because of the unsuccessful attempt to generate other *lat4*$^{-/-}$. In summary, one *lat4*$^{-/-}$ female reached adulthood, showed first no particular phenotype and gave birth to other three *lat4*$^{-/-}$, among which two males reached adulthood. Those latter failed to generate offsprings and lately a histological analysis showed a little number of spermatozoids in their testis. Further analysis was performed at relatively old age. One animal showed a left renal hypertrophy and a right renal atrophy with signs of fibrosis. *lat4*$^{+/-}$ kidney presented microcyst formations reminiscent of *pdk1*$^{+/-}$, which has been shown to be involved in the development of autosomal dominant polycystic kidney disease (Bastos, Piontek et al. 2009). Nevertheless, this observation has not yet been confirmed by more detailed electron microscope imaging. Finally, plasma AA values were lying within normal ranges, whereas 24 hour urine presented elevated levels of several AAs. This last measurement should also be taken with caution due to the above mentioned renal hyper- and atrophy and the late time point of observation. Although one cannot exclude that this survivor family had a second mutation that could compensate the deleterious effect of the absence of Lat4, the relatively normal phenotype of this mouse remains still controversial. The ongoing experiment with the polyclonal antibody, that showed specificity for mLat4, will allow the confirmation of the genotype. Furthermore, a series of backcross with an original 129S strain would elucidate whether that particular background has a rescuing effect on the *lat4*$^{-/-}$ phenotype. It is not excluded that a difference between 129S and C57BL/6 strains might explain such a protective differential impact of *lat4* defect.

Our preliminary results presented in chapter 6.2.3 about the backcrossed *lat4*$^{-/-}$ mice clearly indicate that the mutation has a lethal impact, at least in the C57BL/6 background. The *lat4*$^{-/-}$ newborns were normal at birth but showed a reduced increment in body weight within the following 48 hours: average body weight at 24 hours after birth of 1.1 g for *lat4*$^{-/-}$ versus 1.6 g for *wt* and a net weight gain of 0.1 g versus 0.4 g between 24 and 48 hours (Fig. 27). Therefore the fetal development seems to be normal and the defect in *lat4* appears to be prominent from within the first hours of life. All *lat4*$^{-/-}$ newborns presented a so-called milk spot (a white area caused by the milk in the stomach region), which suggests that the suckling behavior was not impaired and that the mother did not reject the *lat4*$^{-/-}$ offspring. Furthermore, *lat4*$^{-/-}$ pups were reactive and did not present signs of apathy. The mild increase in body weight suggests that the *lat4*$^{-/-}$ intestine could still absorb a substantial degree of nutrients. Further analysis should aim at elucidating the effective *lat4*$^{-/-}$ intestine transport capacity.

7.2 Outlook

In this work we identified an important function of *tat1* for the maintenance of the aromatic AA homeostasis by equilibrating plasma and hepatocytes. This is of particular interest because it attributes for the first time a housekeeping function to a high capacity uniporter, which does not allow an intracellular accumulation of the substrates. Similar analysis should be performed in other knock out mice models that displayed elevated AA in plasma. Furthermore, future studies should aim to characterize the AA transport machinery in the metabolic organs like muscles and liver to better elucidate the role of AA transporters in the regulation of interorgan AA transport reviewed by Brosnan (Brosnan 2003).

In the light of the minor difference in net epithelial transport displayed by our *tat1*$^{-/-}$ and by the published *lat2*$^{-/-}$ (Braun, Wirth et al. 2011), the generation of a double knock out mouse and the analysis of its urinary pattern might elucidate whether other compensatory mechanism are taking place or not. The generation of *lat4* combinatorial knock outs is less promising due to the lethality observed in *lat4*$^{-/-}$. However, the analysis of the urinary pattern of *lat4*$^{+/-}$ in the context of *tat1*$^{-/-}$ and *lat2*$^{-/-}$ might confirm the compensatory role of *lat4*.

The data interpretation of everted gut sacs, microSPECT/CT and tracer administration of in *tat1*$^{-/-}$ has been problematic, probably due to complex metabolic responses and adaptations. A future challenge will be the generation of cell lines with reconstituted transport machinery and the isolation of primary cells for *in vitro* flux studies. This would probably allow controlling the environment and therefore to generate mathematical flux models that would predict AA dynamics in single organs. Furthermore, some additional approaches like microperfusions, micropuncture and microdialysis might allow the validation of the model by dynamic probes sampling.

Finally, the study of different protein rich diets (see 5.3.1) opened new questions about the regulation of transporter proteins: does a specific molecular response to high / low protein load take place in the epithelia? Is such a response different in kidney epithelia than in small intestine in order to fulfill different functions (e.g. avoid waste versus maximize import)? What is the regulatory pathway and how are the AAs sensed? The first approach could be the investigation of up- or down-regulation of the different AA transporters within the different protein diet. Furthermore, a regulation at the level of membrane trafficking should also be included. For instance a phosphorylation site that might act as regulatory element has been found in both, Lat4 and Lat2 (Feric, Zhao et al.). *tat1* presents in the N-terminus a PEST sequence, which has been correlated to a high turnover degree (Rechsteiner and Rogers 1996). More in general, it was demonstrated that Leu plays a role in the control of food intake by AMP-activated protein kinase and mTOR pathway (Cota, Proulx et al. 2006; Lynch, Gern et al. 2006). Nevertheless, the whole mechanism is still not fully understood. Interestingly, a recent publication linked impaired feeding behavior with *pept1*$^{-/-}$ mouse only in the presence of a high protein diet (Nassl, Rubio-Aliaga et al. 2011). The effect was linked to a probable decreased Leptin signaling in the brain and an Arg cross-talk. In nutritional sciences, it becomes evident that the study of nutrients needs to be coupled with the study of the effect that it generates on the transcriptome, proteome and metabolome, since all factors are closely interconnected (Rist, Wenzel et al. 2006; Kussmann, Rezzi et al. 2008). The study of metabolomics has become possible thanks to advance in technologies like liquid chromatography, mass spectrometry and nuclear magnetic resonance spectroscopy. These allow the simultaneous analysis of thousand of metabolites. The future challenge will then be to interconnect all the different informations into a biological hypothesis and on *in silico* model by mean of informatics (Kussmann, Rezzi et al. 2008). These would also allow finding more subtle metabolic compensations in the general homeostasis caused by defective AA transporters with housekeeping function.

8. References

Abbott, N. J., A. A. Patabendige, et al. (2010). "Structure and function of the blood-brain barrier." Neurobiol Dis **37**(1): 13-25.

Altun, A. and B. Ugur-Altun (2007). "Melatonin: therapeutic and clinical utilization." Int J Clin Pract **61**(5): 835-45.

Augustin, M., R. Sedlmeier, et al. (2005). "Efficient and fast targeted production of murine models based on ENU mutagenesis." Mamm Genome **16**(6): 405-13.

Babu, E., Y. Kanai, et al. (2003). "Identification of a novel system L amino acid transporter structurally distinct from heterodimeric amino acid transporters." J Biol Chem **278**(44): 43838-45.

Baker, D. H. (2009). "Advances in protein-amino acid nutrition of poultry." Amino Acids **37**(1): 29-41.

Ballard, S. T., J. H. Hunter, et al. (1995). "Regulation of tight-junction permeability during nutrient absorption across the intestinal epithelium." Annual review of nutrition **15**: 35-55.

Barthe, L., J. F. Woodley, et al. (1998). "An improved everted gut sac as a simple and accurate technique to measure paracellular transport across the small intestine." Eur J Drug Metab Pharmacokinet **23**(2): 313-23.

Bastos, A. P., K. Piontek, et al. (2009). "Pkd1 haploinsufficiency increases renal damage and induces microcyst formation following ischemia/reperfusion." J Am Soc Nephrol **20**(11): 2389-402.

Bauwens, M., T. Lahoutte, et al. (2007). "D- and L-[123I]-2-I-phenylalanine show a long tumour retention compared with D- and L-[123I]-2-I-tyrosine in R1M rhabdomyosarcoma tumour-bearing Wag/Rij rats." Contrast Media Mol Imaging **2**(4): 172-7.

Bier, D. M. (2003). "Amino acid pharmacokinetics and safety assessment." J Nutr **133**(6 Suppl 1): 2034S-2039S.

Biolo, G., P. Tessari, et al. (1992). "Leucine and phenylalanine kinetics during mixed meal ingestion: a multiple tracer approach." Am J Physiol **262**(4 Pt 1): E455-63.

Bodoy, S., L. Martin, et al. (2005). "Identification of LAT4, a novel amino acid transporter with system L activity." J Biol Chem **280**(12): 12002-11.

Bohmer, C., A. Broer, et al. (2005). "Characterization of mouse amino acid transporter B0AT1 (slc6a19)." Biochem J **389**(Pt 3): 745-51.

Boron, W. F. and E. l. Boulpaep (2005). Medical Physiology, Elsevier.

Braun, D., E. K. Wirth, et al. (2011). "Aminoaciduria, but normal thyroid hormone levels and signalling, in mice lacking the amino acid and thyroid hormone transporter Slc7a8." Biochem J **439**(2): 249-55.

Breyer, M. D. and Z. Qi (2010). "Better nephrology for mice--and man." Kidney Int **77**(6): 487-9.

Broer, A., T. Juelich, et al. (2011). "Impaired nutrient signaling and body weight control in a Na+ neutral amino acid cotransporter (Slc6a19)-deficient mouse." J Biol Chem **286**(30): 26638-51.

Broer, S. (2008). "Amino acid transport across mammalian intestinal and renal epithelia." Physiol Rev **88**(1): 249-86.

Broer, S. (2008). "Apical transporters for neutral amino acids: physiology and pathophysiology." Physiology (Bethesda) **23**: 95-103.

Broer, S. and M. Palacin (2011). "The role of amino acid transporters in inherited and acquired diseases." Biochem J **436**(2): 193-211.

Brosnan, J. T. (2003). "Interorgan amino acid transport and its regulation." The Journal of nutrition **133**(6 Suppl 1): 2068S-2072S.

Brosnan, J. T. (2003). "Interorgan amino acid transport and its regulation." J Nutr **133**(6 Suppl 1): 2068S-2072S.

Caballero, B., R. E. Gleason, et al. (1991). "Plasma amino acid concentrations in healthy elderly men and women." Am J Clin Nutr **53**(5): 1249-52.

Cals, M. J., P. N. Bories, et al. (1994). "Extensive laboratory assessment of nutritional status in fit, health-conscious, elderly people living in the Paris area. Research Group on Aging." J Am Coll Nutr **13**(6): 646-57.

Camargo, S. M., D. Singer, et al. (2009). "Tissue-specific amino acid transporter partners ACE2 and collectrin differentially interact with hartnup mutations." Gastroenterology **136**(3): 872-82.

Castellino, P., B. Coda, et al. (1986). "Effect of amino acid infusion on renal hemodynamics in humans." Am J Physiol **251**(1 Pt 2): F132-40.

Castellino, P., R. Levin, et al. (1990). "Effect of specific amino acid groups on renal hemodynamics in humans." Am J Physiol **258**(4 Pt 2): F992-7.

Cheeseman, C. (1992). "Role of intestinal basolateral membrane in absorption of nutrients." Am J Physiol **263**(3 Pt 2): R482-8.

Christensen, H. N. (1990). "Role of amino acid transport and countertransport in nutrition and metabolism." Physiol Rev **70**(1): 43-77.

Christensen, H. N. and D. L. Oxender (1960). "Transport of amino acids into and across cells." Am J Clin Nutr **8**: 131-6.

Cohen, S. A. and K. M. De Antonis (1994). "Applications of amino acid derivatization with 6-aminoquinolyl-N-hydroxysuccinimidyl carbamate. Analysis of feed grains, intravenous solutions and glycoproteins." J Chromatogr A **661**(1-2): 25-34.

Cota, D., K. Proulx, et al. (2006). "Hypothalamic mTOR signaling regulates food intake." Science **312**(5775): 927-30.

Cynober, L., F. Blonde, et al. (1983). "[Measurement of plasma and urinary amino acids with gas chromatography in healthy subjects. Variations as a function of age and sex]." Ann Biol Clin (Paris) **41**(1): 33-8.

Cynober, L. A. (2002). "Plasma amino acid levels with a note on membrane transport: characteristics, regulation, and metabolic significance." Nutrition **18**(9): 761-6.

Daniel, H., B. Spanier, et al. (2006). "From bacteria to man: archaic proton-dependent peptide transporters at work." Physiology (Bethesda) **21**: 93-102.

Danilczyk, U., R. Sarao, et al. (2006). "Essential role for collectrin in renal amino acid transport." Nature **444**(7122): 1088-91.

Danisi, G. and H. Murer (1991). "Inorganic Phosphate Absorption in Small Intestine." in *Comprehensive Physiology*, John Wiley & Sons, Inc.

Dejong, C. H., M. C. van de Poll, et al. (2007). "Aromatic amino acid metabolism during liver failure." J Nutr **137**(6 Suppl 1): 1579S-1585S; discussion 1597S-1598S.

Deutz, N. E., A. J. Wagenmakers, et al. (1999). "Discrepancy between muscle and whole body protein turnover." Curr Opin Clin Nutr Metab Care **2**(1): 29-32.

Dietrich, J. B. (1992). "Tyrosine aminotransferase: a transaminase among others?" Cell Mol Biol **38**(2): 95-114.

Drummond, K. N., A. F. Michael, et al. (1964). "The Blue Diaper Syndrome: Familial Hypercalcemia with Nephrocalcinosis and Indicanuria; a New Familial Disease, with Definition of the Metabolic Abnormality." Am J Med **37**: 928-48.

Eisner, C., R. Faulhaber-Walter, et al. (2010). "Major contribution of tubular secretion to creatinine clearance in mice." Kidney Int **77**(6): 519-26.

Fafournoux, P., C. Remesy, et al. (1983). "Control of alanine metabolism in rat liver by transport processes or cellular metabolism." Biochem J **210**(3): 645-52.

Fang, Z. F., J. Luo, et al. (2009). "Effects of 2-hydroxy-4-methylthiobutyrate on portal plasma flow and net portal appearance of amino acids in piglets." Amino Acids **36**(3): 501-9.

Feric, M., B. Zhao, et al. "Large-scale phosphoproteomic analysis of membrane proteins in renal proximal and distal tubule." Am J Physiol Cell Physiol **300**(4): C755-70.

Fernandez, E., D. Torrents, et al. (2003). "Basolateral LAT-2 has a major role in the transepithelial flux of L-cystine in the renal proximal tubule cell line OK." Journal of the American Society of Nephrology : JASN **14**(4): 837-47.

Fischer, J. E., H. M. Rosen, et al. (1976). "The effect of normalization of plasma amino acids on hepatic encephalopathy in man." Surgery **80**(1): 77-91.

Friesema, E. C., S. Ganguly, et al. (2003). "Identification of monocarboxylate transporter 8 as a specific thyroid hormone transporter." J Biol Chem **278**(41): 40128-35.

Friesema, E. C., J. Jansen, et al. (2005). "Thyroid hormone transporters." Vitam Horm **70**: 137-67.

Galli, F. (2007). "Amino acid and protein modification by oxygen and nitrogen species." Amino Acids **42**(1): 1-4.

Gannon, M. C., J. A. Nuttall, et al. (2002). "The metabolic response to ingested glycine." Am J Clin Nutr **76**(6): 1302-7.

Gannon, M. C., J. A. Nuttall, et al. (2002). "Oral arginine does not stimulate an increase in insulin concentration but delays glucose disposal." Am J Clin Nutr **76**(5): 1016-22.

Gray, H. (1918). Anatomy of the Human Body, Philadelphia: Lea & Febiger.

Grillo, M. A. and S. Colombatto (2007). "S-adenosylmethionine and radical-based catalysis." Amino Acids **32**(2): 197-202.

Gropper, S. S. S., J. L.; Groff, J. L. (2005). Advanced Nutrition and Human Metabolism, Wadsworth.

Halestrap, A. P. and D. Meredith (2004). "The SLC16 gene family-from monocarboxylate transporters (MCTs) to aromatic amino acid transporters and beyond." Pflugers Arch **447**(5): 619-28.

Harper, A. E. and J. C. Peters (1989). "Protein intake, brain amino acid and serotonin concentrations and protein self-selection." J Nutr **119**(5): 677-89.

Hediger, M. A., M. F. Romero, et al. (2004). "The ABCs of solute carriers: physiological, pathological and therapeutic implications of human membrane transport proteinsIntroduction." Pflugers Arch **447**(5): 465-8.

Hoerr, R. A., D. E. Matthews, et al. (1993). "Effects of protein restriction and acute refeeding on leucine and lysine kinetics in young men." Am J Physiol **264**(4 Pt 1): E567-75.

Jager, P. L., W. Vaalburg, et al. (2001). "Radiolabeled amino acids: basic aspects and clinical applications in oncology." J Nucl Med **42**(3): 432-45.

James, J. H., V. Ziparo, et al. (1979). "Hyperammonaemia, plasma aminoacid imbalance, and blood-brain aminoacid transport: a unified theory of portal-systemic encephalopathy." Lancet **2**(8146): 772-5.

Kalogeropoulou, D., L. Lafave, et al. (2008). "Leucine, when ingested with glucose, synergistically stimulates insulin secretion and lowers blood glucose." Metabolism **57**(12): 1747-52.

Kanai, Y. and M. A. Hediger (1992). "Primary structure and functional characterization of a high-affinity glutamate transporter." Nature **360**(6403): 467-71.

Karl, T., R. Pabst, et al. (2003). "Behavioral phenotyping of mice in pharmacological and toxicological research." Exp Toxicol Pathol **55**(1): 69-83.

Keays, D. A., T. G. Clark, et al. (2007). "Estimating the number of coding mutations in genotypic and phenotypic driven N-ethyl-N-nitrosourea (ENU) screens: revisited." Mamm Genome **18**(2): 123-4.

Keays, D. A., T. G. Clark, et al. (2006). "Estimating the number of coding mutations in genotypic- and phenotypic-driven N-ethyl-N-nitrosourea (ENU) screens." Mamm Genome **17**(3): 230-8.

Kim, D. K., Y. Kanai, et al. (2001). "Expression cloning of a Na+-independent aromatic amino acid transporter with structural similarity to H+/monocarboxylate transporters." J Biol Chem **276**(20): 17221-8.

Kim, S. W. and G. Wu (2009). "Regulatory role for amino acids in mammary gland growth and milk synthesis." Amino Acids **37**(1): 89-95.

Klassen, P., P. Furst, et al. (2001). "Plasma free amino acid concentrations in healthy Guatemalan adults and in patients with classic dengue." Am J Clin Nutr **73**(3): 647-52.

Koehnle, T. J., M. C. Russell, et al. (2003). "Rats rapidly reject diets deficient in essential amino acids." J Nutr **133**(7): 2331-5.

Kostandyan, N., C. Britschgi, et al. (2011). "The spectrum of phenylketonuria genotypes in the Armenian population: identification of three novel mutant PAH alleles." Mol Genet Metab **104 Suppl**: S93-6.

Kussmann, M., S. Rezzi, et al. (2008). "Profiling techniques in nutrition and health research." Curr Opin Biotechnol **19**(2): 83-99.

Lahoutte, T., V. Caveliers, et al. (2004). "SPECT and PET amino acid tracer influx via system L (h4F2hc-hLAT1) and its transstimulation." J Nucl Med **45**(9): 1591-6.

Lahoutte, T., V. Caveliers, et al. (2001). "In vitro characterization of the influx of 3-[125I]iodo-L-alpha-methyltyrosine and 2-[125I]iodo-L-tyrosine into U266 human myeloma cells: evidence for system T transport." Nucl Med Biol **28**(2): 129-34.

Lahoutte, T., V. Caveliers, et al. (2002). "Increased tumor uptake of 3-(123)I-Iodo-L-alpha-methyltyrosine after preloading with amino acids: an in vivo animal imaging study." J Nucl Med **43**(9): 1201-6.

Lahoutte, T., J. Mertens, et al. (2003). "Comparative biodistribution of iodinated amino acids in rats: selection of the optimal analog for oncologic imaging outside the brain." J Nucl Med **44**(9): 1489-94.

Langhans, W. (2010). "The enterocyte as an energy flow sensor in the control of eating." Forum Nutr **63**: 75-84.

Lesch, K. P., D. Bengel, et al. (1996). "Association of anxiety-related traits with a polymorphism in the serotonin transporter gene regulatory region." Science **274**(5292): 1527-31.

Lichter-Konecki, U., C. M. Hipke, et al. (1999). "Human phenylalanine hydroxylase gene expression in kidney and other nonhepatic tissues." Mol Genet Metab **67**(4): 308-16.

Lloyd, J. B. and W. J. Whelan (1969). "An improved method for enzymic determination of glucose in the presence of maltose." Anal Biochem **30**(3): 467-70.

Loening, A. M. and S. S. Gambhir (2003). "AMIDE: a free software tool for multimodality medical image analysis." Mol Imaging **2**(3): 131-7.

Lyck, R., N. Ruderisch, et al. (2009). "Culture-induced changes in blood-brain barrier transcriptome: implications for amino-acid transporters in vivo." J Cereb Blood Flow Metab **29**(9): 1491-502.

Lyck, R., N. Ruderisch, et al. (2009). "Culture-induced changes in blood-brain barrier transcriptome: implications for amino-acid transporters in vivo." Journal of cerebral blood flow and metabolism : official journal of the International Society of Cerebral Blood Flow and Metabolism **29**(9): 1491-502.

Lynch, C. J., B. Gern, et al. (2006). "Leucine in food mediates some of the postprandial rise in plasma leptin concentrations." Am J Physiol Endocrinol Metab **291**(3): E621-30.

Maquat, L. E. (1995). "When cells stop making sense: effects of nonsense codons on RNA metabolism in vertebrate cells." RNA **1**(5): 453-65.

Meier, C., Z. Ristic, et al. (2002). "Activation of system L heterodimeric amino acid exchangers by intracellular substrates." EMBO J **21**(4): 580-9.

Meredith, D. and H. C. Christian (2008). "The SLC16 monocaboxylate transporter family." Xenobiotica **38**(7-8): 1072-106.

Moundras, C., C. Remesy, et al. (1993). "Dietary protein paradox: decrease of amino acid availability induced by high-protein diets." Am J Physiol **264**(6 Pt 1): G1057-65.

Murer, H., J. Evers, et al. (1976). "Polarity of proximal tubular epithelial cells in relation to transepithelial transport." Curr Probl Clin Biochem **6**: 173-89.

Nassl, A. M., I. Rubio-Aliaga, et al. (2011). "Amino acid absorption and homeostasis in mice lacking the intestinal peptide transporter PEPT1." Am J Physiol Gastrointest Liver Physiol **301**(1): G128-37.

Nassl, A. M., I. Rubio-Aliaga, et al. (2011). "The intestinal peptide transporter PEPT1 is involved in food intake regulation in mice fed a high-protein diet." PLoS One **6**(10): e26407.

Noguchi, Y., Q. W. Zhang, et al. (2006). "Network analysis of plasma and tissue amino acids and the generation of an amino index for potential diagnostic use." Am J Clin Nutr **83**(2): 513S-519S.

Nuttall, F. Q., K. J. Schweim, et al. (2006). "Effect of orally administered phenylalanine with and without glucose on insulin, glucagon and glucose concentrations." Horm Metab Res **38**(8): 518-23.

Palacin, M., R. Estevez, et al. (1998). "Molecular biology of mammalian plasma membrane amino acid transporters." Physiol Rev **78**(4): 969-1054.

Pappenheimer, J. R. (1993). "On the coupling of membrane digestion with intestinal absorption of sugars and amino acids." The American journal of physiology **265**(3 Pt 1): G409-17.

Park, S. Y., J. K. Kim, et al. (2005). "Reabsorption of neutral amino acids mediated by amino acid transporter LAT2 and TAT1 in the basolateral membrane of proximal tubule." Arch Pharm Res **28**(4): 421-32.

Peters, J. C. and A. E. Harper (1981). "Protein and energy consumption, plasma amino acid ratios, and brain neurotransmitter concentrations." Physiol Behav **27**(2): 287-98.

Peters, J. C. and A. E. Harper (1985). "Adaptation of rats to diets containing different levels of protein: effects on food intake, plasma and brain amino acid concentrations and brain neurotransmitter metabolism." J Nutr **115**(3): 382-98.

Pfeiffer, R., G. Rossier, et al. (1999). "Amino acid transport of y+L-type by heterodimers of 4F2hc/CD98 and members of the glycoprotein-associated amino acid transporter family." The EMBO journal **18**(1): 49-57.

Premen, A. J. (1988). "Potential mechanisms mediating postprandial renal hyperemia and hyperfiltration." FASEB J **2**(2): 131-7.

Przyrembel, H., D. Bachmann, et al. (1975). "Alpha-ketoadipic aciduria, a new inborn error of lysine metabolism; biochemical studies." Clin Chim Acta **58**(3): 257-69.

Qi, Z., I. Whitt, et al. (2004). "Serial determination of glomerular filtration rate in conscious mice using FITC-inulin clearance." Am J Physiol Renal Physiol **286**(3): F590-6.

Ramadan, T., S. M. Camargo, et al. (2007). "Recycling of aromatic amino acids via TAT1 allows efflux of neutral amino acids via LAT2-4F2hc exchanger." Pflugers Arch **454**(3): 507-16.

Ramadan, T., S. M. Camargo, et al. (2006). "Basolateral aromatic amino acid transporter TAT1 (Slc16a10) functions as an efflux pathway." J Cell Physiol **206**(3): 771-9.

Rechsteiner, M. and S. W. Rogers (1996). "PEST sequences and regulation by proteolysis." Trends Biochem Sci **21**(7): 267-71.

Recommendations (1976). "IUPAC Commission on the Nomenclature of Organic Chemistry (CNOC) and IUPAC-IUB Commission on Biochemical Nomenclature (CBN). Nomenclature of cyclitols. Recommendations, 1973." Biochem J **153**(1): 23-31.

Reeves, P. G., F. H. Nielsen, et al. (1993). "AIN-93 purified diets for laboratory rodents: final report of the American Institute of Nutrition ad hoc writing committee on the reformulation of the AIN-76A rodent diet." J Nutr **123**(11): 1939-51.

Rist, M. J., U. Wenzel, et al. (2006). "Nutrition and food science go genomic." Trends Biotechnol **24**(4): 172-8.

Romeo, E., M. H. Dave, et al. (2006). "Luminal kidney and intestine SLC6 amino acid transporters of B0AT-cluster and their tissue distribution in Mus musculus." Am J Physiol Renal Physiol **290**(2): F376-83.

Rossier, G., C. Meier, et al. (1999). "LAT2, a new basolateral 4F2hc/CD98-associated amino acid transporter of kidney and intestine." J Biol Chem **274**(49): 34948-54.

Sallstrom, J., M. Carlstrom, et al. (2010). "High-protein-induced glomerular hyperfiltration is independent of the tubuloglomerular feedback mechanism and nitric oxide synthases." Am J Physiol Regul Integr Comp Physiol **299**(5): R1263-8.

Schimassek, H. and W. Gerok (1965). "Control of the levels of free amino acids in plasma by the liver." Biochem Z **343**(4): 407-15.

Schimassek, H. and W. Gerok (1965). "Control of the levels of free amino acids in plasma by the liver." Biochemische Zeitschrift **343**(4): 407-15.

Seaton, B. and A. Ali (1984). "Simplified manual high performance clinical chemistry methods for developing countries." Med Lab Sci **41**(4): 327-36.

Shalmi, M., H. E. Lunau, et al. (1991). "Suitability of tritiated inulin for determination of glomerular filtration rate." Am J Physiol **260**(2 Pt 2): F283-9.

Shigeoka, T., M. Kawaichi, et al. (2005). "Suppression of nonsense-mediated mRNA decay permits unbiased gene trapping in mouse embryonic stem cells." Nucleic Acids Res **33**(2): e20.

Shikata, N., Y. Maki, et al. (2007). "Multi-layered network structure of amino acid (AA) metabolism characterized by each essential AA-deficient condition." Amino Acids **33**(1): 113-21.

Singer, D., S. M. Camargo, et al. (2009). "Orphan transporter SLC6A18 is renal neutral amino acid transporter B0AT3." J Biol Chem **284**(30): 19953-60.

Slyke, D. D. V. and G. M. Meyer (1913). "Nutrition classics. The Journal of Biological Chemistry. Volume XVI, 1913. The fate of protein digestion products in the body. III. The absorption of amino-acids from the blood by tissues. By Donald D. Van Slyke and Gustave M. Meyer." Nutr Rev **42**(7): 254-6.

Stein, J., H. Daniel, et al. (1994). "Rapid postabsorptive metabolism of nicotinic acid in rat small intestine may affect transport by metabolic trapping." J Nutr **124**(1): 61-6.

Stevens, B. R., H. J. Ross, et al. (1982). "Multiple transport pathways for neutral amino acids in rabbit jejunal brush border vesicles." J Membr Biol **66**(3): 213-25.

Stoll, B., J. Henry, et al. (1998). "Catabolism dominates the first-pass intestinal metabolism of dietary essential amino acids in milk protein-fed piglets." J Nutr **128**(3): 606-14.

Strauss, K. A., E. G. Puffenberger, et al. (2003). "Type I glutaric aciduria, part 1: natural history of 77 patients." Am J Med Genet C Semin Med Genet **121C**(1): 38-52.

Stuart, R. O., A. Pavlova, et al. (2001). "EEG1, a putative transporter expressed during epithelial organogenesis: comparison with embryonic transporter expression during nephrogenesis." Am J Physiol Renal Physiol **281**(6): F1148-56.

Sugiura, S., K. Kitagawa, et al. (2005). "Adenovirus-mediated gene transfer of heparin-binding epidermal growth factor-like growth factor enhances neurogenesis and angiogenesis after focal cerebral ischemia in rats." Stroke **36**(4): 859-64.

Suresh Babu, S. V., M. M. Shareef, et al. (2002). "HPLC method for amino acids profile in biological fluids and inborn metabolic disorders of aminoacidopathies." Indian Journal of Clinical Biochemistry **17**(2): 7-26.

Thony, B. (2010). "Long-term correction of murine phenylketonuria by viral gene transfer: liver versus muscle." J Inherit Metab Dis **33**(6): 677-80.

Tome, D. (2004). "Protein, amino acids and the control of food intake." Br J Nutr **92 Suppl 1**: S27-30.

Uchida, S., A. Kitamoto, et al. (2005). "Chronic reduction in dietary tryptophan leads to changes in the emotional response to stress in mice." J Nutr Sci Vitaminol (Tokyo) **51**(3): 175-81.

van Donkelaar, E. L., A. Blokland, et al. (2010). "Acute tryptophan depletion in C57BL/6 mice does not induce central serotonin reduction or affective behavioural changes." Neurochem Int **56**(1): 21-34.

Vanhove, C., M. Defrise, et al. (2011). "Improved quantification in multiple-pinhole SPECT by anatomy-based reconstruction using microCT information." Eur J Nucl Med Mol Imaging **38**(1): 153-65.

Verrey, F. (2003). "System L: heteromeric exchangers of large, neutral amino acids involved in directional transport." Pflugers Archiv : European journal of physiology **445**(5): 529-33.

Verrey, F., E. I. Closs, et al. (2004). "CATs and HATs: the SLC7 family of amino acid transporters." Pflugers Arch **447**(5): 532-42.

Verrey, F., Z. Ristic, et al. (2005). "Novel renal amino acid transporters." Annu Rev Physiol **67**: 557-72.

Verrey, F., D. Singer, et al. (2009). "Kidney amino acid transport." Pflugers Arch **458**(1): 53-60.

Wilson, M. C., D. Meredith, et al. (2005). "Basigin (CD147) is the target for organomercurial inhibition of monocarboxylate transporter isoforms 1 and 4: the ancillary protein for the insensitive MCT2 is EMBIGIN (gp70)." J Biol Chem **280**(29): 27213-21.

Wu, G. (1998). "Intestinal mucosal amino acid catabolism." J Nutr **128**(8): 1249-52.

Wu, G. (2009). "Amino acids: metabolism, functions, and nutrition." Amino Acids **37**(1): 1-17.

Wybenga, D. R., J. Di Giorgio, et al. (1971). "Manual and automated methods for urea nitrogen measurement in whole serum." Clin Chem **17**(9): 891-5.

Yao, K., J. Fang, et al. (2011). "Tryptophan metabolism in animals: important roles in nutrition and health." Front Biosci (Schol Ed) **3**: 286-97.

Ye, S., S. Dhillon, et al. (2001). "An efficient procedure for genotyping single nucleotide polymorphisms." Nucleic Acids Res **29**(17): E88-8.

9. Curriculum Vitae

Luca Carlo Olivio Mariotta
Date of birth: 10.03.1981
Nationality: Swiss
Place of citizenship: Muralto (TI)
Civil status: Married
E-mail: luca.mariotta@gmail.com

Education and professional activity

2008 – 2012:	University of Zurich, Institute of Physiology: PhD work under the supervision of Prof. Dr. med. François Verrey
2007 – 2008:	University of Zurich: Research Assistant by Prof. Dr. K. Basler
2005 – 2007:	University of Zurich: Master of Science in Molecular and Cellular Biology under the supervision of Prof. Dr. Markus Noll
2002 – 2005:	University of Zurich: Bachelor of Science
2000 – 2002:	ETH Zurich: Biochimestry
1996 – 2000:	Liceo Cantonale di Locarno: Maturity type B

Meeting attendance

2011:	Experimental Biology (EB), Washington, USA
2010:	Deutsche und Skandinavische Physiologische Gesellschaften (DSPG), Kopenagen, DK
2009:	International Union of Physiological Societies (IUPS), Kyoto, JP
2009/10/11/12:	Union of the Swiss Societies for Experimental Biology (USGEB), CH
2008:	Transporters meeting, Murten, CH

Publication list

Verrey F, Singer D, Ramadan T, Vuille-dit-Bille RN, **Mariotta L**, Camargo SM (2009). Kidney amino acid transport. *Pflugers Arch - Eur J Physiol* 458:53–60

Singer D, Camargo SM, Ramadan T, Schäfer M, **Mariotta L**, Herzog B, Huggel K, Wolfer D, Werner S, Penninger J, Verrey F (2012). Defective intestinal amino acid absorption in Ace2 null mice. *AJP Gastrointest Liver Physiol.*

Mariotta L, Ramadan T, Singer D, Guetg A, Herzog B, Stöger C, Palacin M, Lahoutte T, Camargo SM, Verrey F (submitted manuscript). T-type amino acid transporter TAT1 (Slc16a10) is essential for extracellular aromatic amino acid homeostasis control. *J Physiol.*

10. Acknowledgements

First of all I would like to warmly thank François for according me the possibility to work with his "great crew". I'm really grateful for his constant guidance, for all precious advices and for allowing me to present this work at international workshops.

A big thank to the other members of the PhD committee, Prof. Daniel and Prof. Kullak-Ublick, for their great expertise, guidance and encouragement. A special thank also to the people of the ImMed program, ZIRP facility and animal husbandry, in particular to Marija, Matthew and Daniel, who have taken great care of my animals.

I'm really grateful to many former member of the "crew": Tamara, who has traced the project's footsteps; Dustin, who taught me just everything I know; Nadine, who constantly fed me and was always there; Raphael for the scientific discussions in front of a beer; Olga, Chiara, Nicola, Katja, Sandra, Tina, Benjamin, Dong, Lorenz and Thomas for the great start.
Many thanks also to Simone and Brigitte, who always helped, guided and made this work possible. Marta, Monica, Selene, Adriano and Christian for the excellent (*Swiss*-) Italian speaking support: grazie mille! Alok for a great US congress. Special thanks to all other member of the lab for making such a pleasant atmosphere: Elena, Eva, Helen, Sam, Stine, Vicky, Felipe, Ian, Josua, Liviu and Lukas.
A big thank also to the other inhabitants of the Institute of Physiology that I did not mention yet.

Un grazie a tutti gli amici per lo svago sul mezzogiorno e nel weekend. In particular, many thanks to Yuki and Remy for corrections and support on statistic.

The biggest thank you goes to my wife Cristina, who provides a sense to what I do. Finally, I dedicate this work to my family that supported all my studies and always believed in me.